# DEVELOPMENT AND PERFORMANCE EVALUATION OF A DISC TYPE BAMBARA NUT DECORTICATING MACHINE

**BY**

**AJUNWA, Goddey Owoicho**
**M.ENG/SIPET/2018/8401**

**DEPARTMENT OF AGRICULTURAL AND BIORESOURCES ENGINEERING**

**FEDERAL UNIVERSITY OF TECHNOLOGY, MINNA.**

**AUGUST, 2023.**

## ABSTRACT

The trend of post-harvest handling, processing, and storage of pod crops is launched by the removal of the pods or coats and subsequent separation of the same from the seeds; a process known as decorticating in many parts of the country, this act is done traditionally, using several sort techniques such as heap-beating, manual cracking with stones, and trampling by feet. Due to the importance of these crops, several attentions have been pulled towards improving the means of decorticating pod crop. It is in light of this that, a simple decorticator, capable of decorticating several varieties of Bambara nut by just a simple replacement of the decorticating discs was developed. The machine which is a disc-type decorticator, is designed to have rims to which the decorticating members are attached, hence discs specific to a particular variety can be replaced when need be. The machine was evaluated and the result showed that; the values of shelling efficiency ranged from 47.2 % to 96.5 %. The combination of a shelling speed of 250 rpm, plate clearance of 1 mm, fan speed of 1300 rpm, and feed rate of 130 kg/h yielded the highest efficiency of 96.5 %, while the interaction of shelling speed of 150 rpm, plate clearance of 3 mm, fan speed of 1300 rpm, and feed rate 130 kg yielded the lowest efficiency of 47.45 %. The value of clearing efficiency ranged from 70.85 % to 97.22 %. The highest value of 97.22 % was obtained from the combination of shelling speed of 250 rpm, plate clearance of 3 mm, fan speed of 1300 rpm, and feed rate of 110 kg/h, while the interaction between shelling speed of 350 rpm, plate clearance of 3 mm, fan speed of 1300 rpm, and feed rate of 130 kg/h yielded an efficiency of 70.85 %. The value of recovery efficiency ranged from 47.2 % to 99.37 %. The combination of shelling speed of 200 rpm, plate clearance of 2 mm, fan speed of 1200 rpm, and feed rate of 120 kg/h yielded the highest efficiency of 99.37 %, while the interaction of shelling speed of 150 rpm, plate clearance of 3 mm, fan speed of 1300 rpm, and feed rate of 130 kg/h yielded the lowest efficiency of 47.2 %. The value of the percentage loss ranged from 0.63 % to 29.15 %. The combination of shelling speed of 350 rpm, plate clearance of 3 mm, fan speed of 1300 rpm, and feed rate of 130 kg/h yielded the highest percentage loss of 29.15 %, while the interaction of shelling speed of 200 rpm, plate clearance of 2 mm, fan speed of 1200 rpm, and feed rate of 120 kg/h yielded the lowest percentage loss of 0.63 %.

# TABLE OF CONTENTS

# LIST OF TABLES

# LIST OF FIGURES

**Figures** **Page**

# CHAPTER ONE

## 1.0 INTRODUCTION

### 1.1 Background to the Study

Pod crops (also known as pulses), a general term which describes a variety of crops whom seeds or kernels are coated or covered with some sort of casing called “pods”. Pod crops is synonymous to legumes (Wallace *et al.*, 2020) a pod according to the thesaurus dictionary, is a somewhat elongated, two-varved seed vessel, as that of the peer or bean. Pods exhibit dehiscence when dried, a mechanism via which they achieve dispersal.

Pods play numerous important roles in the growth and development of pod crops (pulses). According to Bennette *et al.* (2011), pods play a key role in encapsulating the developing seeds and protecting them from pests and pathogens. They added that pods are active photosynthetic organs during development and that, this occur mainly in the pod walls which is itself a modified type of leaf (Bennette *et al.*, 2011). Vlot *et al.* (2008) put a figure to the contribution to the weight of a particular pod (soya beans) due to the synthesis of pods, stating that this value is 7.34 - 15.6 % of all seed weight. It has also been discovered that pod wall development is strongly associated to seed size and consequently to the pod length, due to the strong correlation between the two morphological characteristics (Diepenbrock, 2000)

Pulses are of tremendous importance, proving useful in various aspects, ranging from nutritional sources to industrial raw materials. Snapp (2018) emphasized on the nutritional importance of legumes (pulses), affirming that “human nutrition and crop-livestock integration are both dependent on the protein rich and diverse amino acid content associated

with legume products". The unique amino acids of legumes contain complements which include tryptophan and lysine (Asif *et al.,* 2013), unique complements that are not present in other sources of protein. Pulse crops provide diversity of nutrients such as the B-group of vitamins, iron, zinc, magnesium, calcium and a variety of amino acids. The nutritional benefits obtainable from pulses are contained in literatures such as (Dahl, 2019)

Due to localized agricultural activities most of the farm lands have been reported degraded significantly in terms of soil nutrients (FAO 2018). If left to persist, FAO reported that, the situation can compromise food production in sub-Saharan Africa (both quantitatively and qualitatively), and the sustainability of existing agricultural production system, thus a need for the revitalization of these farm lands. Pulses have been found to possess a unique ability to biologically fix atmospheric nitrogen into the soil and to enhance the biological turnover of soil phosphorus (FAO, 2018; Unathi *et al.*, 2018; Wiraguna, 2016). A project by an international consortium of eleven partners (LEGUVAL) shows the potentials of legumes as source of plastic products. They also thought that, the left-over biomass of protein extraction could be used as fillers in polymer matrix to improve the properties of plastic materials and as a substrate for biogas anaerobic digestion (Chiara, 2016). Other industrial uses and benefits of pod crops have been published in several literatures such as Bojňanská *et al.* (2021); Voisin *et al.* (2014).

The trend of post-harvest handling, processing and storage of pod crops is launched by the removal of the pods or coats and subsequently separation of same from the seeds, a process known as decorticating or decorticating or shelling (Jun *et al.*, 2018). A corresponding increase in the demand for pod crops has been witnessed due to the overwhelming importance derived from the consortium of these crops coupled with the growing population of Nigeria

and the world at large. In response to these demands, efforts are made toward the growth in production of these crops. Legumes are reported to be the second most consumed food crop globally after cereal. Maphosa and Jideani (2017) confirmed this assertion stating that, "legumes are valued worldwide as a sustainable and inexpensive meat alternative and are considered the second most important food source after cereal". Data from the research by FAO in 2016 also concord with this, showing a value of 335,613,801 metric tons for soya beans falling behind cereals such as rice, maize and wheat. Cowpea for instance, was reported to be grown across the world on an estimated 14.5 million hectares of land per year; yielding about 6.2 million metric tons (Neda and Erena, 2020) the research also reported a 1.5% growth in production per annum over the duration of study (3year). In a review by Akibode and Maredia (2012), it was stated that overall pulse production around the globe had increase at a rate higher than the growth rate in population, both in developing and developed worlds over a period of 14 years. According to him within this period, a stable and modest positive trend in per capital consumption was observed within the context of a declining overall historical trend. In Latin America and South Asia, the expanse of land dedicated to soya bean cultivation has expanded quite rapidly, leading to a production growth rate of 4.3 %. The figure was same for the world at large, making it the second highest crop to experience a per annum growth rate behind cowpea whose value is 4.7 % (Gowda, 2009). He also reported growth rates of 2.2 % and 2.0 % per annum for lentil and pigeon pea respectively over the period of study (that is, 15 years)

The entire vast of these legume yield, irrespective of what purpose or use they are to be put, decorticating is inevitable, hence the importance of this stage of crop processing. There exist several ways of decorticating all embodied in two broad methods; the traditional manual

(conventional) method, which involves activities such as the use of sticks to batter sacks loaded with pulses, the use of mortar and pestle, trampling upon piles of pulses either by humans or animals, manually breaking of pods with the aid of simple tools then hand picking the kernels from the coats; and the machine aided methods which entails the use of agricultural machineries ranging from small self-propelled machines to sophisticated automated machineries (Kabir and Fedel, 2018; Giwa and Akanbi, 2020)

The shift in paradigm from the traditional methods of decorticating to the mechanical methods became imperative in order to meet the increasing demand of this activity. This demand has resulted in the indigenous design and construction of several decorticators for several crops with better performance output and overall advantages over the conventional methods. A modular melon decorticating machine fabricated by Osasumwen, which used friction/rubbing provided by toothed roller drum to peel off melon pods is one of such efforts made towards meeting this demand. The machine showed an average an average percentage of decorticator seeds of 91.1255 %, an average damaged seed of 1.5835 % (Osasumwen *et al.,* 2020). Another inventory team led by Murtala, designed and fabricated a cocoa decorticator, using locally sourced materials. The project which they said was aimed at reduction of production cost and drudgeries associated with the traditional means, showed a throughput capacity of 496.87 kg/hr, with an efficiency of 89.29 % at an operation speed of 219 rpm. Decorticating by this machine is achieved via impact and compressive forces (Murtala *et al.,* 2018). Further contribution to this course by Adu *et al.* (2018) was a groundnut decorticating machine. He also iterated that the machine would eliminate drudgeries associated with the traditional means of this process. Performance evaluation results of this machine showed output capacity of 120 kg/hr., machine damage efficiency of

14 %, cleaning efficiency of 85 % and the decorticating efficiency was 84 %, if ran by a 1 horsepower motor (Adu *et al.,* 2018). There also exist a *Delonix ragia* decorticating machine. The machine which was designed and fabricated by Ojolo and his team uses the principle of impact to shred the pods off the kernel. The machine showed a whole seed recovery of 98.4 % and aa throughput of 56.4 kg/hr. and powered by a 6-kW motor (Ojolo *et al.,* 2019) there exist several other decorticating machines to include; the Bambara nut decorticator by Negedu *et al.* (2018).

The status quo of the present situation arguably reflects a change in the narratives of the processing industry as per decorticating. In spite of this efforts directed towards this aspect of agriculture, a conceptual rational scrutiny shows the existence of gaps, and hence a room for improvement. One of these gaps is the rampancy of the ancient conventional methods despite the existence of all the various machineries. This situation implies that, the lingering problem of affordability is still in the picture. Also, studying through the existing decorticators reviewed that most (if not all) of them are limited in function to a particular crop type, this situation sterns the predicament of commercial medium scale farmers who grow variety of pulses, as it implies ownership of numerous machines of hiring of same, in any case, higher cost of decorticating is incurred. This situation encourages farmers to sell off their produce in un-decorticated, thus launching a stage for underpricing and consequently resulting in under-reward of farmers. These situation plus other devaluing factors associated with the status quo tend to discourage involvement in production agriculture. In light of these gaps, coupled with the importance of the decorticating process it has become imperative for a design that integrates all of these gaps into its design consideration.

## 1.2 Statement of the Research Problem

The growing population of the Nigerian community and the world at large has influenced a direct proportionate growth in the demand of human basic needs, agricultural produce inclusive. The processing chain of most of these agricultural produce starts with decorticating, threshing or de-husking (De Lucia and Assennato, 2016). In many parts of the country, the act of decorticating and its ilk are still done via the primitive manual techniques. A survey done in some parts of Nigeria - the Middle-belt and South-Western zones, about how rural women in villages shelled Bambara nut reviewed that, mostly, the use of a mortar and pestle, to pound on the pods was the predominant technique. In some cases, the pods are placed in a sack and beaten with a stick to remove the shell from the nuts (Ouili *et al.,* 2022).

Extracting clean seeds from pods is a crucial step in processing Bambara nuts, but it is also one of the most time-consuming and challenging tasks. This process has been a major obstacle to large-scale production and processing of this valuable protein-rich crop (Alonge *et al.,* 2017). The separation of the shell from the nuts is done through a local winnowing method. These techniques are labour intensive yet comparatively poor in result, hence a concern for the growing demand of the population (Ouili *et al.,* 2022).

There exist ample machines for decorticating Bambara nut. To the host of this vast list, is a common shortcoming; the persisting issue of high damage (low whole seed recovery rate) to the kernel in form of shatter (Negedu *et al.,* 2018, Adedeji and Danladi, 2016). Review of the previous works on these Bambara nut decorticators showed that, they all depend solely on the principle of impact to achieve decortication. The success of this principle depends exclusively on the discrepancy in the rupture force/energy between the pod/shell and the kernel (Oluwole *et al.,* 2007). This discrepancy however for Bambara nut shrinks as the

crop's moisture content approaches that, ideal for decortication, since the pod gains immense toughness and consequently high rupture force. This fact coupled with the high tendency of the impact principle of decortication to cause shatter at high level of application (as needed to shred Bambara nut pods) (Oluwole *et al.*, 2007) tend to leave a high percentage of the kernel shattered during decortication by these machines.

## 1.3 Aim and Objectives of the Study

The aim of this project is to develop a Bambara nut decorticating machine.

the objectives of the study are to:

i. Design and fabricate a Bambara nut decorticating machine
ii. Evaluate the performance of the machine

## 1.4 Justification for the Study

The relief of farmers from the monotonous and tedious procedures of the conventional decorticating process of the pod crops (Bambara nut) is promised by this project. The simple design of the machine together with the fact that it is made from locally sourced materials is aimed at resolving the issue of unaffordability by local farmers and hence improved products and productivity.

One common loophole associated with the existing Bambara nut decorticators is their high seed shatter-damage tendencies (low whole seed recovery rate) due to their principle of decortication (impact). To attain decortication of Bambara nut by this principle, the impact force has to be high (due to the high rupture force of the pod). This as a result renders these machines low in efficiency. For this project, the decorticator is uniquely designed, paying attention to such these areas resulting in low efficiency/seed damage. Two basic innovation

was incorporated, aimed to curb damage. To curb seed breakage due to high impact force, the decorticator was designed to run at a relatively low speed (of decorticating members), hence low impact. The capability of this machine to simultaneously apply three principles of decortication; impact, attrition and shear (with the latter being the primary principle), aid to curb kernel damage due to high impact force, as in the existing decorticators. Secondly the flexibility of the machine allows for the replacement of the plates/discs. This is useful in that; it gives room for design and utilization of plates with spikes configurations best suited per variety of the crop.

## 1.5 Scope of Work

The scope of work encompassed in this project is strictly limited to that which contributes or aids in developing and evaluating a multipurpose decorticating machine.

# CHAPTER TWO

## 2.0 LITERATURE REVIEW

### 2.1 Meaning of Pod Crops

Pod crops (also known as pulses), a general term which describes a variety of crops whom seeds or kernels are coated or covered with some sort of casing called “pods”. Pod crops is synonymous to legumes (*Wallace et al.,* 2020) a pod according to the thesaurus dictionary, is a somewhat elongated, two-varved seed vessel, as that of the peer or bean. Pods exhibit dehiscence when dried, a mechanism via which they achieve dispersal.

### 2.2 Importance of Pod Crops

Pulses are of tremendous importance, proving useful in various aspects, ranging from nutritional sources to industrial raw materials. Snapp (2018) emphasized on the nutritional importance of legumes (pulses), affirming that “human nutrition and crop-livestock integration are both dependent on the protein rich and diverse amino acid content associated with legume products”. The unique amino acids of legumes contain complements which include tryptophan and lysine (Asif *et al.,* 2013), unique complements that are not present in other sources of protein. Asif *et al.* (2013) reported that, pulse crops provide diversity of nutrients such as the B-group of vitamins, iron, zinc, magnesium, calcium and a variety of amino acids. The nutritional benefits obtainable from pulses are contained in literatures such as (Dahl, 2019)

Due to localized agricultural activities most of the farm lands have been reported degraded significantly in terms of soil nutrients (FAO, 2018). If left to persist, FAO reported that, the situation can compromise food production in sub-Saharan Africa (both quantitatively and

qualitatively), and the sustainability of existing agricultural production system, thus a need for the revitalization of these farm lands. Pulses have been found to possess a unique ability to biologically fix atmospheric nitrogen into the soil and to enhance the biological turnover of soil phosphorus (FAO, 2018; Unathi *et al.*, 2018; Wiraguna, 2016).

## 2.3 Meaning of Decortication and the States of the Act

The trend of post-harvest handling, processing and storage of pod crops is launched by the removal of the pods or coats and subsequent separation of same from the seeds, a process known as decorticating or decorticating or shelling (Jun *et al.,* 2018). The entire vast of pods, irrespective of what purpose or use they are to be put, decorticating is inevitable, hence the importance of this stage of crop processing. There exist several ways of decorticating all embodied in two broad methods; the traditional manual (conventional) method, which involves activities such as the use of sticks to batter sacks loaded with pulses, the use of mortar and pestle, trampling upon piles of pulses either by humans or animals, manually breaking of pods with the aid of simple tools then hand picking the kernels from the coats; and the machine aided methods which entails the use of agricultural machineries ranging from small self-propelled machines to sophisticated automated machineries (Kabir and Fedel, 2018; Giwa and Akanbi, 2020;)

The shift in paradigm from the traditional methods of decorticating to the mechanical methods became imperative in order to meet the increasing demand of this activity. This demand has resulted in the indigenous design and construction of several decorticator for several crops with better performance output and overall advantages over the conventional methods. A modular melon decorticating machine fabricated by Osasumwen, which used friction/rubbing provided by toothed roller drum to peel off melon pods is one of such efforts

made towards meeting this demand. The machine showed an average an average percentage of decorticator seeds of 91.1255 %, an average damaged seed of 1.5835 % (Osasumwen *et al.,* 2020). Another inventory team led by Murtala, designed and fabricated a cocoa decorticator, using locally sourced materials. The project which they said was aimed at reduction of production cost and drudgeries associated with the traditional means, showed a throughput capacity of 496.87 kg/hr, with an efficiency of 89.29% at an operation speed of 219 rpm. Decorticating by this machine is achieved via impact and compressive forces (Murtala *et al.,* 2018). Further contribution to this course by Adu *et al.* (2018), was a groundnut decorticating machine. Performance evaluation results of this machine showed output capacity of 120 kg/hr., machine damage efficiency of 14%, cleaning efficiency of 85 % and the decorticating efficiency was 84 %, if ran by a 1horsepower motor (Adu *et al.,* 2018). There also exist a *Delonix ragia* decorticating machine. The machine which was designed and fabricated by Ojolo and his team uses the principle of impact to shred the pods off the kernel. The machine showed a whole seed recovery of 98.4% and aa throughput of 56.4 kg/hr. and powered by a 6 kW electric motor (Ojolo *et al.,* 2019) there exist several other decorticating machines to include; the Bambara nut decorticator by Negedu *et al.* (2018).

## 2.4 Physical Mechanical Properties of Pods and Their Roles in Design of Processing Equipment

The physical and mechanical properties of crops such as; moisture content, bulk density, grain shape/size, rupture strength, rupture energy and stiffness are key to the design and development of equipment and machines used in the handling, storage and processing of agricultural produce. The following section contains a vivid discussion of some of these

properties, their inter-relationships and their roles in the design of agricultural machines and equipment

### 2.4.1 Rupture strength and energy

Rupture strength (also known as ultimate strength) in the context of agro-materials has been defined as the maximum stress a material can bear (under loading condition) beyond which the material ruptures or breaks down or shatters (Al-Hassani *et al.,* 2014). Aremu *et al.* (2014) stated that, the rupture force is the force at the point on the force deformation curve, at which the compressed shell completely breaks. The rupture point is detected by a continuous decrease of load in the force-deformation curve (Al-Hassani *et al.,* 2014). Some materials exhibit elasticity; that is under gradual (stepwise) loading condition, a corresponding gradual deformation is observed, whereas others do not deform (at least not significantly) in response to loading prior to the ultimate level. Such materials are said to be plastic. In the deformation curve of elastic materials, a region of elasticity exists at the initial loading range before the rupture point is reached. Plastic materials on the other hand remain approximately undeformed in the loading range below that of the rupture force. These phenomena are as shown in the deformation curves for both types of materials.

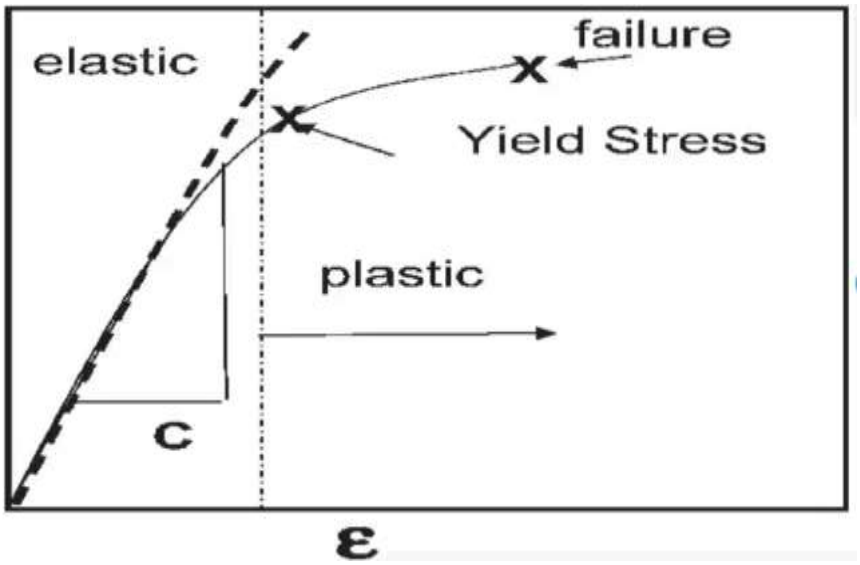


**Figure 2.1:** Stress-strain curves of elastic and plastic materials. (Iskhakov *et al.,* 2022)

Though varies with moisture content, most agro-materials (pods and kernels) exhibit elasticity as, has been revealed previously. Determination of rupture strength of agro-materials based on the loading pattern is basically done in two methods; the compressive loading test and dynamic impact test (Hassan, 2012). Other testing methods are tensile test, torsion test and flexural bending test (Hassan, 2012). The compressive test for rupture strength is carried out to ascertain the maximum stress a material can bear under compressive loading: thus, based on the manner and frequency of loading compressive test maybe dynamic or quasi-static. in the former method the load is applied in a continuous increasing manner until the material ruptures whilst in the later, load application is in a pulse-feed manner. compressive tests are performed on equipment known as universal testing machines. These machines are available in range of sizes and force capacity, spanning between 0.02 to 2000 kN. The universal machines are digitally equipped (with software and applications-specific platens and accessories such as extensometer) which depends on the type of material being tested since a universal machine can be adopted in the testing of various materials by

Simply changing its featuring (provided the force range of the machine encompasses that of the material). Software help to obtain readings to low decimals plus provides plot of the tests (Wang and Wang, 2019). Compressive strengths are usually reported in relationship to a specific technical standard. Aside from the universal testing machine a tensile testing machine could also be used for static compressive test. To achieve this, the gripping Jaws of the tensile apparatus are replaced by anvils and the cross head is made to move towards the stationary grip as reversed to the pulling away in the case of tensile test (Kar, 2018).

## 2.5 Decorticating Mechanisms

The supply and administration of any or blend of the forces required to remove the pods of pulses (decorticating) is achieved via the decorticating mechanism. The decorticating principle (impact, attrition, shear and compression) are applied by the decorticating members which take different shape, motion configuration and force application techniques. Irrespective of the shape, motion configuration and related motion orientation, the mechanism used to administer decorticating force are classified into the following six groups; spike tooth/pegs mechanism, rasp bar mechanism, bar beater mechanism, wire loop mechanism, cutter Blade or syndicator mechanism and hammer mill mechanism or beater type mechanism (Kabir and Fadele, 2019). These member types are also applicable for threshing and shelling unit operations. Selection of the member type depends solely on the decorticating principle or force type it is intended to provide.

### 2.5.1 The spike tooth/peg mechanism

The spike tooth mechanism as the name implies comprises of spikes or pegs of squares or rounded bars or even flat iron pieces attached to a bearing surface (depending on the shape

or working mechanism) by means of either welding or bolting (Fu *et al.*, 2018). The applicability of toothed spike members in decorticating and threshing of various pulses and crop type is achieved by varying the spikes configurations such as spike length, spike shape, (whether rounded, square or flat rods) inter-spike spacing and spike alignment. These variations also play a vital role in determining the efficiency of the mechanism in executing decortications and threshing. The spike toothed mechanism has been found to be the most efficient of all the member types (Fu *et al.*, 2018). it is commonly used with the cylindrical drum shape configuration. when used in this configuration, the spikes are attached around and over the peripheral of a cylindrical drum and it is best for impact force deployment (Kabir and Fadele, 2019). An enormous list of machines whose decorticating, shelling and threshing mechanism are based upon spike toothed members can be made. A multi-crop thresher designed and developed by Iqbal *et al*. (2018) had spike tooth cylindrical configuration in both of its threshing units. One of the drums had flat spikes around its peripheral while the other had rounded bars for threshing of different crops. The actual threshing operation is achieved via beating (impact) on the grains by the spikes against the concave. Performance evaluation carried out on the machine, interacted three factors; cylinder speed and feed rates at four stages each (that is, 700, 800 900 and 1000 rpm; 3.0, 4.0, 5.0 and 6.0 kg respectively) and moisture content at two stages of 9.21 % and 10.81 %. Best result as per efficiency was obtained at the lower moisture content of 9.21 % and speed of 1000 rpm

The spike tooth mechanisms also find usefulness in the decortication of Bambara nut. Design by Adedeji and Danladi (2015), the decorticating member pair are a spike tooth-cylindrical drum and a concave scream. Typical of the spike tooth mechanisms, the extraction of seeds from the pod is achieved by impact force supplied by the rotating spikes. The impact

interaction amongst the nut, the spikes and the concave force, opens the pod thereby releasing the seed which falls through the screen. Again, the performance results from the evaluation of this machine were reported to meet the objectives. A decorticator deficiency of 83 % was achieved. The cleaning efficiency and broken seed percentages were 78.9 % and 49 % respectively. Performance evaluation was conducted at only one level of moisture content of 15.0 % (W.B). The spike tooth decorticating member type has invariably shown a superior performance output for decorticating and threshing functionalities when compared with the other member types. Other designs based on this member type are a Bambara nut decorticator by Aririguzo (2017). In his words results obtained showed that the locally developed decorticator performed creditably well. The machine's threshing and cleaning efficiencies where 97.52 % and 97.88 % respectively with minimal total seed losses of 4.13 % at moisture content of 12.97 %. The black seed (*Nigella Sativa*) native to Egypt is found to be highly medicinal. A decorticating machine for *Nigella Sativa* has also been designed to rip-off pods via the spike tooth drum-concave screen mechanism. The machine was designed in Egypt by Afify *et al.* (2007). The spike drum-concave scream clearance was made un-uniform in decreasing order. A design modification which is meant to achieve spanned and stepwise decortication based on pod sizes. The variation in the clearance were at three levels along the Drum-concave circumference namely; the level closest to the inlet where decortication of the biggest pod size is done, the centre stage where the medium sized pods are decorticated and the level farthest from the inlet (that is close to the outlet) is where the smallest sized pods are shredded off their pods. The clearances for these three levels are 130, 100 and 70 mm respectively. At the initial half of the concave, three radial knives of stainless materials were placed at 100 mm intervals. This knives function to chop the elongated pulse into shorter sizes before furthering into the decorticating gap, thereby reducing the demanded pod

shattering impact, preventing accumulation and curling of long straws around the drum. The machine showed an awesome performance output (see figure 2.2 overleaf). Evaluation of the machine was done under three factors of drum speed (200 250 and 300 rpm), feed rate (of 600 700 800 and 900 kg/h) and moisture content (of 11.82, 13.63 15.72 and 17.61 % WB). Best results of stripping efficiency of 99.31 %, decorticating efficiency of 98.74 %, cleaning efficiency of 95.88 % and 2.63 % of seed losses were obtained under drum speed of 300 rpm feed rate of 600 kg/hr and capsule moisture content of 13.63 % (Afify *et al*. 2007)

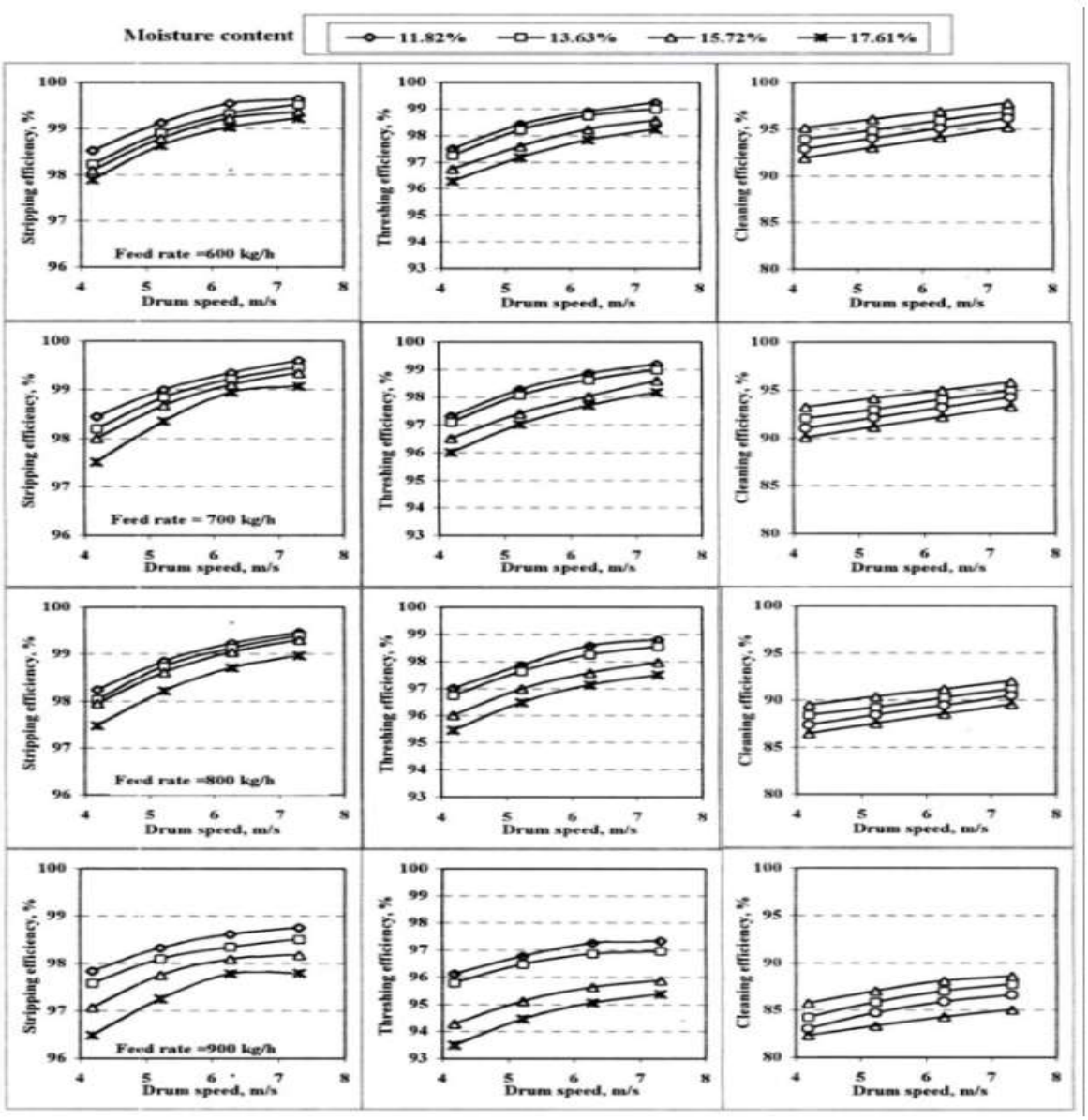


**Figures 2.2:** Effect of drum speed on stripping, threshing and cleaning efficiencies of black seed crop at different conditions of feed rates and seed moisture contents. (Afify *et al*. 2007)

The spike tooth decorticating member type has invariably shown a superior performance output for decorticating and threshing purposes when compared with other member types. A review focused on such comparison was performed by Kailashkumar (2019).

### 2.5.2 The rasp bar member type/mechanism

The term “rasp bar” is analogous to coarse or rough surfaces. It is defined by the lexica dictionary as a coarse file or similar metal tool for scraping filing or rubbing down object of metals, wood or other hard materials. Rasp bar decorticating members comprises thus of unsmooth somewhat projections which are obliquely oriented or randomly inclined on the surface of a metal bar which may be straight or acquitted or could just be a metal with a corrugated surface. Depending on the shape and motion configuration of the member, the rasp could be made directly on the surface of the member (as in a disc or plate member) or could be a couple of rasped bars mounted in a particular order (as in the case of a cylindrical member). The cylindrical-shaped members are the most commonly used - hence rasp bar mechanism is often defined in terms of the cylindrical drum members. It has been described as a cylinder having rasping elements arranged in spaced relation about the peripheral of a cylinder (Li *et al.*, 2020; Jun *et al.*, 2018). Rasps have been modified to take different shapes. They could be the conventional oblique point elevations or could be in the form of slight-narrow inclinations also known as ribs formed as a result of cutting narrow oblique grooves on the surface of the member (bar drum or plate).

Decortication and threshing by rasp members are achieved mainly by friction and compressive actions, rubbing or attrition with little impact Force (Jun *et al*., 2018; Yang and Park, 2019). In tangential axial-flow configuration the grains or pulses flow into the space between a rasped drum and a grating concave screen, the rubbing action sets-in as the drum rotate, sliding its coarse face or rasp over and against the content. The quality and degree of decortication depends on the thickness of stratum or ribbon of grain sitting per-time in the space between the drum and the concave which in turn is a function of the drum concave

clearance. Li *et al.* (2020) aired his observation as regards the effect of drum-concave clearance, stating that; though this clearance is proportional to the grain size, if too thick a ribbon of content is being threshed per time, all the grain pods will not be raked by the rasp and hence a portion of it will be un-threshed, conversely if too thin a ribbon is allowed at a close clearance, a too thorough threshing action results with injuries to a large portion of the grain. Conditioning of the operational state of this mechanism for a quality and efficient output entails configuration to provide values of the three threshing action appropriate to a particular moisture content (yang and Park, 2019). It is as a result of this ample relative configuration requirement that the rasp bar is considered one of the most know-how demanding mechanisms (Li *et al.,* 2020), as a slight shift from the ideal setting reflect on the quality of the grain output. To expand the range for good performance of the rasp mechanism, Li *et al.* (2020) discovered that sheathing the upper surface of the concave grate with an elastic material (for instance, rubber) permit some greater latitude (due to the yield afforded by rubber) than between two metal surfaces and also reduces the purity of cutting and abrading actions of the rasp-since the Pulses drag over the Rubber surface instead of against the metal surface.

The rasp mechanism has been reportedly used to decorticate several pulse crops. An axial-flow thresher for oilseed crops developed by Bansal and Kumar (2009) used the ribbed helical rasp mechanism to thresh the grain within the clearance between its drum and the concave. The grain is threshed as the helical rib raps drag against the grated concave along the axial direction by the action of rubbing. An evaluation of the machine to determine the effects of moisture content, cylinder speed and cylinder-concave clearance) on the quality of thresh of green grain, black grain, soya bean, chickpea and sunflower, show that; best thresh

efficiencies of 99.43, 99.60, 99.40, 90 9.20 and 98.90 % were achieved for the respective crops at the highest set of cylinders speed (S3) and the lowest set of moisture content (M1) and clearance (C1). The test condition is as shown on table below.

**Table 2.1:** Test Condition for Performance Evaluation of an Axial Flow Thresher

| Name of crop | | Greengram | Blackgram | Soyabean | Chickpea | Sunflower |
|---|---|---|---|---|---|---|
| Variety of crop | | K-851 | T-9 | PK-416 | C-235 | CmSH-91A |
| Moisture content of seed, % | $M_1$ | 10.0 | 10.3 | 10.0 | 7.8 | 15.5 |
| | $M_2$ | 12.0 | 11.4 | 12.0 | 10.5 | 23.0 |
| | $M_3$ | 14.0 | 13.4 | 14.0 | 12.2 | 31.5 |
| Cylinder speed, m/s(rpm) | $S_1$ | 9.5(350) | 9.5(350) | 8.2(300) | 8.2(300) | 9.5(350) |
| | $S_2$ | 12.2(450) | 12.2(450) | 11.0(400) | 11.0(400) | 12.2(450) |
| | $S_3$ | 17.6(650) | 17.6(650) | 14.7(540) | 14.7(540) | 17.6(650) |
| Concave clearance, mm | $C_1$ | 5 | 5 | 5 | 5 | 5 |
| | $C_2$ | 10 | 10 | 10 | 10 | 10 |
| | $C_3$ | 15 | 15 | 15 | 15 | 15 |

(Bansal and Kumar 2009)

Conversely the minimum seed damage of 1.10, 1.48, 0.15, 0.27 and 0.225 % (corresponding to the initial order of crops) were recorded for the opposite conditions that is X1, M3 and C3.

The results reflect that, seed damage has a direct proportion with drum-concave clearance and with drum speed too and vice versa.

The Rasp bar mechanism has been shown to be fondly used in ground nut decorticators as evident by the works by Wesley *et al.* (2010); Maduako *et al.* (2006) and Mani *et al.,* (2020). The rasp bar mechanism has also been used in decorticating order food crops such as locust bean (Okunola *et al.,* 2019), melon (Osasumwen *et al.,* 2020).

### 2.5.3 Hammer beater (mill) Mechanism

A hammer beater mechanism consists of a series or gang of hammers (usually four or more) hinged on a central shaft and enclosed within a rigid metal case (Bochat, 2015). Hammer beaters decorticate by the principle of impact, provided by the repeated striking actions of the gang of loosely hinged hammers on a rotating shaft. The gang of hammers is made of rectangular pieces of hardened steel. Customary with all the drum-screen configurations, a hammer beater is fitted with a concave grating screen which provides the support for pulses so as to be impacted against by the gang of hammers. The screen also serves to filter the decorticated kernels from the un-decorticated ones. At the deepest bass of the screen little action of attrition and shearing is administered by this mechanism (Bochat, 2015).

### 2.5.4 The bar beater mechanism

The bar Beater in the context of a cylindrical drum-concave mechanism comprises of two discs (which forms the both ends of a cylinder) connected by straight metal plates or woods (the beaters) spaced at regular intervals along or around the peripheral of the discs. The bar beaters are of various kinds depending on the shape of the material connecting the disc (beaters). Based on these criteria, the rod bar beater, flat bar beater, angles bar beater and

square bar beater have been encountered as beating mechanism in crop decortication, shelling, threshing and dehusking (Murtala, 2018; Fu *et al.*, 2018). Decortication shelling and threshing via this mechanism is by repeated impact, discharged by the beating action of the bars as the drum rotates. The mechanism also provides little of rubbing actions. Over the years the bar beater has undergone several modifications in an attempt to improve on the performance of the mechanism. One of such modification is the covering of the surface of the beater bar structure with a layer of a high grade synthetic cold rubber which is bounded to the flat metal bar. According to the leading patentee (Fu *et al.*, 2018) of this modification the rubber serves double purpose of cushioning the effect of shock transmittable to the machine from the decorticating chamber and also to provide a flexible expandable cylinder-concave clearance hence accommodating perfectly, a range of grain influx (in a perfectly fitting space). Other modifications are described by Fu *et al.* (2018) in his descriptive publication of the bar beater. The flat bar beater has been extensively used for groundnut shelling. Conversely the angle bar beater is found more useful in the extraction of banana fibres, though it is also used in the decortication of pulses.

### 2.5.5 Wire loop type cylinder

In this type of threshing drum there is a hollow cylinder over which a number of wooden or metal steel plates are filtered. On these plates, a number of wire loops are fixed for threshing purposes. This type of cylinder is common in the manually operated Paddy thresher. Holding the bundle against the loop of revolving cylinder does threshing of Paddy crops (Fu *et al*., 2018).

### 2.5.6 Chaff cutter/syndicated type

This is essentially an adoption of chaff cutter for threshing. The crop is fed as done in the case of chaff cutter. After passing through a set of rollers, crop is cut into pieces. Varying the set of gears can vary the size. 3 to 4 serrated blades are fastened to the radial arm of the flywheel. Threshing is done mainly due to cutting helped by Rubbing and impact. The main advantage of the syndicator thresher is that, it can handle crops with higher moisture content. However, chopping knives needs to be sharpened every three to five hours of operation. the machine is more prone to accidents due to positive field rollers (Fu *et al*., 2018).

## 2.6 Decorticating Principles

The shredding of pods and the subsequent removal of pits from same requires the systematic application of force termed force principles. This systematic application of force results in a one or more of the various mechanisms that results in material failure (In this case, pods failure) and hence yielding decortications of pulses. The main principles of decortications employed by processing machines for decorticating are as discussed below.

### 2.6.1 Impact

Wang *et al.* (2011) described a simple model of a body as an assembly of molecules held in a clustered unit by bonds. The cluster of bonds cooperatively operates synergistically to form a relatively strong molecule cluster. These bonds help the body to resist forces tending to shatter the material by absorbing the energy induced by the force in form of elastic strain energy. Thus, when the stored energy accumulates beyond or exceeds (at a time) the critical value that can be borne by the material, rupture set in. Hu *et al.* (2015) stated that the initiation of microscopic material failure is associated with the collective disruption of atomic bonds which is derived by the potential energy stored in the atomic bonds. Microscopic material

failure sets in when the elastic strain energy density accumulate beyond a critical value known as the rupture energy of the material. Beyond this value the atoms and molecules parking are disrupted and visible deformation of the material could be observed (Hu *et al.,* 2015; Davies *et al.,* 2019). Grain rupturing may be explained to be due to the need to release excess internal energy (the elastic strain energy) as during rupturing, the stored energy is radiated in the form of brief high-intensity pulse of pressure energy into the environment (Davies *et al*., 2019).

In some materials a dissipative function which is due to material inelastic deformation, damage and other possible intrinsic dissipative mechanism in a mechanical system (mechanical energy state) leads to the reduction of material strength and ultimately resulting in the rupturing of the material. In this case it is said that; material failure is dominantly due to energy dissipation whilst in other materials the intrinsic dissipation mechanism or inelastic deformation is negligible during the deformation process before failure. In this case no gradual losing of strength is observed, the failure is due to elastic strain energy at a time, exceeding the initial critical material bond strength. The material talked about earlier are said to exhibit elasticity (elastic materials), why the later scenario describes brittle materials (Hu *et al.,* 2015). Material disintegration could be at the sub atomic level atomic-level molecular level or simply fragmentation of a whole in which case clusters of molecules fall off the whole. Disintegration at below the molecular level is initiated by bombardment of particles ejected or projected buy an instrument known as particle Photon accelerator. Whist, fragmentation can be due to application of external force as in impact by a moving object. During an impact the kinetic energy of the incident mass is transferred to the impacted body in accordance with the law of conservation of momentum. A portion of this kinetic energy is

absorbed and stored within the bounds of the material as the aforementioned elastic strain energy, which is responsible for material fracture at some values beyond the critical one for such a material. The rupture resistance of a material gives the numerical critical value of stored strength energy beyond which fracture sets-in for that material.

Decortication by the principle of impact is based on the idea of stored strain energy as discussed below. In designing for an impact-based decorticator irrespective of the configuration used, the members are designed with provision for a means to administer impact. Typically, the spike-tooth and hammer member types are synonymous to the impact decorticating principle (Jun *et al.*, 2018). The general design model often includes a space known as the clearance (usually housed between the decorticating members), a casing, a chute or a hopper, and an effluent opening. The chute serves to receive the pulse into the space where they are exposed to repeated striking or beating by the moving tooth or arms of the dynamic members: in the process, transferring their kinetic energies to the pods and hence the impact and rupturing process explained earlier follows. Further impact with the casing of the section and amongst pulses also aid further decortication. The speed of the dynamic member, amongst other factors, is a critical factor upon which the quality of decortication leans, since energy transfer is a direct function of this speed.

### 2.6.2 Attrition (Rubbing)

Attrition commonly known as wear is the damaging, gradual removal or deformation of material at solid surfaces due to mechanical or chemical processes. Wear in terms of mechanical processes is analogous to friction as it usually sequels friction in the context of materials rubbing. Tribology: a study field dedicated just the study of wear and related processes seeks to bring to light all aspects of wear, ranging from types and respective

mechanisms, stages etc. at the various levels of sub atomic, atomic, nano-sizes and material sizes. The complexity of the process and nature of wear has been evident in the lack of understanding of its mechanisms. In the nano-scale especially, the mechanism of both friction and wear are unclear and often elusive (Kim *et al*., 2012). Several mechanisms have been hypothesized. One of such hypothesis states that; wear on the nano-scale is mainly understood through two processes of: plastic deformation (that is the nano recoverable change in shape of material without it breaking) and surface/near-surface material fracture (breaking and detachment of particles of a material) (Akchurin *et al.*, 2017). The process: atomic attrition is yet another major hypothesized mechanism of wear at the atomic level. This hypothesis is of the opinion that; wear is due to the transfer of atoms from one surface to another via a series of bond breaking and bond forming chemical reactions of contacting surfaces. This hypothesis is claimed to have been validated by investigations performed under the atomic force microscope (Kim *et al.*, 2012). Tabor (2000) sequel to their investigations deduced that; friction although independent of the macroscopic contact area is in fact, proportional to the true contact area. The true contact area they explained in terms of surface asperity. According to them, during surface contact the microscopic irregularities push and fit into one another (forming the true contact area) subsequently forming strong bonds at this contact points, whose strengths are sufficient enough that, continuous sliding over each surface results in continual tearing away of tiny Fragments of the materials due to accumulated strain energy.

Based on the tribo-system and mechanisms, wear is classified into the following types; adhesive wear, abrasive wear, surface fatigue, fretting wear, erosive wear, corrosion and

oxidation wear. Others are cavitation, diffusive wear and impact wear. Each of the wear type is caused by one or a multiple blend of these mechanisms (Varenberg, 2013;).

### 2.6.3 Shear

material shell is due to shear stress (which in turn is induced by shear force) is defined to be the force tending to cause deformation of a material by slippage along the plane or planes parallel to the imposed stressed (Khurmi and Gupta, 2005). Khurmi and Gupta explained that; shear stress is induced on a body when it is subjected to two equal and opposite forces acting tangentially across the resisting section, as a result of which the body tends to share of the section. Unlike normal stress which arises from the force vector components which acts perpendicular to the cross-sectional area of the material it acts upon, the force vector components resulting in shear stress acts parallel to the materials cross-section. The mechanisms of material deformation via sharing have been widely studied and reported at various scales or degree.

As mentioned earlier, shear deformation is due to shear stress-when these stresses are induced on a material, the relative position of the atoms changes while storing strain energy. When local deformation exceeds certain limit, the bonding forces between the atoms are destroyed, causing cracks to occur. This is the basic mechanism that initiates any type of deformation. The means of extension and propagation of a crack which is a function of the type of stress determines the deformation type that succeeds the crack (Guijun and Soo-jin, 2019). In material shear deformation, the applied force (shear stress) is directed to a particular plane (acting against a non-parallel counter Force in the opposite direction) as a result, change in relative position of atoms/molecules and subsequent breaking of the inter-atomic/ molecular bonding force is localized just too the stressed plane (the plane parallel to the stressed one

and sitting in-between the stressed zones), thereby resulting in crystal dislocation along this plane (Guijun and Soo-Jin, 2019). Application of further shear stress posterior to the dislocation results in the movement of dislocations, but only if they applied shear stress is large enough to overcome the resistance to dislocation motion. This motion of dislocation is along the shear plane and is known as slip (which is the actual description of plastic shear deformation) (Yang and Park, 2019). Slip occurs when the shear stress applied to the slip direction on the slip surface reaches a certain critical value known as the “critical resolved shear stress" (Yang and Park, 2019). Schmidt *et al.* (1979) proposed a model that predicts the value of shear stress along the slip direction on the slip plane that is critical to initiating or creating crystal dislocation motion as $\tau_c = \delta \cos\varphi \cos\lambda$

Where; $\tau_c$ is the critical resolved shear stress, $\delta$ is the tensile stress, $\varphi$ is the angle between the slip direction and the direction of the applied force, $\lambda$ is the angle between the normal of the slip plane and the direction of the applied force and $\cos\varphi \cos\lambda$ is the Schmidt factor (M)

### 2.6.4 Compressive force

The compressive strength of a material is the capacity of the material to withstand loads tending to reduce size (compress) as opposed to tensile strength which withstands loads tending to elongate (extend). The ultimate compressive strength of a material is that value of uniaxial compressive stress beyond which the material fails completely (plastically) (Khurmi and Gupta, 2004). Compressive Force when applied on a body tends to shrink or reduce the size of the material in a direction parallel to the compressive force. At the atomic level, during compression, the molecules or atoms under and parallel to the load are forced together (close packing) as a result, forces arise throughout the entire material which opposes both tension and compression as atoms of the material seek to find an equilibrium position. This is the

basis of mechanism behind rupture or failure under compressive Force (Fischer and Anthony, 2007). Material failure under compressive Force has been explained by various failure mechanisms. variations in the mechanism of failure has been largely attributed to a number of factors such as; means and condition of force application, direction of force application, structural composition of the material, pre-existing faults or flaws on the material (initial misalignment of the load-bearing tows and intersection of the load-bearing tows and through thick reinforcing tows) (Pinson *et al*., 1991) compressive failure mechanisms include Buckling, kink band formation (kinking), shear crippling etc. Material failure under compressive loading may be due to one or more of the mechanisms working harmoniously (Lee, 2014).

The mechanism of failure of pulses on the accord of compressive force which hence aids decortication depends on the nature of the pulse and its condition as at the time of decortication and the force application condition. For pods with approximately brittle characterization, rupturing mechanism under compressive Force could be by axial splitting, shear fracture, or ductile failure; depending on the level of constraints in the direction perpendicular to that of the compressive force (confining pressure). The above mechanisms ensue respectively with zero confinement, moderate confinement and high confinement (Fischer and Anthony, 2007). Not much work has been done to investigate the mechanisms (at the atomic and nano-scale) of compressive failure in agro materials hence, only a little could be discussed to this regard. In the decortication of pods by a decorticating machine, compression is mostly used along with other principles of decortication. It is often a secondary principal, aiding a final touch on the extraction of kernels from their pods plus, push them through the grating screen.

Without an exception the compressive principle (at least a little of its) is administered at the lowest point of the drum concave mechanism (Jun *et al*., 2018). One decorticating mechanism whose decorticating principle is primarily based on compressive force is; the twin-roll drum, commonly used for the dehulling of sunflower and cotton seeds.

Another decorticating mechanism which has been found viable in the administration of compressive force is the reciprocating piston. This mechanism combines impact and compressive Force to break and extract kernels from their pods. This mechanism has been used in the design and fabrication of an apricot (*Prunus armeniaca L.*) and pit decorticator (Kate *et al*., 2018). A typical model of a compressive mechanism of decorticating is as shown below.

## 2.7 Decorticating Theories

The mechanisms (members) via which decortication is achieved are classified based on varying criteria. Member pair structure, mount orientation, members relative motion configuration, feed flow direction relative to member are some of the criteria upon which decorticating members are classified.

### 2.7.1 Based on member pair structure

According to both literatures and perceptions, the classes of decorticating members based on pair structure are; the drum-concave pair, the twin-drum (double roll-drums), the double disc or plate members and the centrifugal or arms-case members (Kabir and Fedele, 2018).

#### *2.7.1.1 The Drum concave pair*

as the name implies, this shilling pair comprises of a cylindrical drum whose peripheral is equipped with the decorticating mechanism (for example, spikes, rasps etc.) and a concave

grating screen whose diameter is a bit larger than the cylinder but oriented such that its circumferential axis conforms with that of the cylinder. the pair are both encased in the decorticating section and configured such that the concave sits just beneath the cylinder, forming a clearance within which pulses are held and are proffered the interactive decorticating mechanisms of the pair. the concave is grated and perforated as in a screen such that, only particles of equal or lesser sizes as the decorticated kernels can pass through, hence, ensuring that only decorticated seeds leave the section. The intensity of decortication depends on such factors as drum speed, drum concave clearance and the degree of corrugation of the grate of the concave (Kabir and Fedele, 2018; Kailashkumar, 2019).

#### *2.7.1.2 The twin-drum (double roller drum) pair*

Typically comprising of two identical drums; this decorticating technology is prominent for its proficiency in delivering compressive stress. it is characterized by a system of mating drum pair, with somewhat corrugated or toothed, or in most cases, helically ribbed surfaces that aid the hurling of pods off kernels in a progressive fashion as the pulses are fed-in (Zhang *et al*., 2014). The operating principle of this pair type employs the coactions of two identical drums axled in a parallel orientation. The clearance between the drums is adjustable. Administration of compressive force is at the drum-drum interface (the clearance between the peripherals of the drums). The configuration of the machine is such that, as the drum(s) rotate(s) they pick up pulses that falls on them from the chute (at the upper part), rolling them along into the drum-drum interface region (the plane along which the peripherals of a drums are closes). This space or clearance is made to be slightly narrower than the diameter of the pulse (at its minimum point of separation) yet slightly larger than the kernel. the motion of the drums together with some sort of mechanisms on the surface of the drum helps to push

and force the Pulse through the Narrow clearance where they are compressed and hence decorticated (Lisa *et al.,* 2013). Variations and modifications of this mechanism could be due to the nature of the surface of the drum, the orientation of the drums, the motion of the drums etc.

The degree of the decortication here is a function of the relative motion of the drum(s), the nature of the surfaces of the drums, the rotating speed(s) of the drum(s) and the clearance between the drums.

#### *2.7.1.3 The double disc (or plates) pair*

the disc type decorticator comprises of a pair of circular plates whose surfaces are corrugated usually serrated. The corrugated faces of the plates form the decorticating interface or bounds. The usual assembly comprises of a hollow cylindrical casing within which the pair of relatively rotatable juxtaposed plates with coacting radiating grooved or other forms of corrugated surfaced are oppositely faced. one of the plate is hollowed at its centre to conform to the diameter of a cylindrical casing and is attached to one end of the cylinder (with the corrugated face pointed away from the length of a cylinder) as the stationary pair, and the second plate (the rotary plate) is either attached to a driving shaft from the opposite side of the stationary one or to a helical shaft which runs from the other end of the cylinder through its hollow and extending outwards beyond the stationary plate (such that the rotary plate is attached parallel to the stationary one with the decorticating faces facing each other). The helical shaft serves the purpose of transmitting drive to the rotating plate and conveying pulses into the decorticating space in the horizontal orientation, or to aid controlled pulse feeding by gravity in the vertical orientation. Pulse feed is perpendicular to the orbit of disc rotation through the hollow of the stationary plate into the decorticating space. When fed into

the space, seeds, by virtue of the relative rotation of the plate and the coactions of the corrugated faces tend to assume a position of alignment with the grooves and the approach while resting in opposed grooves at a position normal to the plate. the adjustable plates clearance plus the depth of the opposed grooves is such that the pressure is applied to the edges of the pulses as the normal position is approached, whereby the seed shell is cracked or shattered or in modified cases which permits for handling of wetted seeds, if the pulses are suitably wetted in advance, it is opened at the edge seam to permit the pit to be squeezed out of the shell by further abrasion and Pressure exerted by the coacting rubber faces. Secondary customization to enhance efficient decortication may include; a mechanism to recollect and return un-decorticated pulses, altering the grooving depth and patterns on the plates, optimizing the plate-plate clearance and the rotating speed of the plates (Nishad, 2022)

#### *2.7.1.4 The vane centrifugal member pair*

This theory comprises of fixed arms extending from a central axis (the rotating shaft) radially at regular spacing that rotates within a casing whose curvature arms to the orbit of rotation of the arms. This pair type is most useful in processing operations that requires impact force. The impact is provided by the coacting action of the rotation of the arms and the internal surface of the casing. One common example of this member type is the hammer beater type (Fu *et al.,* 2018).

# CHAPTER THREE

## 3.0 MATERIALS AND METHODS

### 3.1 Material Selection

Material selection entails deciding on the most appropriate materials to be used for the project (the fabrication of the machine), considering all factors that together tend to affect the design, fabrication, performance, viability, ownership and maintenance of the machine. The factors thus considered whilst selecting materials to the above regards are embodied into economic factors and engineering factors (material properties).

Economic factors according to Saravacos *et al.* (2012) entail;

- The cost of the materials
- Availability of the material

Engineering factors entails the physio-mechanical properties of materials which according to Saravacos *et al.* (2012) includes

- Machineability of the material
- Durability/strength of the material
- Corrosion resistance of the material
- Reliability

### 3.2 Materials used

For the project, the materials used comprises of those used for the fabrication of the machine and the bio material used for the testing of the machine.

### 3.2.1 Biomaterial

The biomaterial used for the testing of the machine is Bambara nut of the variety Local-1

### 3.2.2 Materials used for machine construction

Based on the above factors, the materials used for the construction of the machine are;

i. Galvanized metal sheet (2 mm and 6 mm thickness)
ii. Angle iron ($50 \times 50 \times 60$) mm
iii. Steel shaft of grade C-8 ($\emptyset = 30\ mm$)
iv. Mild steel sheet (2 mm thickness)
v. Cast iron ($\emptyset = 5\ mm$)
vi. Pulleys ($\emptyset = 60\ mm, 300\ mm\ and\ 325\ mm$)
vii. V-belt (A-type)
viii. Bolts and nuts (17 mm and 13 mm)
ix. bearings

## 3.3 Design Considerations

The aspects considered for design are economic performance and safety.

The performance aspects encompassed in the design framework includes;

- Efficiency
- Effectiveness
- Power and drive
- Throughput capacity

For the safe functioning of the machine, the design was done bearing in mind;

- Machine stability
- Operability
- Operator's/environmental safety

## 3.4 Design Criteria/General Design Analysis

A general design (basics) for the functionality and performance of the machine is primarily dependent on the properties of the pulses Negedu *et al.* (2018). The aspects considered for the design are: dimensions/sizes of machine parts, conformity of adjoining parts, fitting of drive system, technicalities of functions, appropriation of inputs for desired response, power requirement of the machine, and conformity of the units/assembly strength to all interfering factors (that is, safety). The theoretical general design is as shown below. Note that, for adjustable designs, specific design for a desired output or performance (which is crop dependent) is obtained by simply substituting the desired variables into the general design formula.

### 3.4.1 Determination of hopper height

Design assumptions:

The hopper is a conical frustum, opened at both ends. The larger upper end forms the feeding interface, while the lower end connects to the inlet pipe.

The hopper is designed with a capacity so as to allow for smooth pulse in feed thus avoiding choke and more importantly, it is designed such that, the maximum resultant weight (vertical downward weight) at the base do not exceed the bearing capacity of the flow regulator at the base of the hopper, that is $\sum \rho_p \rho_p g \approx \rho_p v_h g \leq bearing\ strength\ of\ regulator$

The angle of slant of the walls of the hopper (reference to the horizontal plane) is selected such that, it is slightly greater than the angle of repose of the pulse, that is $\theta \geq \alpha$. $\theta$ on the other hand, is kept at minimal, such that the hopper sides are slanted enough to provide maximum support for content.

Thus, considering the above assumptions, the hopper capacity is determined based on the density relation, to determine the volume required to accommodate the desired mass of pod, and based on the obtained volume, the height of the hopper was determined based on the formula for a truncated cone (having assumed the lower and upper openings);

$$V_h = \frac{1}{3}\pi h(r_1^2 + r_1 r_2 + r_2^2) \tag{3.1}$$

Therefore;

$$h = 3V_h/(\pi(r_1^2 + r_1 r_2 + r_2^2)) \tag{3.2}$$

Where;

$V_h$ is the volume of the hopper;

$h$ is height of the conical frustum;

$r_1$ and $r_2$ are the radius of the upper (larger) opening and of the lower (smaller) opening of the hopper respectively.

### 3.4.2 Determination of the height of delivery channel

Criteria/designs: The base and the top diameters (internal) of the delivery pipe are equal to the circular cuts on the center of the upper stationary decorticating disc and on the plate that covers the base of the hopper respectively. This is so as to allow for the perfect conformity

of hopper-pipe and pipe-decorticating section, and hence smooth transient of pulses from hopper through pipe into the decorticating section. Thus;

$$D_{pi} = D_{ds} = D_{ph} \tag{3.3}$$

The pipe's height is such that, the maximum acquired kinetic energy (due to height of fall) with which the pod hits the decorticating section is not beyond the fracture energy of the kernel, thus preventing cracking or fracture damage to the kernel. That is, acquired kinetic energy of pod ≤ fracture energy of kernel. Thus;

$$^1/_2\, mv^2 \leq E_{fk} \tag{3.4}$$

But acquired kinetic energy = potential energy at state of rest, which is in this case, the height of the pipe $H_p$ plus the vertical distance between the lower end of the pipe and the dispersing plate on which the pods fall on ($h_v$), in the decorticating section. Thus;

$$^1/_2\, mv^2 = mg\left(H_p + h_v\right) \tag{3.5}$$

Substituting equation (3.5) into equation (3.4) gives;

$$mg\left(H_p + h_v\right) \leq E_{fk} \tag{3.6}$$

Interpolating to obtain $H_p$ yields;

$$H_p \leq \frac{E_{fk}}{mg} - h_v \tag{3.7}$$

Where; $H_p$ is the height of the delivery channel pipe;

$E_{fk}$is the fracture energy ($J$);

$h_v$ is the vertical distance between the lower end of the pipe and the dispersing plate on which the pods fall on (m);

$m$ is the mass of the pod (kg) and $g$ is acceleration due to gravity;

$h_{v.max}$ the maximum possible clearance between the plates $=$ the case height $-$ $2$(thickness of plates $+$ thickness of case sheet)

The delivery channel thus, has to be set to a value less than $H_p$ as in equation 3.7

### 3.4.3 Design of the decorticating plates

Design criteria: the decorticating member is a pair of concentric facing disc, whose internal surfaces are equipped with the decorticating spikes or corrugation (depending on the intended principle). For the evaluation purpose of this machine, the discs are equipped with spikes. The spikes are mounted on both the facing surfaces of the plates such that, the spikes interloop or coact smoothly as the dynamic disc rotates. The spikes are mounted radially, forming 2 spike fronts on the rotary disc, and 1 front on the stationary disc respectively. Inter front spacing ($2x_f$) on the discs is only slightly greater than twice the largest principal diameter of the pit ($2D_{mp}$) it is meant to decorticate, such that, when interloped with the opposite pair, the looped spacing ($x_f$) is only slightly greater than the largest diameter of the pit ($D_{mp}$). Also, the inter spike spacing on the furthest front on the rotary disc serves as the screen, thus, this spacing is such that only decorticated pods can pass through it and hence out of the decorticating section into the conveyor slid pan.

### 3.4.4 Design of the blower

#### *3.4.4.1 Determination of air discharge speed and discharge rate*

Assumption: the blower is meant to blow off lighter particles (chaff) from the pit or kernel, hence it is designed such that, the dynamic pressure of its air stream (as a function of its flow rate) is same as the component of the force per unit area in the direction of air flow ($p_h/\cos\emptyset$) attained by the pit, due to it kinetic energy in falling through the distance $'h'$ to the point of air column.

The dynamic pressure of a fluid is given by Bernoulli's equation, as;

$$p_d = {}^1\!/_2\,\rho v^2 \tag{3.8}$$

And the pressure gained by a body in falling through a height $'h'$ is given by;

$$p_h = \frac{k.E}{A.h} \tag{3.8}$$

$k.E$ is the kinetic energy of the body in falling through $'h'$, $A$ is the projected area of the body, and $h$ is the height through which the body has fallen. Therefore, by our design assumption, we have that;

$${}^1\!/_2\,\rho_a v_a^2 = \frac{k.E_p}{A_p.h\cos\emptyset} \tag{3.9}$$

$$\text{But } k.E_p = {}^1\!/_2\,m_p v_p^2 \tag{3.10}$$

Substituting (3.10) into (3.9) yields;

$${}^1\!/_2\,\rho_a v_a^2 = \frac{m_p v_p^2}{2A_p.h\cos\emptyset} \tag{3.11}$$

But the velocity of the pit $v_p$ in falling through $h$ is obtained from the equation of motion as;

$$v_p = \sqrt{2gh} \tag{3.12}$$

Thus, putting (3.12) in (3.11) we obtain;

$$^1/_2\, \rho_a v_a^2 = \frac{m_p.\left(\sqrt{2gh}\right)^2}{2A_p.h\cos\emptyset} \tag{3.13}$$

By interpolating the above to obtain $v$, we have that;

$$v_a = \sqrt{\frac{2m_p g}{\rho_a A_p.\cos\emptyset}} \tag{3.14}$$

From the relation, $discharge\ rate\ (Q) = flow\ velocity\ (v) \times discharge\ area(A)$, we obtain the required air discharge rate that blows chaff in the direction of the air as;

$$Q = \sqrt{\frac{2m_p g}{\rho_a A_p.\cos\emptyset}} \times A_d = v_a \times A_d \tag{3.15}$$

The parameters are as defined below

$v_a$ is the velocity of air flow at the outlet in $ms^{-1}$

$m_p$ is the mass of the pit (kernel);

$\rho_a$ is the density of air at standard temperature and pressure (S.T.P);

$A_p$ is the maximum projectable area of the pit;

$\emptyset$ is the angle the fan outlet protrusion makes with the vertical axis;

$A_d$ is the cross-sectional area of the discharge outlet (volute opening);

$g$ is acceleration due to gravity

### *3.4.4.2 Determination of the speed (rpm) of the blower shaft, based on the discharge rate*

By applying the continuity equation, we know that the flow rate at the outlet $(Q_{out}) =$ the flow rate at the inlet $Q_{in}$

That is;

$$Q_{out} = Q_{in} \tag{3.16}$$

But, $Q_{in}$ is given by Oyelami *et al.*, *(2008*) as,

$$Q_{in} = 2\pi r_i b_i V_{ri} \tag{3.17}$$

Where; $r_i$ is the volute's inside radius;

$b_i$is the fan vane width at the suction eye;

$V_{ri}$, the radial component of the air absolute velocity is the same as the inlet velocity ($V_{in}$), since there are no vane guard.

From equation 48, we obtain $V_{ri} = V_{in}$ as;

$$V_{in} = \frac{Q_{in}}{2\pi r_i b_i} \tag{3.17}$$

Thus,

The relationship between the air inlet velocity ($V_{in}$) and the linear velocity of the vane at the volute inside radius $V_{v.in}$ is given by Oyelami *et al*. (2008) as;

$$V_{in} = V_{v.in} \tan \beta_i \tag{3.18}$$

Where; $\beta_i$ is the inlet vane angle

From equation (3.18), it follows hence that; $V_{v.in} = {V_{in}}/{\tan \beta_i}$

The RPM equivalent of this velocity which is same as the blower shaft/pulley speed $(N_f)$ is given by $N_f = 60V_{v.in}/2\pi\, r_i$

Based on the design assumption, this is the vane speed that yields a flow rate just enough to lift and blow the kernel or pit itself. Thus, the actual speed is set below this value so as to avoid lifting and consequently, blowing off of the actual kernel or pit.

The fan speed, is therefore set to 1100 rpm.

### 3.4.5 Design of drive mechanisms (belts pulleys and bearings) of the decorticating section

#### *3.4.5.1 Fitting the drive speeds and the size of the pulleys*

To fit the speeds of the driven pulleys, the velocity ratio relationship by Khurmi and Gupta (2005) is used. By the relation we have that;

$$N_1 D_1 = N_2 D_2 \tag{3.19}$$

Where;

$N_1$ the speed of the motor

$D_1$ the diameter of the motor pulley

$N_2$ the speed of the decorticating pulley

$D_2$ the diameter of the decorticating pulley

from equation (3.19), we have that; $D_2 = N_1 D_1 / N_2$

### *3.4.5.2 Determination of the length of the belt*

The length of an open belt running over two pulleys is given in terms of pulley diameter by the relation by Khurmi and Gupta (2004);

$$L = \frac{\pi}{2}(D_1 + D_2) + 2x + \frac{(D_1 - D_2)^2}{4x} \tag{3.20}$$

Note that, the center distance ($x = 11.75inches = 298.45mm$) is estimated from design configuration.

### *3.4.5.3 Determination of angle of contact ($\theta$) and angle of wrap ($\alpha$)*

The angle of contact also known as the angle of lap of belt on the smaller pulley is a very important parameter for successful transmission of drive when two pulleys of different diameters are used for a drive. This angle of contact is given by Khurmi and Gupta (2005) as;

$$\theta = (180^{\circ} - 2\alpha)\frac{\pi}{180} rad \tag{3.21}$$

The angle of wrap $\alpha$ is given by;

$$sin\alpha = D_2 - D_1/2x \tag{3.22}$$

### *3.4.5.4 Determination of driving tensions in the belt*

The tensions in both the tight ($T_1$) and slack ($T_2$) sides of the belt are key, since they are determinant factors of both the power transmitted by the belt and the torsional moments on shafts. The tension ($T_1$) of the tight side of the belt is dependent on the belt's maximum tension ($T_u$) and centrifugal tension ($T_c$,) by the relation

$$T_u = T_1 + T_c \tag{3.23}$$

$T_c$ is caused by centrifugal force, and is given by;

$$T_c = m_{b/l}.v_b^2 \tag{3.24}$$

Where; $T_c$ is centrifugal tension;

$v_b$ is the velocity of the belt;

$m_{b/l}$ is mass of belt per unit length

$$m_{b/l} = cross\ sectioal\ arae\ of\ belt\ \times unit\ lenght \times density\ of\ belt\ material$$

The tension on the tight side of the belt $T_1$ from equation (3.23) is given as $T_1 = T_u - T_c$

$T_u$, the maximum tension in the belt is given as;

$$T_u = maximum\ permissibe\ belt\ tensile\ stress(\sigma) \times belt\ crosssectional\ area(A)$$

According to Khurmi and Gupta (2004), the tension on the slack side $T_2$ is obtained from the equations of "ratio of driving tension" given for v-belt in equations 3.25 below as;

$$2.3log\left[\frac{T_1}{T_2}\right] = \mu.\theta cosec\beta \tag{3.25}$$

Where; $\mu$ is coefficient of friction = 0.3 for rubber-cast iron contact (dry)

$\theta$ is the angle of contact at the smaller pulley in radian;

$\beta$ is half the groove angle of the pulley;

Thus, by interpolating to make $T_2$ the tension in the slack side of the belt the subject of the formula of equation 3.25 yields

$$T_2 = \frac{2.3log.T_1}{\mu.\theta cosec\beta} \tag{3.25}$$

#### *3.4.5.5 Determination of the power transmitted by the belt*

This is given in terms of the tension and the velocity of the belt as;

$$P_b = (T_1 - T_2)v_b \tag{3.26}$$

Note that, the center distance $(x)$ is estimated from design configuration.

### 3.4.6 Design of drive mechanisms (belts and pulleys) of the blower section

Following the same procedures as in section 3.4.5, we design for the fan drive as below

#### *3.4.6.1 Fitting the drive speeds and the size of the blower pulleys*

The fan is driven by the decorticating shaft, via the aid of a v-belt drive, hence the fan driver pulley (mounted on the decorticating shaft) and the driven pulley are selected so as to deliver the desired fan speed of 1100 rpm, with respect to the predetermined decorticating shaft speed ($\mathrm{N_d} = 200$ rpm). This is done using equation (3.19), with $N_1,\ D_1,\ N_2,\ D_2$ replaced with $N_d$, the speed of the decorticating shaft; $D_d$, the diameter of the blower driver pulley; $N_b$, the speed of the blower driven shaft/pulley and $D_b$, the diameter of the blower driven pulley respectively.

#### *3.4.6.2 Determination of the length of blower belt*

This is done using equation (3.20), with $D_1$ and $D_2$ as the diameters of the fan driven pulley and the fan driving pulley respectively, $x$ is the centre distance of the drive

#### *3.4.6.3 Determination of angle of contact ($\theta$) and angle of wrap ($\alpha$)*

The angle of contact and of wrap for the blower drive are both determined as in equations 3.21 and 3.22 respectively, using parameters for the blower section

#### *3.4.6.4 Determination of driving tensions in the belt*

The tensions in both the tight ($T_1$) and slack ($T_2$) sides of the fan belt are obtained using the same procedures as in tensions in the decorticator belt, equations 3.23. through to 3.25

#### *3.4.6.5 Determination of the power transmitted by the blower driver belt*

This is obtain using equation (3.26), and substituting the parameters for the blower drive

### 3.4.7 Design of shafts

The shafts are designed for both strength and torsional rigidity, so as to successfully withstand both bending and twisting (torsional) moments under instantly applied load, while transmitting power from the motor to the driven components without failure of any form. The American Society of Mechanical Engineers (ASME) has stated ultimate specifications upon which working designs of shafts are based. According to ASME code for design of transmission shaft; the maximum permissible working stress ($\sigma_u$) in tension or compression may be taken as 84 MPa and 112 MPa for shafts with and without allowance for key ways respectively, while maximum permissible shear stress ($\tau_u$) may be taken as 42 Mpa and 56 Mpa for shafts with and without allowance for key ways respectively.

Shaft design was based on that of a solid subjected to fluctuating torsional and bending load, along with axial load, since that shaft are vertically oriented and are subjected to axial load. Based on this, the equivalent twisting moment ($T_e$) and the equivalent bending moment ($M_e$) are given by Khurmi and Gupta (2004) as;

$$T_e = \sqrt{(K_m \times M + \alpha F_a\, D/8)^2 + (K_t \times T)^2} = \frac{\pi}{16} \times \tau_a D^3 \quad (3.27)$$

$$M_e = \frac{1}{2}[K_m + M + \alpha F_a\, D/8] + \sqrt{(K_m + M + \alpha F_a\, D/8)^2 + (K_t \times T)^2} = \frac{\pi}{32} \times \sigma_a D^3 \quad (3.28)$$

Where; $T_e$ is equivalent twisting moment;

$M_e$ is equivalent bending moment;

$F_a$ is the axial load $(N)$

$\alpha$ is the column factor $= 1$ for solid shaft;

$T$ maximum torque transmitted by the shaft; $(N/M)$

$M$ is the maximum bending moment induced on the shaft $(N/M)$. Force and moment analysis along the shafts are performed to determine the maximum bending moments. In the analysis, all forces/weight (vertical and horizontal) are considered.

$K_m$ is the combine fatigue and shock factor for bending $= 2$

$K_t$ is the combine fatigue and shock factor for bending $= 1.5$

$\tau_a$ is the permissible (allowable) stress in shear of the shaft $(N/m^2)$

$$= ultimate\ stress\ in\ shear\ of\ material(\ \tau_u)/factor\ of\ safety(f.s)$$

$\sigma_a$ is the permissible (allowable) stress in tension of the shaft $(N/m^2)$

$$= ultimate\ stress\ in\ shear\ of\ material(\ \sigma_u)/factor\ of\ safety(f.s)$$

$D$ is the desired diameter of the shaft;

Formula parameters as per the design are obtained as below;

- Maximum bending moment on the shaft

The maximum bending moment is obtained by carrying out a bending moment analysis on the drive system, using the rules of the sum of forces and moment of a body in equilibrium. Hence, applying the um of forces and the sum of moment rules, we have;

$$\sum F_V = 0 \tag{3.29}$$

$$\sum M_{V.A} = 0 \tag{3.30}$$

Where; $\sum F_V$ and $\sum M_{V.A}$ are the sum of vertical forces acting on the shaft, and the moment of forces about point $A$ on the shaft.

- Maximum torsional moment on the shaft

The torsional moment on the shaft is given by

$$T = (T_1 - T_2)R \tag{3.31}$$

Where; $T_1$ and $T_2$ are the tensions in the tight and slack sides of the belt, $R$ is distance from point of application of force (the outer fiber of the shaft) to the axis of rotation.

- The axial load $F_a$

The axial load $F_a$ is same as the weight of disc $W_{disc}$.

- The permissible stress in shear and tension

The permissible (allowable) stress in shear of the shaft is;

$$\tau_a = \tau_u / f.s \tag{3.32}$$

The permissible (allowable) stress in tension of the shaft is;

$$\sigma_a = \sigma_u / s.f \tag{3.33}$$

The same procedure is used to determine the diameter of the blower shaft

### 3.5.7 Determination for power requirement of the machine

The total power requirement for running the machine is supplied by an electric motor, which will offset for all the power requirement of the several aspects of the machine. Thus, the total machine power requirement is the summation the power requirement of the decorticating section and that of the blowing section. Thus,

$$P_m = P_{d.s} + P_{b.s} \tag{3.34}$$

#### *3.5.7.1 Power requirement of the decorticating section ($P_{d.s}$)*

The power requirement of the decorticating section $P_{d.s}$ is the sum of the power required to drive the decorticating members and to decorticate the pod. This sum is given as;

$$P_{d.s} = P_{disc} + P_{shaft} + P_{pulley} + P_{decort} \tag{3.35}$$

- The power required to drive the disc ($P_{disc}$)

The power required to drive the disc is given by Khurmi and Gupta (2004) as;

$$P_{disc} = T_{disc}\omega_d \tag{3.36}$$

$$T_{disc} = (W_{plate} + W_{pod} + W_{spikes})r_{disc} \tag{3.37}$$

Therefore;

$$P_{disc} = T_{disc}.\omega_d = W_{disc}r_{disc}.\omega_d \tag{3.38}$$

Note that, all weights are obtained in terms of density and volume as,

$$W = \rho vg = \rho\pi r^2 tg = \rho\pi r^2 hg \tag{3.39}$$

Where;

$T_{disc}$ is torque on rotary disc due to weight of disc, spikes and that of the pods it bears;

$W_{plate}$ is the weight of the plate;

$W_{spikes}$ is the weight of the spikes on the plate;

$r_{disc}$ is the radius of the decorticating disc;

$\omega_d$ is the angular velocity of the disc as obtained from $N_2$;

$W_{pod}$, the maximum possible weight of pods borne by the disc (in the decorticating space between the discs), assuming a filled space, given by;

$$W_{pod} = \sum_1^{n_{ph}} \rho_p V_p \tag{3.40}$$

Where;

$n_{ph}$ is the maximum number of pods that can be held within the decorticating space;

Therefore, by equation 3.35 and 3.37, we have that;

$W_{disc} = W_{plate} + W_{spikes} + W_{pod} = (\rho vg)_{plate} + n(\rho vg)_{spikes} + W_{pod}$

$$= (\rho \times \pi r^2 t \times g)_{plate} + n(\rho \times \pi r^2 h \times g)_{spike} + W_{pod} \quad (3.41)$$

$\rho_{plate}$ is the density of the disc material;

$r_{plate}$ is the radius of the lower disc;

$t_d$ is the disc material thickness;

$n$ is the number of spikes on the lower disc;

$\rho_{spike}$ is the density of the spike material;

$r_{spike}$ is the radius of the spikes;

$h_{spike}$ is the height of the spikes;

$v_{disc}$ and $v_{spike}$ are the volumetric content of the disc and spike materials respectively.

$W_{pod}$ the weight of equal volume of pod as the capacity of the decorticating chamber given by;

$$W_{pod} = \rho v g = \rho(\pi r^2 h)g \quad (3.42)$$

Note that the chambers '$h$' height is equal as the height of the spikes.

$W_{disc}$ is hence obtain using equation (3.41) above.

Therefore, $T_{disc}$ is obtained by equation (3.31) and $P_{disc}$ is hence obtained using equation (3.37)

$$P_{disc} = T_{disc}\omega_d \quad (3.43)$$

$$\text{But, } \omega_d = 2\pi N_d/60 \tag{3.44}$$

- Power to drive the shaft $(P_{shaft})$

The power required to drive the shaft is given by equation 3.34, that is;

$$P_{shaft} = T_{shaft} \times \omega_d \tag{3.45}$$

$$\text{But,} \quad T_{shaft} = W_{shaft} \times r_{shaft} = (\rho\pi r^2 lg)_{shaft} \times r_{shaft} \tag{3.46}$$

Where,

$T_{shaft}$ is shaft torque;

$W_{shaft}$ is the shaft weight;

$r_{shaft}$ is the radius of the shaft;

$\rho_{shaft}$ is the density of shaft material;

And $l$ is the length of the shaft;

- Power to drive the pulley$(P_{pulleys})$

The power to drive the pulley is calculated in accordance with the procedures as in $P_{shaft}$ above. Thus;

$$P_{pulleys} = (T)_{pulleys} \times \omega_d \tag{3.47}$$

But,

$$(T)_{pulleys} = (W.r)_{d.pulley} + (W.r)_{b.pulley} \tag{3.48}$$

Where,

$W_{d.pulley}$ is the weight of the decorticator driven pulley;

$r_{d.pulley}$ is the radius of the decorticator driven pulley;

$W_{b.pulley}$ is the weight of the blower driver pulley;

$r_{d.pulley}$ is the radius of the blower driver pulley;

- Power to decorticate the pod ($P_{pod}$)

The power required for the removal of the kernel by splitting open the pod is a function of the fracture resistance of the pod. To this regard, the force applied by the decorticating member must be set equal to the rupture force of the pod. By the power formula, we know that;

$$P_{pod} = T_{pod}\omega_d \tag{3.49}$$

But;

$$T_{pod} = F_{pod.r}r_{fn} \tag{3.50}$$

Thus, for $n_{s/f}$ number of spikes per front, we have that;

$$T_{pod} = n_{s/f}(F_{pod.r}r_{fn}) \tag{3.51}$$

For the total torque for $n_f$ number of fronts, the torque will be obtained by the sum;

$$\sum T_{pod} = \sum_{n=1}^{n=n_f} n_{s/f}\,(F_{pod.r}r_{fn}) \tag{3.52}$$

Therefore, total power requirement for decortication is given by;

$$P_{pod} = \sum T_{pod} \cdot \omega_d \tag{3.53}$$

Where;

$P_{pod}$ is the power requirement for pod decortication;

$T_{pod}$ is the torque due to the decorticating force;

$r_{fn}$ is the radius from the axis of rotation of the disc to a front;

That is; $r_{f1}$ the radius to the first front of spike arrays and $r_{f2}$ the radius to the second front of spikes array;

$n_f$ is the number of spikes front or arrays;

$n_{s/f}$ is the number of spikes per front;

$F_{pod.r}$ is the rupture force of the pod;

Thus, substituting this value into equation 3.51 to find $T_{pod}$ for the spike front, gives;

Torque for first front array spikes as;

$$T_{pod1} = n_{s/f}(F_{pod.r} r_{f1}) \tag{3.54}$$

and Torque for second front array of spikes as;

$$T_{pod2} = n_{s/f}(F_{pod.r} r_{f2}) \tag{3.55}$$

Hence, total torque is obtained according to equation (3.52);

Total power requirement for decorticating pod is hence obtained by equation (3.53).

And $P_{d.s}$ is subsequently obtained using equation (3.35)

#### *3.5.7.2 Determination of the Power requirement of the blower ($P_{blower}$)*

This was computed to be $= 84.321\text{W}$

Total power required by the machine ($P_m$) according to equation (3.34) was thus calculated. That is;

Considering a factor of safety of 1.5, the minimum motor power to drive the machine was computed as;

$$machine\ power = P_m \times f.s \tag{3.56}$$

## 3.5 Machine Construction

### 3.5.1 Material purchase

Purchase of materials needed for the machine construction, was done at the Minna central market.

### 3.5.2 Machine components fabrication and assembly

Solid Works (CAD) software version 2020 was used for the drawings of the Machine. The working and assembled drawings are presented in appendix B. The machine was fabricated in Technology Incubation Center, Minna Niger State. Fabrication activities were majorly cutting of materials into desired shapes and sizes, formation of materials into suiting shapes by bending, forging and filing, drilling of materials for bolt slots, welding of several parts into machine component parts. The tools used mainly, for the fabrication were welding machine, angle cutter, drilling machine, measuring tape, hammer and lathe machine.

### 3.5.3 Description of the machine

The machine altogether is designed to comprise of seven (7) main functional sections as discussed

i. **The hopper:** Th hopper is deigned to have the shape of a truncated cone with a volume value of $7.143 \times 10^{-3}\ m^{-3}$. The upper and lower openings are of radius 0.215 m and 0.152 m respectively, and a vertical height of 0.215 m. the hopper was constructed with a 2 mm thick mild steel sheet.

ii. **The in-let/feed pipe:** The hopper sits on the delivery channel, which is a circular pipe with diameter that conforms to the lower opening of the hopper (0.304 m). the pipe is 0.1524 m long and it connects the hopper to the decorticating section.

iii. **The decorticating section:** This section comprises of a cylindrical casing of diameter $2.794 \times 10^{-1}\ m$, which houses the decorticating discs. The decorticating discs are circular plates made of cast iron of 5mm thickness and one of each of their faces is equipped with spikes of 0.0381 m height. The spikes are solid circular rods of radius 2.5 mm of cast-iron material. The upper plate has a circular cut of diameter 0.304 m, through which the delivery pipe enters into the decorticating section. Both discs are bolted to rims on the upper casing and on the shaft that enters into the section from beneath the casing. Also, within the decorticating casing is a pan that sits just beneath the lower decorticating disc and slants into the vertical delivery channel. The casing and the slanted pan are both made of 2 mm thick galvanized metal sheets

iv. **The delivery channel:** This is a cuboid channel that serves as a guard for the pods with chaffs from the decorticating section, through the blower face, onto the conveyor belt. The channel is $2.794 \times 10^{-1}\ m$ wide and $6.35 \times 10^{-2}\ m$ thick and stretches

through a height of $5.842 \times 10^{-} m$. This channel is constructed with a 2 mm thick galvanized metal sheet. Close to the lower end of the channel ($5.08 \times 10^{-2} m$ from the base), there is a protrusion whose length spans across the breath of the channel and is $7.62 \times 10^{-2} m$ wide for the discharge of blown chaffs. The lower end of the channel opens unto a conveyor belt.

v. **The conveyor belt**: The conveyor belt is an endless leather belt of width 0.254 m running horizontally over two shafts placed at 0.508 m apart. The conveyor belt conveys the kernel to the outlet, which is just a simple chute of $2.794 \times 10^{-1} m$ by $5.08 \times 10^{-2} m$

vi. **The aerodynamic cleaning section (blower):** The blower unit comprises of a cylindrical casing with a protrusion of same dimension as the chute ($2.794 \times 10^{-1} m$ by $5.08 \times 10^{-2} m$) from the circumference into the delivery channel. The casing is made of 2 mm thick mild steel and is of height $1.016 \times 10^{-1} m$, and diameter $3.302 \times 10^{-1} m$. This casing houses the fan, which is a radial type with five vanes mounted radially on a hollow shaft of 30 mm inner diameter.

vii. **The frame:** The frame is rigidly made of angle bars to provide support and rigidity to all the components of the machine, and it holds all the parts together

### 3.5.4 Working principle of the machine

The pod is fed into the hopper, which is designed to have the shape of a truncated cone. The bottom (smaller opening) of the hopper is equipped with a flow regulator (gate), to aid regulate the feed rate of the pods into the inlet, so as to check overfeeding hence a potential choke and entanglement of the decorticating plates.

From the hopper, the pulses go down through the vertically positioned cylindrical inlet pipe (which is attached to the lower portion of the hopper and extending downwards into the decorticating section) by gravity into the decorticating section. The lower end of the inlet pipe fits into a circular cut on the upper stationary plate of the decorticator, to allow for inflow of pulses into the section. The linear vertical orientation of the hopper, the inlet pipe and the decorticating chamber allows for the pulses to flow in, through these sections by gravity.

Pass the inlet pipe; the pulses are ushered directly into the decorticating chamber. This is where the actual decortications or removal of seed from pods is done. The decorticating member is the double-discs type, and oriented for a transverse feeding. The arrangement comprises of a double concentric disc equipped with spikes that face each other (adjustably mated) and enclosed in a cylindrical casing. The upper plate is attached to a rim on the inside of the upper end of the cylindrical casing by means of bolts and nuts such that a circular cut on its centre conforms to the opening of the inlet pipe. The lower rotary plate is attached (also by means of bolts and nuts) to a rim on the power shaft (which is driven by means of a v-type belt drive by a vertically mount-type motor) which enters into the section from beneath the lower end of the casing. On the rotary disc, a circular plate of equal diameter as the cut on the upper disc is attached (aligned with the cut) by means of a rod at the midpoint of the disc, protruding slightly upwards from floor of the bearing disc such that the materials entering the section falls on this plate before touching the floor of the rotary disc. A narrow bar is obliquely welded flat on the surface of this plate which in conjunction with the centrifugal force helps to splatter fed materials radially into the toothed regions of the plate where rigorous tooth interloping/mating occurs when the machine runs. This section is uniquely designed with provision for the replace-ability of the discs; a strategy upon which

the multi pod decorticating ability of the machine depends. The machine via the mating action of the spikes of the decorticating discs reaps pods off the kernels by the triple principles of shearing, impact and a bit of compression. Discs configurations such as the number of spikes per disc, the inter/intra spike spacing, length of spikes and disc-disc clearance, constitutes the variations amongst the discs and all depends on the pulse for which they are meant to decorticate. Effluent of decorticated seeds and chaff from this section is aided by a double action of fling and push. The fling action is provided by the centrifugal force due to the rotation of the lower disc, which by; throw seeds off the disc in all radial directions. The push on the other hand is on the frontal materials (pre-fed) by the adjacent descending ones (freshly fed). The seeds and chaff thrown off the disc all collect on the slide conveyor pan beneath the lower disc.

The slide conveyor tray as earlier mentioned is located just beneath the decorticating section, also encased in same cab as the discs. It is slightly tilted downwards such that the seeds and chaffs that fall on it converges, due to the vibration of the machine, towards a protrusion (opening) to which the cleaning section of the machine may be linked (by means of flanges).

The cleaning section of the machine is designed as an integral part of the decorticating machine. From the decorticating section, the seeds with the shredded pods pass through the link (the decorticator-cleaner link) into a hollow channel, where they are allowed to fall through (in between) an attached blower and an opening on the opposite side of the blower, thus cutting across the direction of flow of the air blown by the blower, hence lighter materials (mostly chaff) are blown along with the breeze in its direction. The cleaned seeds fall through unto a conveyor belt (whose assembly comprises of an endless leather belt, which runs over two rollers), which conveys the seeds to the outlet chute.

### 3.5.4 Cost analysis of the machine

The material specification and costing for the construction of the machine was determined on the basis of material cost, labour cost and overhead cost using equation 3.42 below

$$\text{Total cost of fabrication} = \text{CM} + \text{CL} + \text{CO} \quad (3.57)$$

Where;

$C_M$ = Material cost is the cost of all materials used in the fabrication of the machine

$C_L$ = Labour cost involves the cost of direct human services rendered during the fabrication process and is assumed to be 30 % of the material cost

$C_O$ = Overhead cost represents all in-direct miscellaneous expenses incurred during construction of the machine, including cost of feeding and transportation, assumed to be 20 % of the material cost.

Equation 3.18 is re-written as

$$\text{CP} = 0.2\text{CM} + 0.3\text{CM} + 0.2\text{CM} \quad (3.58)$$

## 3.6 Design of Experiment

The experiment was designed to capture four machine functional parameters; decorticating speed (A), plate clearance (B), blower speed (C), and feed rate (D) (independent variables) using a central composite rotatable design (CCRD) of response surface methodology (RSM). In order to obtain the required data, the range of values of each of the four variables (k) was determined as reported by Gana *et al.,* (2017) and is presented in Table 1. The total number of runs for the four variables (k = 4) and five levels (-α, -1, 0, 1 and +1) experiments was determined by the expression: $2^k$ ($2^4$= 16 factorial points) + 2k (2 × 4 = 8 axial points) + 6

(center points: six replications) as 30 (Cukor *et al.*, 2011) and raised by the design software. the design is shown in Table 4.1 in the appendix.

To evaluate the performance, hence optimize the machine, as per the levels of the factors considered, four performance determinant variables namely; decorticating speed, plate clearance, feed rate and blower speed were used at several levels table 4.1. Interaction of the levels of these factors was done according to the print by the design of experiment (DOE) by the Design expert stat ease ® 360 Software as discussed in section 4.1. Based on the design of the experiment, five decorticating speeds were varied: 150 rpm, 200 rpm, 250 rpm, 300 rpm, and 350 rpm. The plate clearance was varied as follows: 1 mm, 2 mm, 3 mm, 4 mm, and 5 mm. The fan speed was varied between 1100 rpm, 1200 rpm, 1300 rpm, 1400 rpm, and 1500 rpm. The feed rate ranged from 110 kg/h, 120 kg/h, 130 kg/h, 140 kg/h, and 150 kg/h. The experiment was conducted at the National Technology Incubation Centre Minna, Niger State, Nigeria. The design of experiment is as shown on Table 3.1.

**Table 3.1:** Experimental design for the performance evaluation of the machine

| Std | Run | A:Speed of shelling | B:Plate clearance | C:Speed of Blower | D:Feed Rate | Shelling Efficiency | Recovery Efficiency | Cleaning Efficiency | Percentage Loss |
|---|---|---|---|---|---|---|---|---|---|
| | | rpm | mm | rpm | kg/h | % | % | (%) | % |
| 12 | 1 | 300 | 4 | 1200 | 140 | | | | |
| 16 | 2 | 300 | 4 | 1400 | 140 | | | | |
| 20 | 3 | 250 | 5 | 1300 | 130 | | | | |
| 28 | 4 | 250 | 3 | 1300 | 130 | | | | |
| 5 | 5 | 200 | 2 | 1400 | 120 | | | | |
| 22 | 6 | 250 | 3 | 1500 | 130 | | | | |
| 19 | 7 | 250 | 1 | 1300 | 130 | | | | |
| 25 | 8 | 250 | 3 | 1300 | 130 | | | | |
| 1 | 9 | 200 | 2 | 1200 | 120 | | | | |
| 29 | 10 | 250 | 3 | 1300 | 130 | | | | |
| 8 | 11 | 300 | 4 | 1400 | 120 | | | | |
| 9 | 12 | 200 | 2 | 1200 | 140 | | | | |
| 10 | 13 | 300 | 2 | 1200 | 140 | | | | |
| 3 | 14 | 200 | 4 | 1200 | 120 | | | | |
| 4 | 15 | 300 | 4 | 1200 | 120 | | | | |
| 30 | 16 | 250 | 3 | 1300 | 130 | | | | |
| 13 | 17 | 200 | 2 | 1400 | 140 | | | | |
| 21 | 18 | 250 | 3 | 1100 | 130 | | | | |
| 24 | 19 | 250 | 3 | 1300 | 150 | | | | |
| 6 | 20 | 300 | 2 | 1400 | 120 | | | | |
| 14 | 21 | 300 | 2 | 1400 | 140 | | | | |
| 27 | 22 | 250 | 3 | 1300 | 130 | | | | |
| 17 | 23 | 150 | 3 | 1300 | 130 | | | | |
| 2 | 24 | 300 | 2 | 1200 | 120 | | | | |
| 26 | 25 | 250 | 3 | 1300 | 130 | | | | |
| 15 | 26 | 200 | 4 | 1400 | 140 | | | | |
| 7 | 27 | 200 | 4 | 1400 | 120 | | | | |
| 23 | 28 | 250 | 3 | 1300 | 110 | | | | |
| 18 | 29 | 350 | 3 | 1300 | 130 | | | | |
| 11 | 30 | 200 | 4 | 1200 | 140 | | | | |

## 3.7 Machine Performance Evaluation

The multipurpose decorticator so developed was tested with peanut, the pod which the fitting of the pod-dependent aspects of the machine (such as the disc and the decorticating force) was based. The general performance of the machine was understudied at various levels of four independent (determinant) factors, that tend to affect the responses of the machine.

### 3.7.1 Performance index calculation

To obtain the data required for the optimization of the machine, 4 kg of peanuts (denoted as $M_p$) was used for each varied run. This quantity was fed into the machine after being set as desired and allowed to run empty for 30 seconds. The time taken until the last pod is decorticated is noted as $(T_d)$. The mass of decorticated seeds and not broken (whole seeds) were recorded as $(M_{hs})$. The mass of the decorticated seeds but broken were recorded as $(M_{bs})$. The mass of the chaff collected at the blower outlet was collected and recorded as $(M_{ch})$. The mass of the pods that came out un-decorticated were also recorded as $(M_{us})$. Prior to machine testing, 4kg of the pod was measured and hand broken in a careful setting, ensuring that no seed nor peel was lost. The mass of the seed was taken as $(M_{s.max})$, and the mass of the peel (chaff) was also recorded as $(M_{ch.max})$.

The following indices used for optimization were calculated per run using the relations below.

i. Decorticating efficiency $\eta_D = \frac{M_{hs}+M_{bs}}{M_{S.max}} \times 100\ \%$ (3.59)

ii. Whole seed recovery $R_\varepsilon = \frac{M_{hs}}{M_{s.max}} \times 100\ \%$ (3.60)

iii. Cleaning efficiency $C_\varepsilon = \frac{M_{ch}}{\eta_D(M_{ch.max})} \times 100\ \%$ (3.61)

iv. Percentage loss $L = \frac{M_p - (M_{hs} + M_{bs} + M_{ch} + M_{us})}{M_p} \times 100\ \%$ (3.61)

### 3.7.2 Statistical analysis

An analysis of variance (ANOVA) was carried out to estimate the effects of the main variables and their likely effects on the responses (Gana *et al.*, 2017).

Design expert stat ease ® 360 Software was employed, to optimize independent and dependent variables using numerical techniques. By applying the desirability functions method in RSM, a number of solutions were obtained for the optimum covering criteria with desirability close to 1, and the first solution with desirability closest to 1 was selected.

# CHAPTER FOUR

## 4.0 RESULTS AND DISCUSSION

### 4.1 Results

#### 4.1.1 Machine Performance Evaluation

After the design and construction of the machine were completed, the effects of the independent variables on the dependent variables were determined. The results of the effects of the decorticating speed, plate clearance, fan speed, and feed rate of the machine are shown in Table 4.1. The values of decorticating efficiency ranged from 47.2 % to 96.5 %. The combination of decorticating speed of 250 rpm, plate clearance of 1 mm, fan speed of 1300 rpm, and feed rate 130 kg/h yielded the highest efficiency of 96.5 %, while the interaction of decorticating speed of 150 rpm, plate clearance of 3 mm, fan speed of 1300 rpm, and feed rate 130 kg yielded the lowest efficiency of 47.45 %. The value of clearing efficiency ranged from 70.85 % to 97.22 %. The highest value of 97.22 % was obtained from the combination of decorticating speed of 250 rpm, plate clearance of 3 mm, fan speed of 1300 rpm, and feed rate of 110 kg/h, while the interaction between decorticating speed of 350 rpm, plate clearance of 3 mm, fan speed of 1300 rpm, and feed rate of 130 kg/h yielded an efficiency of 70.85 %. The value of recovery efficiency ranged from 47.2 % to 99.37 %. The combination of decorticating speed of 200 rpm, plate clearance of 2 mm, fan speed of 1200 rpm, and feed rate of 120 kg/h yielded the highest efficiency of 99.37 %, while the interaction of decorticating speed of 150 rpm, plate clearance of 3 mm, fan speed of 1300 rpm, and feed rate of 130 kg/h yielded the lowest efficiency of 47.2 %. The value of the percentage loss ranged from 0.63 % to 29.15 %. The combination of decorticating speed of 350 rpm, plate

clearance of 3 mm, fan speed of 1300 rpm, and feed rate of 130 kg/h yielded the highest percentage loss of 29.15 %, while the interaction of decorticating speed of 200 rpm, plate clearance of 2 mm, fan speed of 1200 rpm, and feed rate of 120 kg/h yielded the lowest percentage loss of 0.63 %.

## 4.2 Discussion

### 4.2.1 Effects of Independent Variables on Machine Performance Parameters

The machine performance parameters investigated in this study include decorticating efficiency, cleaning efficiency, recovery efficiency, and percentage loss, and the responses are shown in Table 4.1.

#### *4.2.1.1 Decorticating Efficiency*

The effects of independent variables on the decorticating efficiency indicated that it decreased with an increase in the speed of decorticating, feed rate, and plate clearance but remained constant with the fan speed. A statistical analysis of the experimental variance was performed using software (Design Expert StatEase® 360). Table 4.2 shows the results of the statistical analysis of the variance of the data obtained from the results, for the determination of effects, contributions, the model coefficient, the test for lack of fits, and the significance of the variables and their respective interactions on the decorticating efficiency. The significant model terms were identified at the 5% significant level. The quadratic regression model and fitted model equations developed to predict the decorticating efficiency with respect to functional machine parameters (independent variables) were given as shown in equations 4.1

The results in Table 4.2 showed that the model equation was significant ($P \leq 0.001$), and the model F-value of 33.44 implies the model is significant. There is only a 0.01 % chance that

an F-value this large could occur due to noise. P-values less than 0.0500 indicate model terms are significant. The results also showed that decorticating speed (A), plate clearance (B), and feed rate (D) were significant model terms ($P \leq 0.05$). It can be clearly observed that plate clearance has the highest significant effects on the decorticating efficiency, with a coefficient of estimation of 8.09.

The obtained coefficient of variation (C.V.) of 4.33 % was low, falling within the threshold of less than 10 %. This means that the deviation between predicted and experimental values was within the recommended value (Maran and Manikanda (2012); Gana *et al.,* (2017)). The coefficient of determination R value of 0.9843 indicated that the model equation was capable of predicting about 98.43 % of the differences between the predicted and experimental values. Therefore, the model was not capable of accounting for about 0.057 % of the variation. The R-squared coefficient of correlation of 0.969 was high and very close to one, as recommended by Gana (2016), Xin and Saka (2008). However, the authors went on to say that a high $R^2$ value does not necessarily imply that the regression model equation is good because it will increase when a new variable is added, even if the new variable is insignificant. Hence, adjusted and predicted $R^2$ were suggested to be used to test the model's sufficiency. Based on that, it was observed that the predicted R-squared and adjusted R-squared values were in logical conformity with each other, with values of 0.847 and 0.940, respectively. This means that the experimental data were well fitted. The adequate precision is greater than the recommended threshold value of 4.

The regressed decorticating efficiency model is given as

$$S_{\mathrm{E}} = 86.11 + 5.21A - 8.09B - 0.4108C - 8.50\mathrm{D} - 0.3962AB + 0.2675\mathrm{AC} + 0.6525AD + 0.7787\ \mathrm{BC} + 0.5738\mathrm{BD} - 0.7300\mathrm{CD} - 5.70A^2 - 1.21B^2 - 0.3940C^2 - 4.12^2 \quad (4.1)$$

where, $S_{\mathrm{E}}$ = Decorticating Efficiency (%)

A = Decorticating Speed (rpm)

B = Plate Clearance (mm)

C = Fan Speed (rpm)

D = Feed Rate (kg)

It is important to add that the variable A in the model has a positive coefficient, implying direct proportionality, while B and D have a negative coefficient, implying indirect proportionality. That is, an independent increase in B or D decreased the decorticating efficiency, while an increase in A increased the decorticating efficiency.

#### *4.2.1.2 Simulation and Confirmation of the Model*

The model equation obtained was simulated and the decorticating efficiency was observed to be within the experimental range. From Table 4.3 the actual value of decorticating efficiency was observed to be in close conformity with the predicted value verifying the need that the model equation can be used to determine the best decorticating efficiency at various operating condition within the range of experimental value.

#### *4.2.1.3 Relationship between Plate Clearance and Decorticating Speed with respect to Decorticating Efficiency*

The effects of plate clearance and decorticating speed on decorticating efficiency at a constant fan speed of 1300 rpm and feed rate of 130 kg/h were presented in Figures 4.1 and 4.2. The response surface is presented in Figure 4.1, while the contour plot is presented in Figure 4.2. As the plate clearance increased from 2 mm to 4 mm, the decorticating efficiency decreased from 84 % to 66 %. The decrease could be due to more space that allowed the seed to pass out of the decorticating chamber without being dehulled. This indicated that the plate clearance significantly influenced the decorticating efficiency. This agreed with the report of Gitau *et al.* (2013), where the decorticating efficiency of groundnut decorticators was affected by the decorticator clearance, such that as the clearance increased, decorticating efficiency decreased, and too much decrease in the clearance resulted in compressing forces that the nuts experienced. The decorticating efficiency increased from 84 % to 90 % as the speed increased from 200 to 250 rpm, and then remains almost constant to a value of 93 % with further increase in speed to 300 rpm. This could be the result of the increased energy and impact force associated with the higher speed.

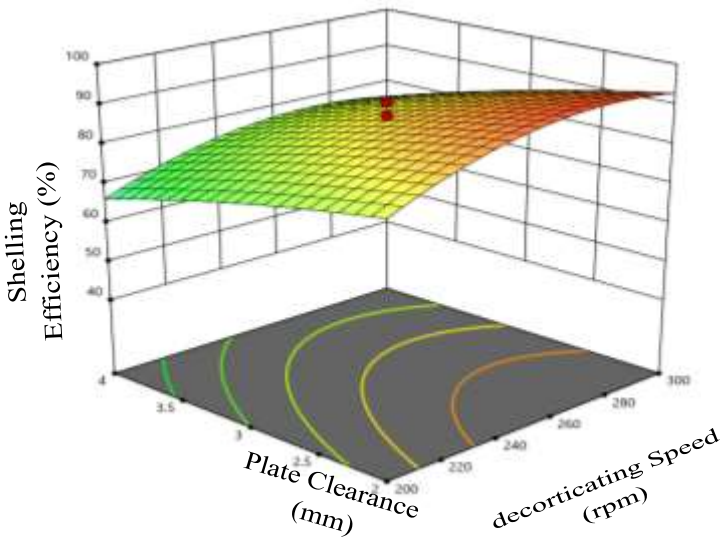


**Figure 4.1:** Response Surface for Decorticating Efficiency with Respect to Plate Clearance and Decorticating Speed

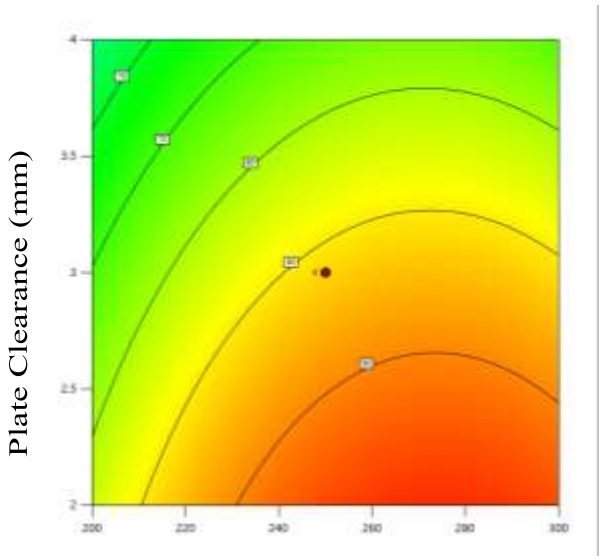


**Figure 4.2:** Contour Plot for Decorticating Efficiency with Respect to Plate Clearance and Decorticating Speed

### *4.2.1.4 Relationship between Fan Speed and Plate Clearance with respect to Decorticating Efficiency*

The effects of fan speed and plate clearance on decorticating efficiency at a constant decorticating speed of 130 rpm and plate clearance 3 mm are presented in Figures 4.3 and 4.4. The decorticating efficiency remained almost constant at 73 % as the blower speed increased from 1200 rpm to 1400 rpm. This indicates that the fan speed has no effect on decorticating efficiency (P 0.05). It was obvious that the plate clearance had an impact on the decorticating efficiency. The decorticating efficiency increased from 73 % to 86 %, as the decorticating speed increases from 200 rpm to 250 rpm and then remain constant with further increased in speed to 300 rpm.

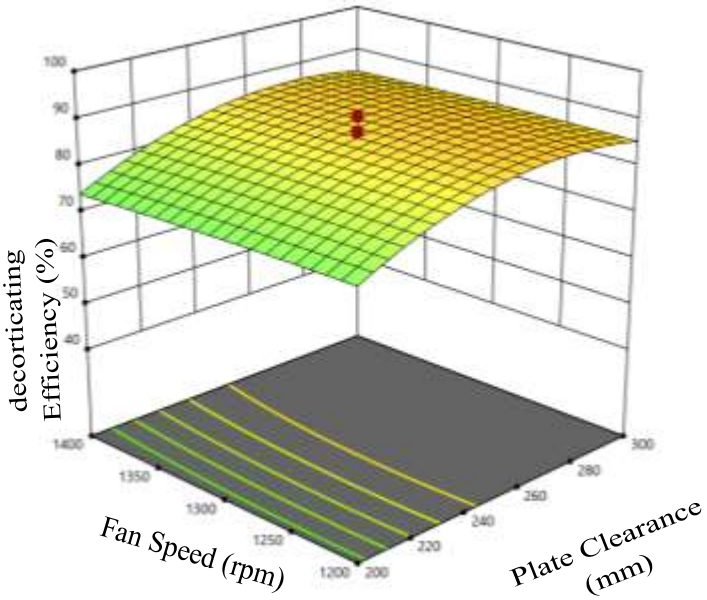


**Figure 4.3:** Response Surface for Decorticating Efficiency with Respect to Fan Speed and Plate Clearance

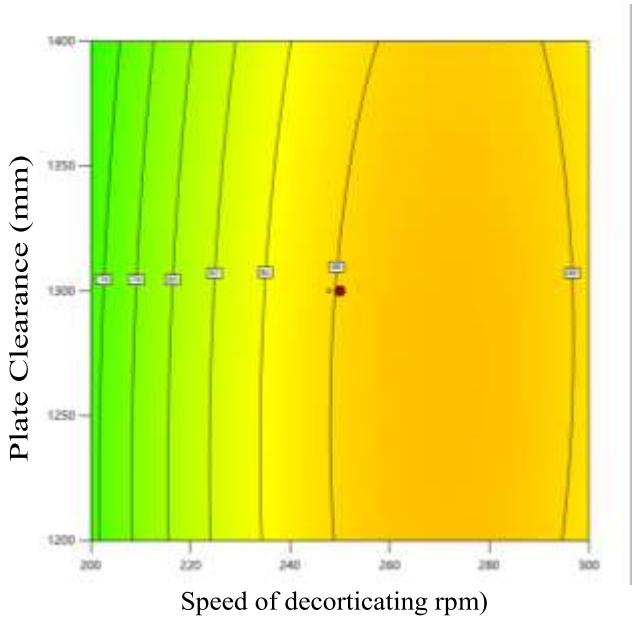


**Figure 4.4:** Contour Plot for Decorticating Efficiency with Respect to Fan Speed and Plate Clearance

#### *4.2.1.5 Relationship between Feed Rate and Decorticating Speed with respect to Decorticating Efficiency*

The effects of feed rate and decorticating speed on decorticating efficiency at a constant fan speed of 1350 rpm and a plate clearance of 3 mm are presented in Figures 4.5 and 4.6. The decorticating efficiency remains constant with a value of 80 % as the feed rate increased 120 kg/r to 130 kg/h and then decreases to 61 % with further increase in feed rate speed to 140 kg/h. This could be the result of more impact among the seeds than between the seed and the decorticating mechanism. Which resulted in insufficient impact force for decorticating the seed. This is in line with the report of Gitau *et al*. (2013), in which an increase in feed rate decreases decorticating efficiency and percent fines. At higher feed rates, the number of seeds entering the sheller per unit time increases, and some seeds may be hitting other seeds instead of the hard rubber surface, resulting in insufficient impact for decorticating. The decorticating

efficiency increased from 80 % to 89 % as the speed increases from 200 to 250 rpm and then remain almost constant with further increase in speed to 300 rpm.

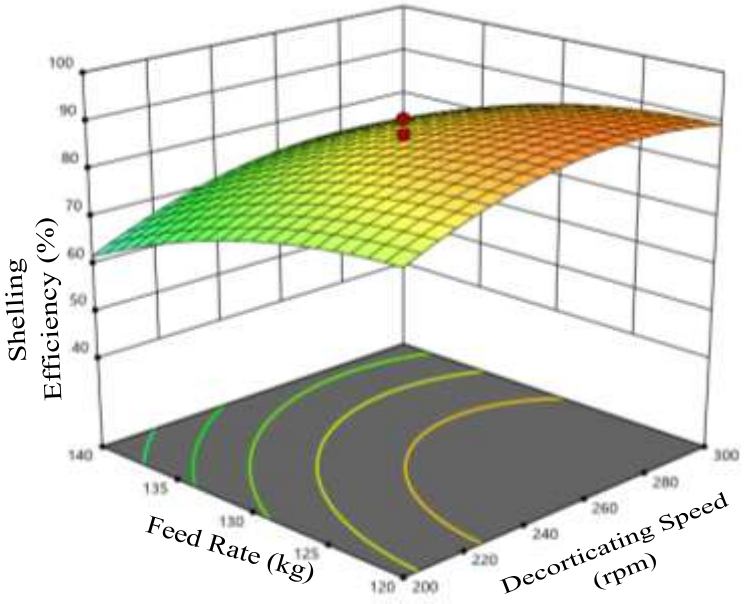


**Figure 4.5:** Response Surface for Decorticating Efficiency with Respect to Feed Rate and Speed of Decorticating

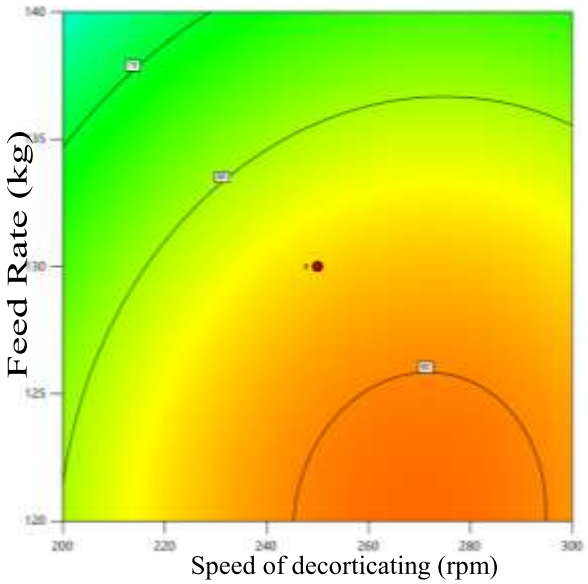


**Figure 4.6:** Contour Plot for Decorticating Efficiency with Respect to Feed Rate and Decorticating Speed

### *4.2.2.1 Cleaning Efficiency*

The effects of independent variables (decorticating speed, plate clearance, plate speed, and feed rate) on the cleaning efficiency were presented in Table 4.1. The cleaning efficiency remains constant with increases in decorticating speed and plate clearance but increases with the speed of the fan and decreases with increases in feed rate. The results in Table 4.4 showed that the model equation was significant ($P \leq 0.001$), and the model F-value of 21.68 implies the model is significant. There is only a 0.01 % chance that an F-value this large could occur due to noise. P-values less than 0.0500 indicate model terms are significant. Fan speed (C) and feed rate (D) were also found to be significant model terms ($P \leq 0.001$). It can be clearly observed that the fan speed (C) has the highest significant effect on the cleaning efficiency with value of 5.98. The lack of fit F-value of 2.48 indicates that the lack of fit is insignificant in comparison to the pure error. A large lack of fit f-value due to noise has a 16.37 % chance

of occurring. The coefficient of variation (C.V.) of 24.56 % obtained was low, below the threshold value of not greater than 10 %. This means that the deviation between predicted and experimental values was within the recommended threshold (Maran and Manikanda (2012); Gana *et al.,* (2017)). The coefficient of determination R value of 0.9760 indicated that the model equation was capable of predicting about 97.60% of the differences between the predicted and experimental values. Therefore, the model was not capable of accounting for about 2.4 % of the variation. The R-squared coefficient of correlation of 0.9526 was very close to one, as recommended by Gana (2016), Xin and Saka (2008). However, the authors went on to say that a high $R^2$ value does not necessarily imply that the regression model equation is good because it will increase when a new variable is added, even if the new variable is one of consequence or order. Hence, the adjusted and predicted $R^2$ were suggested to be used to test the model's sufficiency. Based on that, it was observed that the predicted R-squared and adjusted R-squared values were in logical conformity with each other, with values of 0.7625 and 0.9089, respectively. This indicates that the experimental data were well fitted.

The regressed decorticating efficiency model is given as

$$C_{\mathrm{E}} = 72.78 + 0.8338A - 0.193B + 5.98C - 9.77\mathrm{D} + 1.82AB - 0.5281\mathrm{AC} - 1.21AD - 1.45\mathrm{BC} - 1.17\mathrm{BD} - 3.69\mathrm{CD} + 0.0789A^2 + 1.48B^2 + 0.9164\,C^2 + 2.06D^2 \quad (4.2)$$

It is important to add that the variable both A and C in the model have positive co-efficient implying a direct proportionality. That is independent increased in A or C increases the cleaning efficiency.

#### *4.2.2.2 Simulation and Confirmation of the Model*

The model equation obtained was simulated, and the cleaning efficiency was observed to be within the experimental range. From Table 4.5, the actual value of cleaning efficiency was observed to be in close conformity with the predicted value, verifying the need for the model equation to be used to determine the best cleaning efficiency at various operating conditions within the range of the experimental value.

#### *4.2.2.3 Relationship between Plate Clearance and Decorticating Speed with respect to Cleaning Efficiency*

The effects of plate clearance and decorticating speed on cleaning efficiency at a constant fan speed of 1300 rpm and feed rate of 130 kg/h were presented in Figures 4.7 and 4.8. The response surface is presented in Figure 4.7, while the contour plot is presented in Figure 4.8. The cleaning efficiency remains constant with the increased plate clearance from 2 mm to 4 mm. Also, the cleaning efficiency remained constant with the increased in speed of decorticating from 200 to 300 rpm. This indicated that the two variables have no any significant effects on the decorticating efficiency.

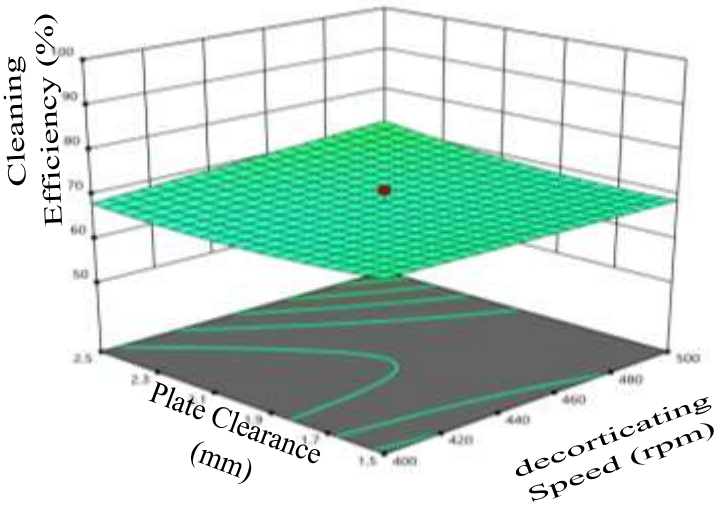


**Figure 4.7:** Response Surface for Cleaning Efficiency with Respect to Plate Clearance and Decorticating Speed

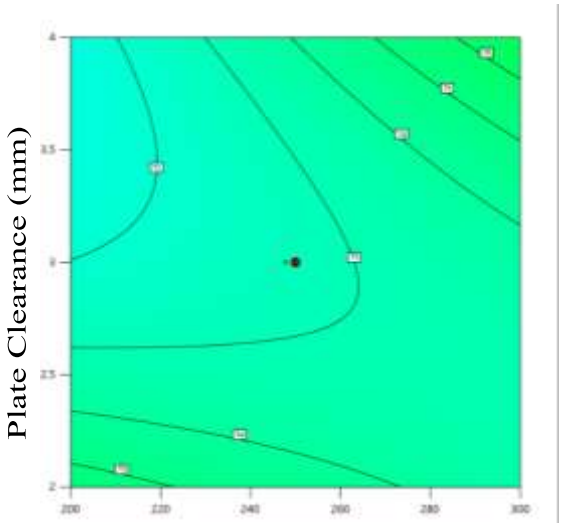


**Figure 4.8:** Contour Plot for Cleaning Efficiency with Respect to Plate Clearance and Decorticating Speed

### *4.2.2.4 Relationship between Fan Speed and Plate Clearance with respect to Cleaning Efficiency*

The effects of fan speed and plate clearance on cleaning efficiency at a constant decorticating speed of 250 rpm and feed rate of 130 kg/h are presented in Figures 4.9 and 4.10. The cleaning efficiency remained almost constant at 62 % as the plate clearance increased from 2 mm to 4 mm. This indicates that plate clearance has no significant effects ($P \leq 0.05$) on the cleaning efficiency. Also, the cleaning efficiency decreased from 624 % to 80.153 % as the fan speed increased from 1200 to 1400 rpm. This could be the result of more flow energy associated with higher fan speeds, resulting in high airflow that lifts more lighter materials. This agreed with the findings of Al-Shamiry and Yahya (2020), in which increase in speed resulted to increase in blown grain.

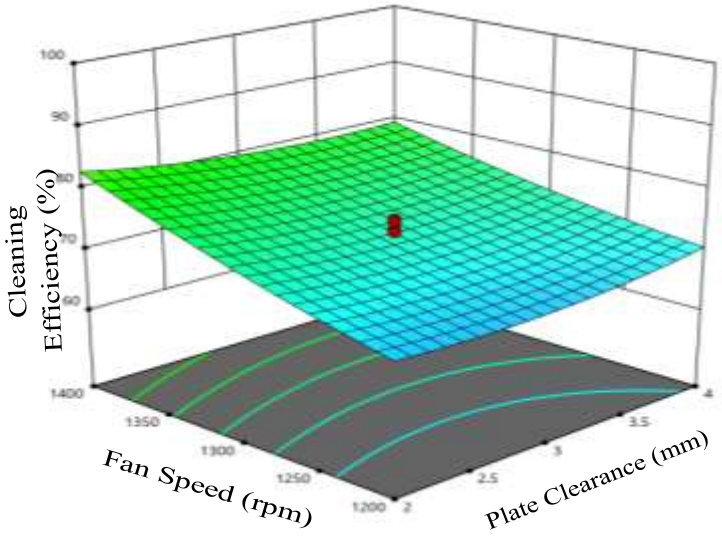


**Figure 4.9:** Response Surface for Cleaning Efficiency with Respect to Fan Speed and Plate Clearance

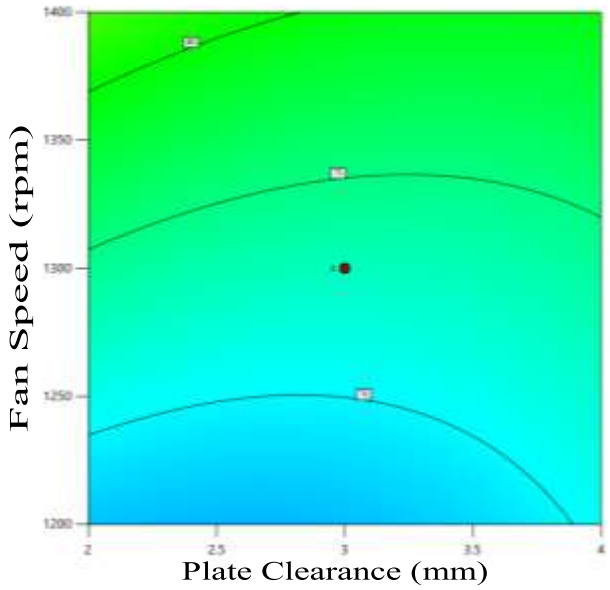


**Figure 4.10:** Contour Plot for Cleaning Efficiency with Respect to Fan Speed and Plate Clearance

### *4.2.2.5 Relationship between Feed Rate and Plate Clearance with respect to Cleaning Efficiency*

The effects of feed rate and plate clearance on cleaning efficiency at a constant decorticating speed of 250 rpm and a fan speed of 1300 rpm are presented in Figures 4.11 and 4.12. The cleaning efficiency remained almost constant at 86.5% as the plate clearance increased from 2 mm to 4 mm. This indicates that the plate clearance has no significant effects on the cleaning efficiency. The cleaning efficiency decreased from 86.5 % to 67 % as the feed rate increase from 120 kg/h to 140 kg/h. This can be as result of more particles obstructing airflow. This is consistent with Simonyan and Simonyan (2008) report, which suggested that an increase in load intensity on the sieve may be the cause of the decline in cleaning efficiency against feed rate. The airflow is impeded by several particulates. Also, Simonyan and Simonyan (2008) reported that increase in load intensity on the sieve may be the cause

of the decline in cleaning efficiency against feed rate. The airflow is impeded by several particulates.

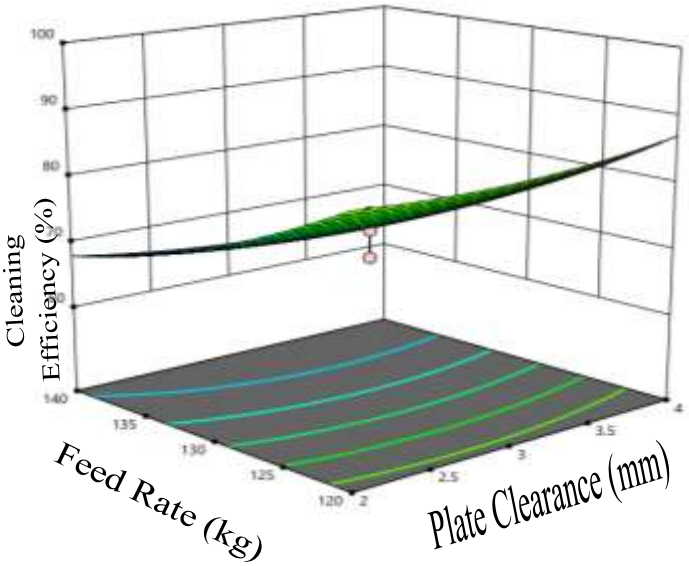


**Figure 4.11:** Response Surface for Cleaning Efficiency with Respect to Feed Rate and Plate Clearance

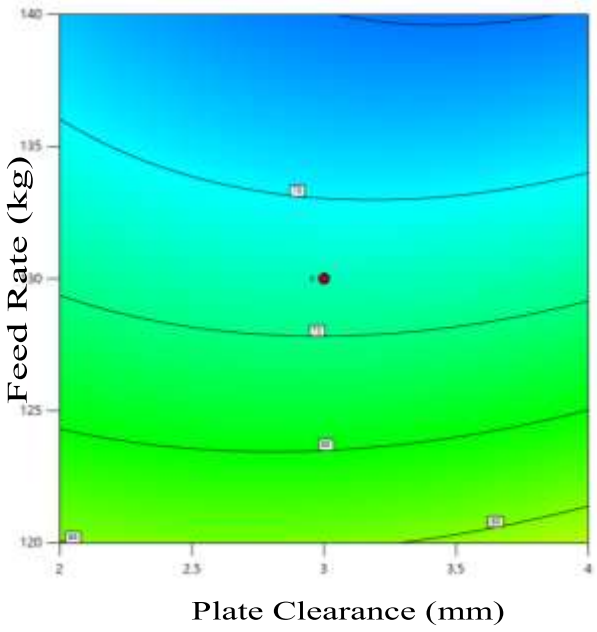


**Figure 4.12:** Contour Plot for Cleaning Efficiency with Respect to Feed Rate and Plate Clearance

#### *4.2.3.1 Recovery Efficiency*

The effects of independent variables (decorticating speed, plate clearance, plate speed, and feed rate) on the recovery efficiency were presented in Table 4.1. The recovery efficiency decreased with increases in feed rate, speed of the fan, speed of decorticating, and plate clearance.

The results in Table 4.6 showed that the model equation was significant ($P \leq 0.001$), and the model F-value of 19.12 implies the model is significant. There is only a 0.01 % chance that an F-value this large could occur due to noise. P-values less than 0.0500 indicate model terms are significant. The findings also revealed that all variables were significant ($P \leq 0.001$). It can be clearly observed that the plate clearance (B) has the most significant effects on the recovery efficiency. The lack of fit F-value of 1.33 indicates that the lack of fit is insignificant in comparison to the pure error. A large lack of fit f-value due to noise has a 39.75 % chance of occurring.

The coefficient of variation (C.V) of 2.355 % obtained was low, below the threshold value of not greater than 10 %. The coefficient of determination R value of 0.9731 indicated that the model equation was capable of predicting about 97.31 % of the differences between the predicted and experimental values. Therefore, the model was not capable of accounting for about 1.08 % of the variation. The R-squared correlation coefficient of 0.9469 was high and very close to one, as recommended by Gana (2016) and Xin and Saka (2008). However, the authors went on to say that a high $R^2$ value does not necessarily imply that the regression model equation is good because it will increase when a new variable is added, even if the new variable is one of consequence or order. Hence, adjusted and predicted $R^2$ were suggested to be used to test the model's sufficiency. Based on that, it was observed that the

predicted R-squared and adjusted R-squared values were in logical conformity with each other, with values of 0.757 and 0.8974, respectively. This means that the experimental data were well fitted.

The regressed decorticating efficiency model is given as

$$R_{\mathrm{E}} = 91.4 - 3.76A - 3.12B - 0.1283C - 2.73\mathrm{D} + 0.2475AB + 0.89\mathrm{AC} + 0.5050AD + 0.4763\ \mathrm{BC} + 0.2788\mathrm{BD} - 0.3912\mathrm{CD} - 2.84A^2 - 2.02B^2 + 0.8773\ C^2 + 0.3235D^2 \quad (4.5)$$

where, $R_{\mathrm{E}}$ = Seed Recovery Efficiency (%)

A = Decorticating Speed (rpm)

B = Plate Clearance (mm)

C = Fan Speed (rpm)

D = Feed Rate (kg)

It is important to add that all the variables have negative coefficient, implying indirect proportionality, implying indirect proportionality. That is independent and increased in A or B or C or D decreases the recovery efficiency.

#### *4.2.3.2 Simulation and Confirmation of the Model*

The model equation obtained was simulated, and the recovery efficiency was observed to be within the experimental range. From Table 4.7, the actual value of recovery efficiency was observed to be in close conformity with the predicted value, verifying the need for the model

equation to be used to determine the best seed recovery efficiency at various operating conditions within the range of the experimental value.

#### *4.2.3.3 Relationship between Plate Clearance and Decorticating Speed with respect to Seed Recovery Efficiency*

The effects of plate clearance and decorticating speed on cleaning efficiency at a constant fan speed of 1300 rpm and feed rate of 130 kg/h were presented in Figures 4.13 and 4.14. The response surface is presented in Figure 4.13, while the contour plot is presented in Figure 4.14. The recovery efficiency remains almost constant at 93.8 % as the plate clearance increases from 2 to 3 mm, and then decreases significantly to 86.5% with further increases in the plate clearance to 4 mm. The decreased could be due to crushing of the seed as result of compressing force generated from too much decrease in the clearance. This agrees with report of Gitau *et. al*. (2013), where too much decrease in the clearance resulted in compressing forces that the nuts experience. As the clearance reduces, the pods are compressed. Al-Shamiry and Yahya (2020), reported that the broken percentage of a thresher attached to the tractor increase in concave clearance reduction. Also, the recovery efficiency remains almost constant with a value of 93.8 % to 93.4 %, and then decreases significantly to 85 % with further increases in the speed to 300 rpm.

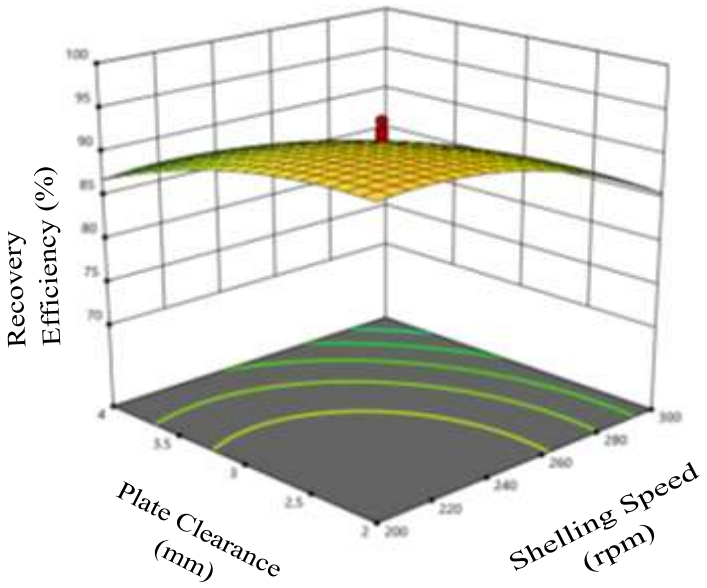


**Figure 4.13:** Response Surface for Seed Recovery Efficiency with Respect to Plate Clearance and Decorticating Speed

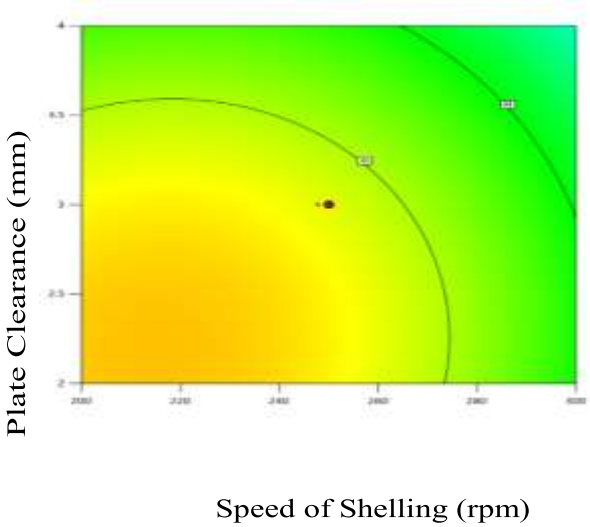


**Figure 4.14:** Contour Plot for Seed Recovery Efficiency with Respect to Plate Clearance and Decorticating Speed

***4.2.3.4 Relationship between Fan Speed and Plate Clearance with respect to Seed Recovery Efficiency***

The effects of fan speed and plate clearance on recovery efficiency at a constant decorticating speed of 250 rpm and feed rate of 130 kg/h are presented in Figures 4.15 and 4.16. The

recovery efficiency remains constant with a value of 91.8 % as the fan speed increased from 1200 to 1400 rpm. The recovery efficiency remains constant with a value of 91.8 % as the decorticating speed increased from 200 to 250 rpm, and then decreased to 85 % as the speed was increase to 300 rpm.

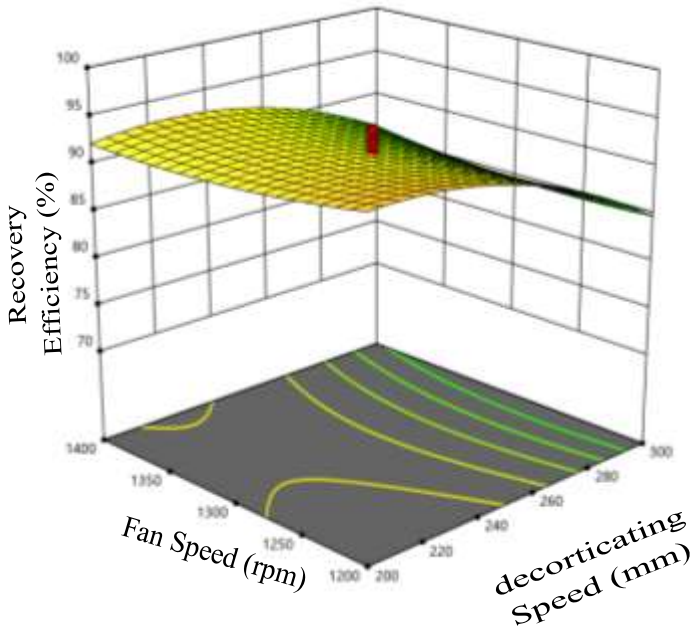


**Figure 4.15:** Response Surface for Seed Recovery Efficiency with Respect to Fan Speed and Decorticating Speed

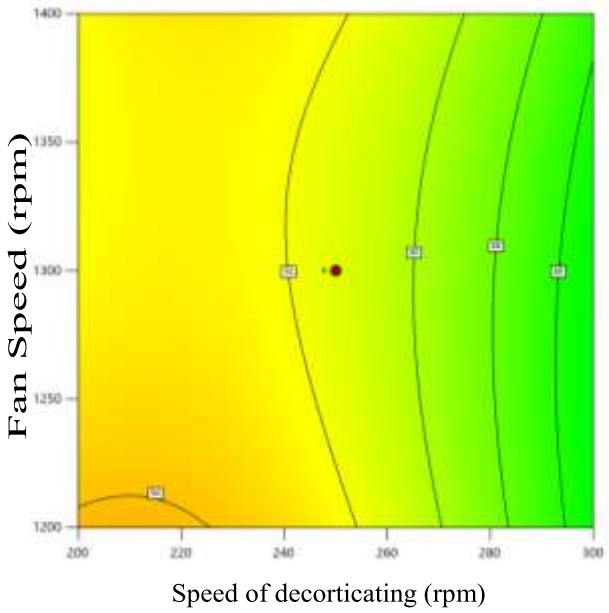


**Figure 4.16:** Contour Plot for Seed Recovery Efficiency with Respect to Fan Speed and Speed of Decorticating

### *4.2.3.5 Relationship between Feed Rate and Plate Clearance with respect to Recovery Efficiency*

The effects of feed rate and plate clearance on recovery efficiency at a constant decorticating speed of 250 rpm and a fan speed of 1300 rpm are presented in Figures 4.17 and 4.18. As the feed rate increased from 120 kg to 140 kg, the recovery efficiency decreased from 95 % to 90 %. This could be the result of more impact among the seeds than between the seed and the decorticating mechanism. Which resulted in insufficient impact force for decorticating the seed. This is in line with the report of Gitau *et al*. (2013), in which an increase in feed rate decreases recovery efficiency. At higher feed rates, the number of seeds entering the sheller per unit time increases, and some seeds may be hitting other seeds instead of the hard rubber surface, resulting in insufficient impact for decorticating. Also, the recovery

efficiency remains almost constant at 95 % as the plate clearance increases from 2 to 3 mm, and then decreases to 88 % with further increases in the plate clearance to 4 mm.

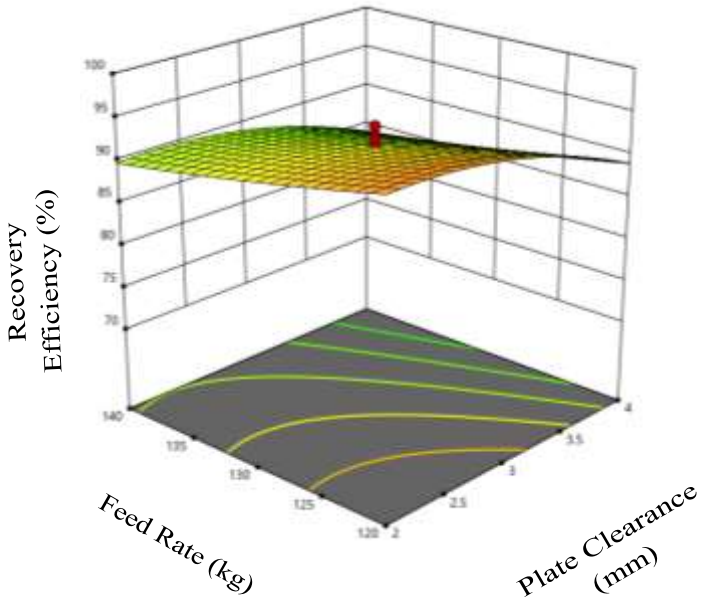


**Figure 4.17:** Response Surface for Recovery Efficiency with Respect to Feed Rate and Plate Clearance

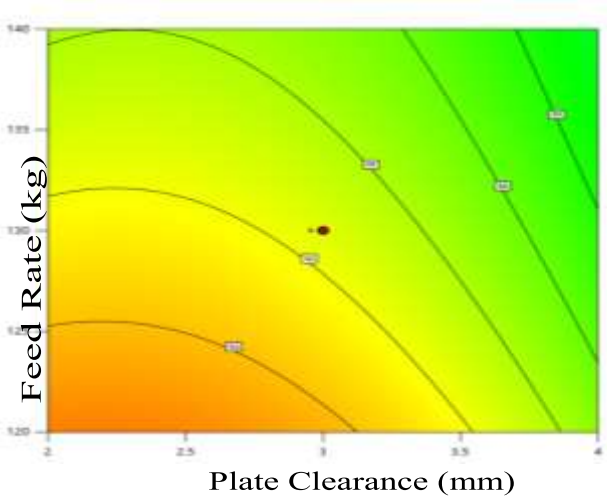


**Figure 4.18:** Contour Plot for Recovery Efficiency with Respect to Feed Rate and Plate Clearance

#### *4.2.3.1 Percentage Loss*

The effects of independent variables (decorticating speed, plate clearance, plate speed, and feed rate) on the percentage loss were presented in Table 4.1. The percentage loss increased with increases in feed rate, speed of the fan, speed of decorticating, and plate clearance. Table 4.8 below shows the results of the statistical analysis of the variance of the data obtained from the results for the determination of effects, contributions, the model coefficient, the test for unfitness, and the not insignificant nature of the variables and their respective interactions on the percentage loss. The not-insignificant model terms were identified at a 5 % significance level. The quadratic regression model and fitted model equations developed to predict the decorticating efficiency with respect to functional machine parameters (independent variables) were given as shown in equation 4.7.

The results in Table 4.8 showed that the model equation was significant ($P \leq 0.001$), and the model F-value of 74.7 implies the model is significant. There is only a 0.01% chance that an F-value this large could occur due to noise. P-values less than 0.0500 indicate model terms are significant. All of the variables were also found to be significant model terms ($P \leq 0.001$). The lack of fit F-value of 0.53 indicates that the lack of fit is insignificant in comparison to the pure error. A large lack of fit f-value due to noise has a 81.47 % chance of occurring.

The coefficient of variation (C.V) of 8.88 % obtained was low, below the threshold value of not greater than 10%. This means that the deviation between predicted and experimental values was not as large as reported by Maran and Manikanda (2012) or Gana *et al.* (2017). The coefficient of determination R value of 0.9929 indicated that the model equation was capable of predicting about 99.29 % of the differences between the predicted and experimental values. As a result, the model was unable to account for approximately 0.007

% of the variation. The R-squared coefficient of correlation of 0.9859 was very high and very close to one, as recommended by Gana (2016); Xin and Saka (2008). However, the authors went on to say that a high $R^2$ value does not necessarily imply that the regression model equation is good because it will increase when a new variable is added, even if the new variable is of consequence or order. Hence, adjusted and predicted $R^2$ were suggested to be used to test the model's sufficiency. Based on that, it was observed that the predicted R-squared and adjusted R-squared values were in logical conformity with each other, with values of 0.9481 and 0.9727, respectively. This means that experimental data were well fitted.

The regressed decorticating efficiency model is given as

$$P_{\mathrm{L}} = 8.5 + 3.7A + 2.78B - 0.06C + 2.65\mathrm{D} - 0.2388AB - 0.7625\mathrm{AC} - 0.5138AD - 0.4675\ \mathrm{BC} - 0.4063\mathrm{BD} + 0.3825\mathrm{CD} + 2.99A^2 + 1.36B^2 - 0.9123C^2 - 0.0673D^2 \quad (4.7)$$

where, $P_{\mathrm{L}}$ = Percentage Loss (%)

A = Decorticating Speed (rpm)

B = Plate Clearance (mm)

C = Fan Speed (rpm)

D = Feed Rate (kg)

The variables A, B and D in the fitted model have a positive coefficient, implying direct proportionality, implying direct proportionality.

#### *4.2.3.2 Simulation and Confirmation of the Model*

The model equation obtained was simulated, and the percentage loss was observed to be within the experimental range. From Table 4.9, the actual value of the percentage loss was observed to be in close conformity with the predicted value, verifying the need for the model equation to be used to determine the least percentage loss at various operating conditions within the range of the experimental value.

#### *4.2.3.3 Relationship between Plate Clearance and Decorticating Speed with respect to Percentage Loss*

The effects of plate clearance and decorticating speed on percentage loss at a constant fan speed of 1300 rpm and feed rate of 130 kg/h were presented in Figures 4.19 and 4.20. The response surface is presented in Figure 4.19, while the contour plot is presented in Figure 4.20. The percentage loss remains constant as with value of 6 % as the plate clearance increased from 2 mm to 3 mm and then increased to 11.5 % with further increase in plate clearance to 4mm. This could be as result of more space created that allows the grains pass without decorticating. Also, the decorticating efficiency remains constant with the value of 6% as the decorticating speed increased from 200 to 250 rpm and then increased to 14 % with further increase in speed to 300 rpm. This could be as result of more impact energy that crushed the grain at high speed of decorticating. This result is in agreement with the results found by Al-Shamiry and Yahya (2020), where the percentage of grain breakage and grain loss increased with increase in plate speed

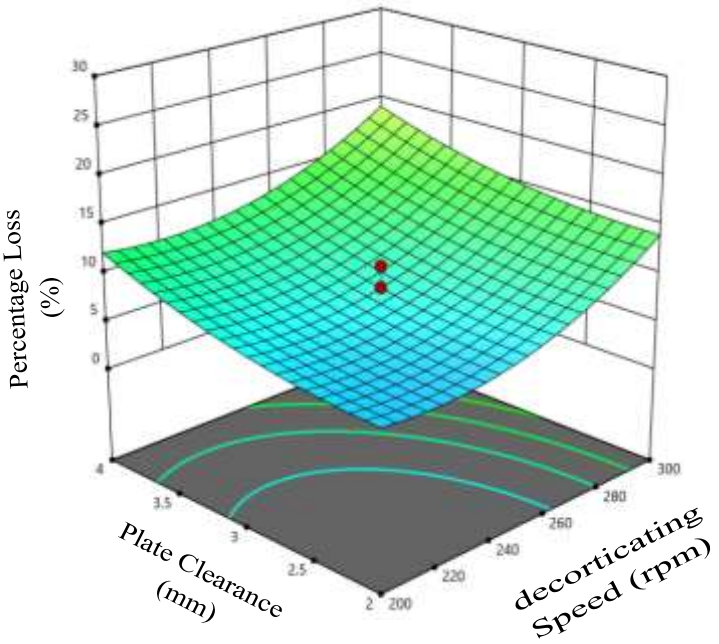


**Figure 4.19:** Response Surface for Percentage Loss with Respect to Plate Clearance and Decorticating Speed

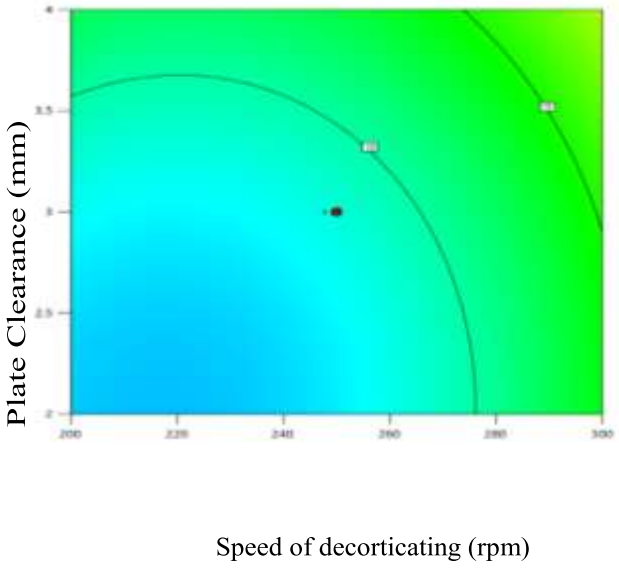


**Figure 4.20:** Contour Plot for Percentage Loss with Respect to Plate Clearance and Decorticating Speed

### *4.2.3.4 Relationship between Fan Speed and Plate Clearance with respect to Percentage Loss*

The effects of fan speed and plate clearance on percentage loss at a constant decorticating speed of 250 rpm and feed rate of 130 kg are presented in Figures 4.21 and 4.22. As the fan speed increased from 1200 to 1400 rpm, the percentage loss remains constant. This could be as result of the volume of air generated is not enough to blowing away the grains particles. Also, the percentage loss increased remains constant with a value of 6 % as the plate clearance increased from 2 to 3 mm and then increase to 13 % with further increase in clearance to 4 mm.

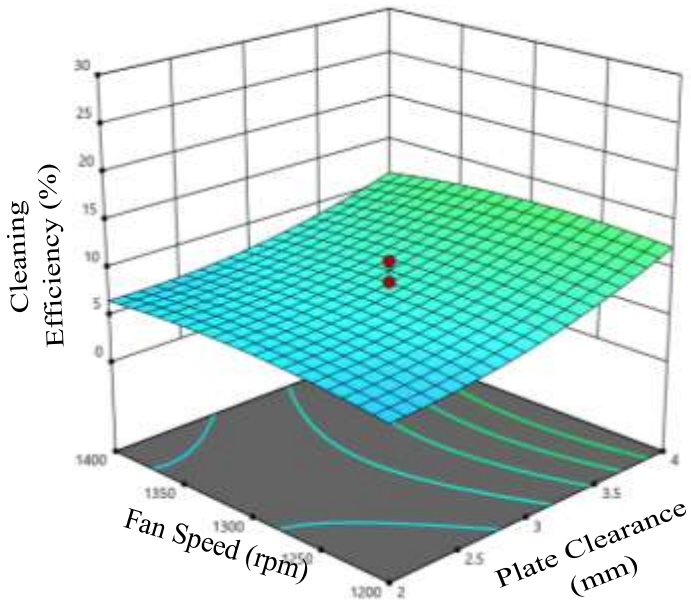


**Figure 4.21:** Response Surface for Percentage Loss with Respect to Fan Speed and Plate Clearance

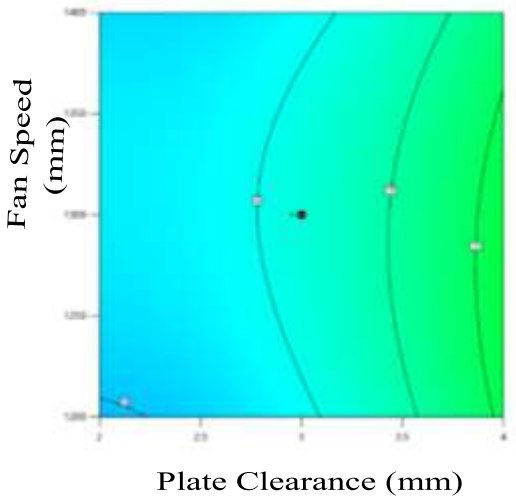


**Figure 4.22:** Contour Plot for Percentage Loss with Respect to Fan Speed and Plate Clearance

### *4.2.3.5 Relationship between Feed Rate and Plate Clearance with respect to Percentage Loss*

The effects of feed rate and plate clearance on percentage loss at a constant decorticating speed of 250 rpm and a fan speed of 1300 rpm are presented in Figures 4.23 and 4.24. The percentage loss increased from 5 to 10% as the feed rate increased from 120 to 140 kg/h. This could be the result of more impact among the seeds than between the seed and the decorticating mechanism. Which resulted in insufficient impact force for decorticating the seed. This is in line with the report of Gitau *et al*. (2013), in which an increase in feed rate increased the percentage loss. At higher feed rates, the number of seeds entering the sheller per unit time increases, and some seeds may be hitting other seeds instead of the hard rubber surface, resulting in insufficient impact for decorticating. Also, the percentage loss remains constant at value 5 % as the plate clearance increased from 2 to 3 mm and then increase to 10 % with further increase in plate clearance to 4 mm.

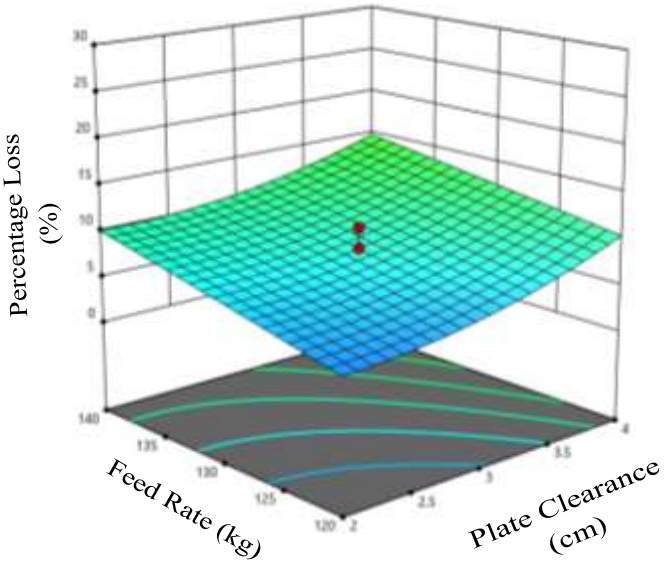


**Figure 4.23:** Response Surface for Percentage Loss with Respect to Feed Rate and Plate Clearance

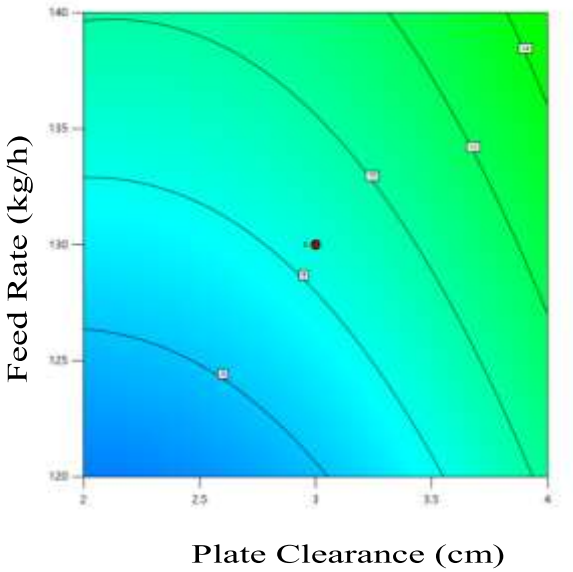


**Figure 4.24:** Contour Plot for Percentage Loss with Respect to Feed Rate and Plate Clearance

# CHAPTER FIVE

## 5.0 CONCLUSION AND RECOMMENDATIONS

### 5.1 Conclusion

i. A decorticating machine to decorticate a range of Bambara nut varieties by simple replacement of the plates was designed using solid works computer aided design software, version 2020. in accordance to standard methods. Measured engineering properties of Bambara nut relevant for its decortication aided in fitting the crop specific parameters (spikes spacing and decorticating force), hence the decorticating machine was constructed.

ii. the parameters needed for the estimation of the performance indices were successfully obtained via the evaluations of the machine. From the ANOVA performed on the evaluation data, the performance on the bases of the machine's variables obtained showed that; the best shelling efficiency of 96.5 % occurred at variable combinations of; shelling speed of 250 rpm, plate clearance of 1 mm, feed rate of 130 kg/h and fan speed of 1300 rpm, the throughput at this condition was found to be 86.4 kg/h. while, the best performance of cleaning of 92.22 % occurred at a shelling speed = 250 rpm, plate clearance = 3 mm, fan speed = 1300 rpm and feed rate = 110 kg/h

## 5.2 Recommendation

The study recommends that other types of decorticating member (discs) such as the rasp bar type (for frictional decorticating principles) be used for improves performance.

The study further recommends that more shelling disc should be constructed for other nuts or pods using the specification of their Engineering Properties.

## 5.3 Contribution to Knowledge

This research work identifies a novel technology that can be adopted by agricultural machines for decorticating operations. The effects of the machine speed, hopper opening on recovery efficiency, cleaning efficiency and separation was evaluated. The performance evaluation of the machine resulted to recovery efficiency of 99.37%, compared to typical range of 70% to 92% as seen in the literatures reviewed herein.

## REFERENCES


Adedeji M.A. And W.Y. Danladi (2016): Modification and Construction of Motorized Bambara Nut Decorticating Machine. *Global Advanced Research Journal of Engineering, Technoogy and Innovation* (ISSN: 2315-5124) Vol 5(1) Pp. 001-006, February, 2016. Available Online Http://Garj.Org/Garjeti/Ndex.Htm. Copyright © 2016 Global Advanced Research Journals

Adu, James & Ejiko, Samuel & Peters, Osayemi. (2018). Design and Fabrication of Groundnut Shelling Machine. *Grin Research Journal. 19.*

Afify M. K., M. A. El-Sharabasy., M. M. A. Ali (2007): Development of a Local Threshing Machine Suits for Threshing Black Seed (Nigella Sativa). *Misr J Ag Eng*, 24(4) 699724.

Akchurin, A. (2017). Generation of wear particles in lubricated contacts during running-in. University of Twente.

Akibode, S., & Maredia, M. K. (2012). Global and regional trends in production, trade and consumption of food legume crops.

Al-Hassani, H. M. A., Abd Alamir, J. S., & Hamad, N. T. (2014). First diagonal cracking and ultimate shear of reactive powder concrete T-beams without stirrups. *Journal of Engineering and Sustainable Development*, 18(5), 149-164.

Alonge, A., Ossom, I., & Bassey, E. (2017). Design modification and performance testing of a Bambara groundnut sheller. Chemical Engineering Transactions, 58, 367-372.

Al-Shamiry F. M. S and Yahya N. M. A (2020). The Performance Evaluating of Thresher Machine Attached to the Tractor, *IJRDO - Journal of Agriculture and Research*, 6(3). Pp-7-16

Aremu A. K., Ademuwagun A. A. And Ogunlade C. A (2014): Effects of Moisture Content and Loading Orientation on Some Mechanical Properties of the African Oil Bean Seed (Pentaclethra Macrophylla Benth). *African Journal of Agricultural Research* Vol. 9(49), Pp. 3504-3510, 4 December, 2014 Article Number9C31A2F48862 DOI: 10.5897/AJAR2014.9109 ISSN 1991-637X

Aririguzo, J. C. (2017). "Evaluation of Performance of an Indigenous Bambaranut Decorticating Machine. American Journal of Engineering Research, 6(7), 06-10.

Asif, M., Rooney, L.W., Ali, R. & Riaz, M.N. 2013. Application and Opportunities of Pulses in Food System: A Review. Critical Reviews in Food Science and Nutrition, 53(11): 1168–1179.

Bansal N K and Shiv Kumar Lahan (2009): Design and Development of an Axial Flow Thresher for Seed Crops. Juu~Nal Of Agncujtural Engtneenng Vol. &{I). January-March, 2009.

Bennett, Emma & Roberts, Jeremy & Wagstaff, Carol. (2011). The Role of the Pod in Seed Development: Strategies for Manipulating Yield. The New Phytologist. 190. 838-53. 10.1111/J.1469-8137.2011.03714.X.

Bochat, A., Wesolowski, L., & Zastempowski, M. (2015). A comparative study of new and traditional designs of a hammer mill. Transactions of the ASABE, 58(3), 585-596.

Bojňanská, T., Frančáková, H., Líšková, M., & Tokár, M. (2021). Legumes–the alternative raw materials for bread production. Journal of Microbiology, Biotechnology and Food Sciences, 2021, 876-886.

Chiara Benetti (2016): Sustainable Production of Plastics and Biogas from Legume Residues. BE-Sustainable Magazine, April 26, 2016 Edition.

Christy Sprague: Santa Fe - New Pinto Bean for Michigan October 19, 2015.

Cukor, G., Jurkovic, Z., & Sekulic, M. (2011). Rotatable Central Composite Design of Experiments Versus Taguchi Method in the Optimization of Turning. (METABK 5091) 17-20.

Dahl, Wendy. (2019). Health Benefits of Pulses. 10.1007/978-3-030-12763-3.

Davies, T. R., McSaveney, M. J., & Reznichenko, N. V. (2019). What happens to fracture energy in brittle fracture. xmltex\break?> Revisiting the Griffith assumption. Solid Earth, 10(4), 1385-1395.

De Lucia, M., & Assennato, D. (2016). Agricultural engineering in development: post-harvest operations and management of foodgrains. FAO Agricultural Services Bulletin (FAO).

Diepenbrock, Wulf. (2000). Yield Analysis of Winter Oilseed Rape (Brassica Napus L.): A Review. Field Crops Research. 67. 35-49. 10.1016/S0378-4290(00)00082-4.

FAO, IFAD, UNICEF, WFP and WHO (2018) The State of Food Security and Nutrition in the World 2018. Building climate resilience for food security and nutrition. Rome: FAO.

FAO/WHO Expert Committee on Food Additives. Meeting, & World Health Organization. (2016). Evaluation of certain food additives and contaminants: eightieth report of the Joint FAO/WHO expert committee on food additives (Vol. 80). World Health Organization.

Fischer-Cripps and Anthony. C. (2007). Introduction to contact mechanics (Vol. 101). New York: Springer.

Fu J., Chen, Z., Han, L., & Ren, L. (2018). Review of grain threshing theory and technology. *International Journal of Agricultural and Biological Engineering*, 11(3), 12-20.

Gana I.M, Agidi G, Idah PA, Anuonye JC. (2017). Development and Testing of an Automated Grain Drinks Processing Machine. Food and Bioproducts Processing, *Journal of the European Federation of Chemical Engineering: Part C. Elsevier*. 2017;104:19-31. Www. Elsevier.Com/Locate/Fbp

Gana I.M. Development and Optimization of Functional Parameters of an Automated Grain Drinks Processing Machine [Unpublished Phd. Engineering Thesis]. Minna: Federal University of Technology; 2016

Gitau A. N., Mboya P., Njoroge B. N. K. And Mburu M (2013). Optimizing the Performance of A Manually Operated Groundnut (Arachis Hypogaea) Decorticator. Open Journal of Optimization, 2013, 2, 26-32

Giwa S., & Akanbi, T. (2020). Mechanization Of Melon Processing And Novel Extraction Technologies: A Short Review. Scientific African. 9. E00478. 10.1016/J.Sciaf.2020.E00478.

Gowda, C. L. L., Rao, P. P., & Bhagavatula, S. (2009). Global trends in production and trade of major grain legumes.

Guijun, Yang & Soo-Jin P. (2019). Deformation of Single Crystals, Polycrystalline Materials, And Thin Films: A Review. Materials. 12. 2003. 10.3390/Ma12122003

Hassan, A. M. T., Jones, S. W., & Mahmud, G. H. (2012). Experimental test methods to determine the uniaxial tensile and compressive behaviour of ultra-high performance fibre reinforced concrete (UHPFRC). Construction and building materials, 37, 874-882.

Hu, X., Vatankhah-Varnoosfaderani, M., Zhou, J., Li, Q., & Sheiko, S. S. (2015). Weak hydrogen bonding enables hard, strong, tough, and elastic hydrogels. Advanced materials, 27(43), 6899-6905.

Iqbal, I., Suhardi, S., & Nirisnawati, S. A. (2018). Multipurpose Power Thresher Performance Test. J. Ilm. Rekayasa Pertan. dan Biosist., 6(1), 12-16.

Iskhakov, I., Frolov, I., & Ribakov, Y. (2022). Experimental Verification of Theoretical Stress-Strain Model for Compressed Concrete Considering Post-Peak Stage. Materials, 15(17), 6064.

Jun S. P., Yoo, H. S., & Choi, S. (2018). Ten years of research change using Google Trends: From the perspective of big data utilizations and applications. Technological forecasting and social change, 130, 69-87.

Kabir A. A. & Fadele, Oluwaseyi. (2019). Open Access Journal of Agricultural Research a Review of Shelling, Threshing, De-Hulling and Decorticating Machines. 3. 1-10.

Kabir AA And Fedele OK (2018): A Review of Shelling, Threshing, De-Hulling and Decorticating Machines J Agri Res 2018, 3(1): 000148.

Kailashkumar, E. B (2019): Study of Different Kinds of Threshers & Factors Influencing Threshing of Crops: A Review. International Journal for Scientific Research & Development| Vol. 6, Issue 12, 2019| ISSN (Online): 2321-0613.

Kar, S. K., Anshuman, D. A., Raj, H., & Singh, P. P. (2018, August). New design and fabrication of smart helmet. In IOP Conference Series: Materials Science and Engineering (Vol. 402, No. 1, p. 012055). IOP Publishing.

Kate, R. S., Khalate, S. A., & Deokate, R. J. (2018). Overview of nanostructured metal oxides and pure nickel oxide (NiO) electrodes for supercapacitors: A review. Journal of Alloys and Compounds, 734, 89-111.

Khurmi, R. S., & Gupta, J. K. (2004). A Text Book of Machine Design. 14th Reprint.

Khurmi, R.S. And Gupta, J.K. (2005) A Textbook of Machine Design. 14th Edition, Eurasia Publishing House (PVT.) Ltd, Ram Nagar, New Delhi.

Kim, H. J., Yoo, S. S., & Kim, D. E. (2012). Nano-scale wear: a review. International Journal of Precision Engineering and Manufacturing, 13, 1709-1718.

Lee, M. (2014). GIS-based route risk assessment of hazardous material transport.

Li X., Du, Y., Guo, J., & Mao, E. (2020). Design, simulation, and test of a new threshing cylinder for high moisture content corn. Applied Sciences, 10(14), 4925.

Lisa Buchholz, Jody Hanson and Janelle Mauch (2013): Design and Evaluation of a Sunflower Dehuller to Aid in Precision Planting. Project Report Submitted as Part of the Course ABEN487: Senior Design Project II

Maduako, J. N., Saidu, M., Matthias, P., & Vanke, I. (2006). Testing of an engine-powered groundnut shelling machine. Journal of Agricultural Engineering and Technology, 14, 29-37.

Mani A. & P, Manishkumar & M, Krishna & Uthappan, Karthick. (2020). Groundnut Peeling Shelling Machine. International Research Journal on Advanced Science Hub. 2. 136-139. 10.47392/irjash.2020.51.

Maphosa, Y., & Jideani, V. A. (2017). The role of legumes in human nutrition. Functional food-improve health through adequate food, 1, 13.

Maran, P. J., & Manikanda S. (2012). Response Surface Modeling and Optimization of Process Parameters for Aqueous Extraction of Pigments from Pea Fruit Dye Pigin, 95, 465-472.

Murtala O. I, Elijah A. A and Timothy A. A. (2018): Design, Fabrication and Testing of Cocoa Depodding Machine. Mindanao Journal of Science and Technology Vol.16 (2018) 11-24

Neda, Erana & Erena, Zelalem. (2020). Expounding the Production and Importance of Cowpea (Vigna Unguiculata (L.) Walp.) In Ethiopia. Cogent Food and Agriculture. 6. 1769805. 10.1080/23311932.2020.1769805.

Negedu, A. M., Irtwange, S.V and Ijabo, O. J (2018): Design and Fabrication Of Bambara Groundnut (Vigna Subterranea (L) Verdc) Combined Sorter, Sheller And Cleaning Machine. International Journal of Scientific & Engineering Research Volume 9, Issue 4, April-2018 1785 ISSN 2229-5518.

Nishad, P., Singh, J., Naik, R. K., Patel, S., Mangaraj, S., Mishra, N., & Thakur, R. R. (2022). Design and development of a circular disc type efficient automatic decorticator for Charoli (Buchanania lanzan). Journal of Food Processing and Preservation, e16634.

Ojolo, S., Orisaleye, J., Ogundare A. & Damilola, Kadiri. (2019). Development of A Delonix Regia Decorticating Machine. Engineering Reports. 1. 10.1002/Eng2.12058.

Okunola, A. A., Adekanye, T. A., Ayooluwa, A., Okonkwo, C. E., Alake, S. A., Olayanju, T. M. A., & Adewumi, A. D. (2019). Development Of A Locust Bean Seed Dehulling Cum Washing Machine. International Journal of Mechanical Engineering and Technology (IJMET), 10(1), 1321-1330.

Oluwole F., A. Abdulrahim and R. Olalere. "Evaluation of Some Centrifugal Impaction Devices for Shelling Bambara Groundnut". *Agricultural Engineering International: the CIGR Ejournal.* Manuscript PM 07 007. Vol. IX. October, 2007

Osasumwen G. O., Aniekan E. I., Lucky E. C. (2020): Design and Fabrication of a Modular Melon Depodding Machine for Optimum Performance in Nigerian Agricultural Sector. European Mechanical Science (2020), 4(3):103112doi: Https://Doiorg/10.26701/Ems.729747

Ouili, A. S., Ouoba, A., Nankangre, H., Compaore, C. O. T., Nikiema, M., & SidikiOuattara, A. (2022). Post-Harvest Management Practices of Bambara Groundnut (Vigna Subterranea (L.) Verdc) Seeds in Burkina Faso.

Oyelami, A. T., Olaniyan, O. O., Iliya, D., & Idowu, A. S. (2008). The design of a closed type impeller blower for a 500 kg capacity rotary furnace. Journal of Engineering Development Institute, 12(1), 50-56.

Pinson, G.S., Melville, D.J. And Cox, D.R.S. (1991) Decortication of Tropical Oilseeds and Edible Nuts (NRI Bulletin No. 42). [Working Paper].

Saravacos, G. D., & Kostaropoulos, A. E. (2012). Handbook of food processing equipment (Vol. 2012, pp. 331-381). Kluwer Academic/Plenum.

Schmidt, F. L., Pearlman, K., Hunter, J. E., & Shane, G. S. (1979). Further tests OF the schmidt-hunter bayesian validity generalization procedure 1. Personnel Psychology, 32(2), 257-281.

Simonyan K. J. And Yiljep Y. D. (2008) "Investigating Grain Separation and Cleaning Efficiency Distribution of a Conventional Stationary Rasp- Bar Sorghum Thresher" Agricultural Engineering International: The CIGR Ejournal Manuscript PM 07 028. Vol. X. August, 2008. Pp. 1-12

Snapp, S., Rahmanian, M., & Batello, C. (2018). Pulse crops for sustainable farms in sub-Saharan Africa. United Nations.

Tabor, D. (2000). The Hardness of Metals. Oxford University Press.

Uguru, H., Akpokodje, O. I., & Altuntaş, E. (2021). A Study on Rupture Resistance of Groundnut (Cv. SAMNUT 22) Kernel. Turkish Journal of Agricultural Engineering Research, 2(1), 19-33.

Unathi Gulwa, Nobulungisa Mgujulwa and Solomon T. Beyene (2018) "Benefits of Grass-Legume Inter-Cropping in Livestock Systems." African Journal of Agricultural Research 13, No. 26: 1311-1319.

Varenberg, M. (2013). Towards A Unified Classification of Wear. Friction, 1, 333-340.

Vlot, A. C., Liu, P. P., Cameron, R. K., Park, S. W., Yang, Y., Kumar, D., ... & Klessig, D. F. (2008). Identification of likely orthologs of tobacco salicylic acid-binding protein 2 and their role in systemic acquired resistance in Arabidopsis thaliana. The Plant Journal, 56(3), 445-456.

Voisin, Anne-Sophie & Gueguen, Jacques & Huyghe, Christian & Jeuffroy, Marie-Helene & Magrini, Marie-Benoît & Jean-Marc, Meynard & Mougel, Christophe & Pellerin, Sylvain & Pelzer, Elise. (2014). Legumes for Feed, Food, Biomaterials and Bioenergy in Europe: A Review. Agronomy for Sustainable Development. 34. 10.1007/S13593-013-0189-Y.

Wallace, A. J., Armstrong, R. D., Grace, P. R., Scheer, C., & Partington, D. L. (2020). Nitrogen use efficiency of 15N urea applied to wheat based on fertiliser timing and use of inhibitors. Nutrient Cycling in Agroecosystems, 116(1), 41-56.

Wang, M., & Wang, C. (2019). Bulk properties of biomaterials and testing techniques. Reference Module in Biomedical Sciences: Encyclopedia of Biomedical Engineering.

Wang, P., Chou, W., Nie, A., Huang, Y., Yao, H., & Wang, H. (2011). Molecular dynamics simulation on deformation mechanisms in body-centered-cubic molybdenum nanowires. Journal of Applied Physics, 110(9), 093521.

Wesley, B. J., Swamy, R., Babu, B. H., & Reddy, T. Y. (2010). Modification of Groundnut thresher for Decorticating Groundnut Pods and Castor. Agricultural Science Digest, 30(1), 23-25.

Wiraguna, E. (2016). Enhancement of Fixation Nitrogen in Food Legumes. Journal of Agricultural Studies. 4. 1. 10.5296/Jas.V4i2.9065.

Xin L., & Saka S. (2008). Optimization of Japanese Beech Hydrolysis Treated with Batch Hot Compressed Water by Response Surface Methodology. *Inter. Journal of Agricultural Biological and Engineering 1(2), 239-245.*

Yang, G., & Park, S. J. (2019). Conventional and microwave hydrothermal synthesis and application of functional materials: A review. Materials, 12(7), 1177.

Zhang, Y., Zuo, T. T., Tang, Z., Gao, M. C., Dahmen, K. A., Liaw, P. K., & Lu, Z. P. (2014). Microstructures and properties of high-entropy alloys. Progress in materials science, 61, 1-93.

# APPENDICES

## Appendix A: design considerations

### 3.3 Design considerations

#### 3.4.1 Determination of the hopper height

This was found according to equation (3.1) as shown below

$$V_h = \frac{1}{3}\pi h(r_1^2 + r_1 r_2 + r_2^2$$

For the present design, $r_1 = 6\ inches = 0.152\ m$, $r_2 = 1.75\ inches = 0.044\ m$.

$$h = \sqrt{{h_s}^2 - (r_1 - r_2)^2}$$

where $h_s$ is slant height of the cone $= 9.5\ inches = 0.241\ m$

$$h = \sqrt{0.241^2 - (0.152 - 0.044)^2} = 0.215\ m$$

therefore,

$$V_h = \frac{1}{3}\pi \times 0.215(0.152^2 + 0.152 \times 0.044 + 0.044)$$

$$V_h = 7.143 \times 10^{-3}\ m^3$$

#### 3.4.2 Design of the delivery channel

by equation (3.3), we have that;

$$D_{pi} = D_{ds} = D_{ph} = 3.5 inches = 0.089\ m$$

Considering equation (3.7), hence fitting the height of the delivery channel, we have that;

$E_{fk} = 0.116\ Nm$ and average mass $m$ of Bambara nut kernel was found to be $1.7 \times 10^{-3}$.

$h_{v.max}$ the maximum possible clearance between the plates $=$ the case height $-$ $2(\text{thickness of plates} + \text{thickness of case sheet}) = 0.1524 - 2(0.005 + 0.002) =$ $0.1404\ m$

Therefore;

$$H_p \leq \frac{0.116}{1.7 \times 10^{-3} \times 9.8} - 0.1404 = 6.823\ m$$

The delivery channel thus, has to be set to a value less than this. It was set to 6 inches = 0.1524 m

### 3.4.4 Design of the blower

- Determination of air discharge speed and discharge rate

The parameters are as defined below, with their values for the test pod (Bambara nut)

$v_a$ is the velocity of air flow at the outlet in $ms^{-1}$

$m_p$ is the mass of the kernel = 0.404 g = $4.04 \times 10^{-4}\ kg$ (Christy, 2015);

$\rho_a$ is the density of air at s.t.p $= 1.3\ kgm^{-3}$

$A_p$ is the maximum projectable area of the pit $= 6.851 \times 10^{-5}\ m^{-2}$ (Christy, 2015);

$\emptyset$ is the angle the fan outlet protrusion makes with the vertical axis $= 70^o$

$A_d$ is the cross-sectional area of the discharge outlet (volute opening) $= (11 \times 3)\ inches = 2.129 \times 10^{-2}\ m^2$

$g$ is acceleration due to gravity$= 9.8\ ms^{-2}$

Thus, substituting the values into equation (3.14), we obtain $v_a$ as in below.

$$v_a = \sqrt{\frac{2 \times 4.04 \times 10^{-4} \times 9.8}{1.3 \times 6.851 \times 10^{-5} \cos 70^o}} = 16.122\ ms^{-1}$$

Substituting this value into equation (3.15), we obtain the discharge rate as;

$$Q_{out} = v_a \times A_d = 16.122 \times 2.129 \times 10^{-2}$$

This gives $Q = 0.343\ m^3 s^{-1}$

Design for the speed (rpm) of the blower shaft, based on the discharge rate

$r_i$ the volute's inside radius $= 3\frac{1}{4}\ inches = 0.083\ m$

$b_i$ the fan vane width at the suction eye $= 1.5\ inches = 0.038\ m$

$V_{ri}$, the radial component of the air absolute velocity is the same as the inlet velocity ($V_{in}$), since there are no vane guard.

From equation (3.17), we obtain $V_{ri} = V_{in}$ as;

$$V_{in} = \frac{Q_{in}}{2\pi r_i b_i} = \frac{0.343}{2\pi \times 0.085 \times 0.038}$$

Thus, $V_{in} = 16.857\ ms^{-1}$

The linear velocity of the vane at the volute inside radius $V_{v.in}$ is hence obtained using equation (3.18)

$V_{in} = V_{v.in} \tan \beta_i$

Where; $\beta_i$ the inlet vane angle $= 30°$

From equation (3.18), it follows hence that;

$$V_{v.in} = {}^{V_{in}}/_{\tan \beta_i} = {}^{16.857}/_{\tan 30°}$$

Thus, $V_{v.in} = 29.197\ ms^{-1}$

The rpm equivalent of this velocity which is same as the blower shaft/pulley speed $(N_f)$ is given by;

$$N_f = 60V_{v.in}/2\pi\, r_i = 60 \times 29.197/2\pi \times 0.083 \approx 3359\ rpm$$

Based on the design assumption, this is the vane speed that yields a flow rate just enough to lift and blow the kernel itself. Thus, the actual speed is set below this value so as to avoid lifting and consequently, blowing off of the actual kernel or pit.

The fan speed, is therefore set to 1100 rpm.

### 3.4.5 Design of drive mechanisms (belts and pulleys) of the decorticating section

- Fitting the drive speeds and the size of the pulleys

$N_1 = 1000\ rpm$, $D_1 = 60\ mm$, $N_2 = 200\ rpm$, $D_2 =$?

from equation (3.19), we have that; $D_2 = N_1 D_1 / N_2$

Therefore, $D_2 = 1000 \times 60/200 = 300\ mm$

- Determination of the length of belt

The length of the belt was obtained using equation (3.20) as in below

Note that $x = 11.75\ inches = 298.45\ mm$

$$L = \frac{\pi}{2}(60 + 300) + 2 \times 298.45 + \frac{(60 - 300)^2}{4 \times 298.45} = 1.210 \times 10^3\ mm$$

- Determination of angle of contact ($\theta$) and angle of wrap ($\alpha$)

The angle of contact according to equation 3.21 is given by;

$\theta = (180^{\circ} - 2\alpha)\frac{\pi}{180} rad$

The angle of wrap $\alpha$ is obtained according to equation (3.22) as in below;

$$\alpha = \sin^{-1}(\frac{300 - 60}{2 \times 298.45}) = 23.708^{\circ}$$

Hence, $\theta$ is obtained using equation (3.21)

$$\theta = (180^{\circ} - 23.708)\frac{\pi}{180} rad = 2.728\ rad$$

- Determination of driving tensions in the belt

Following the procedure in section for determination of driving tension, we obtain the parameters as below.

$$m_{b/l} = cross\ sectioal\ arae\ of\ belt\ \times unit\ lenght \times density\ of\ belt\ material$$

For the selected belt material, area = $9.0 \times 10^{-5}\ m^2$

Density of double woven reinforced rubber = $1250\ kg/m^3$

Therefore;

$$m_{b/l} = 9.0 \times 10^{-5}\ m^2 \times 1 \times 1250\ kg/m^3 = 0.113$$

And

$$v_b = \pi D_1 N/60 = \pi \times 0.06 \times 1000/60 = 3.142\ ms^{-1}$$

Thus;

$$T_c = 0.113 \times 3.142^2 = 1.116\ N$$

The tension on the tight side of the belt $T_1$ from equation (3.23) is given as $T_1 = T_u - T_c$

$T_u$, the maximum tension in the belt is given as;

$$T_u = maximum\ permissibe\ belt\ tensile\ stress(\sigma) \times belt\ crosssectional\ area(A)$$

For the selected belt type, $\sigma = 4.0\ MN/m^2$ and $A = 9 \times 10^{-5}\ m^{-2}$.

Therefore;

$$T_u = \sigma \times A = 4.0 \times 10^6 \times 9 \times 10^{-5} = 360\ N$$

Thus,

$$T_1 = T_u - T_c = (360 - 1.116)\ N = 358.884\ N$$

$\mu$ the coefficient of friction = 0.3 for rubber-cast iron contact (dry)

$\theta$ is the angle of contact at the smaller pulley (in radian $= 2.728\ rad$ )

$\beta$ is half the groove angle of the pulley ($35^o/2$)

Thus, substituting values into equation (3.25) yields,

$$2.3log\left[\frac{358.884}{T_2}\right] = 0.3 \times 2.728cosec(35/2)^{\circ}$$

This gives $T_2 = 23.532\ N$

- The power transmitted by a belt

This is obtained by substituting values for the parameters into equation (3.26), thus;

$$P_b = (358.884 - 23.532)3.142 = 1053.676W = 1.054\ KW$$

Note that, the center distance $x = 11.75\ inches = 298.45\ mm$

### 3.4.6 Design of drive mechanisms (belts and pulleys) of the blower section

- Fitting the drive speeds and the size of the blower pulleys

The blower peed was determined by substituting the parameters values into equation (3.19)

$$N_d D_d = N_b D_b$$

Where; $N_d = 200\ rpm$, $D_d = 325\ mm$, $N_b = 1100\ rpm$, $D_b$ =?

Thus, substituting the values and obtaining $D_b$, we have;

$$D_b = N_d D_d / N_b = 200 \times 325/1100 = 59.09$$

A pulley of diameter 60 mm is thus selected for the blower

- Determination of the length of blower belt: using equation (3.20),

That is;

$$L = \frac{\pi}{2}(D_1 + D_2) + 2x + \frac{(D_1 - D_2)^2}{4x}$$

where; $D_1 = 325$ mm, $D_2 = 60$ mm, $x$ the centre distance of the drive $= 381$ mm.

Therefore;

$$L = \frac{\pi}{2}(325 + 60) + 2 \times 381 + \frac{(325 - 60)^2}{4 \times 381}$$

$$L = 1366.787\ mm$$

A belt of length 1366mm is selected.

- Determination of angle of contact ($\theta$) and angle of wrap ($\alpha$)

By equation 3.21, that is;

$$\theta = (180^{\circ} - 2\alpha)\frac{\pi}{180}\ rad$$

The angle of wrap $\alpha$ is given by equation 3.22 as;

$$sin\alpha = \frac{D_2 - D_1}{2x}$$

Thus,

$$\alpha = \sin^{-1}(\frac{325 - 60}{2 \times 381}) = 20.351^{\circ}$$

Hence,

$$\theta = (180^{\circ} - 2 \times 20.351^{\circ})\frac{\pi}{180}\ rad$$

Therefore, $\theta = 2.431\ rad$

- Determination of driving tensions in the belt

The tensions in both the tight ($T_1$) and slack ($T_2$) sides of the fan belt are obtained using the same procedures as in tensions in the decorticator belt, equation (3.23).

Thus, $T_u = T_1 + T_c$

but we know from equation (3.24) that; $T_c = m_{b/l}.v_b^2$

Where; $T_c$ is centrifugal tension;

$m_{b/l}$ the mass of belt per unit length = $0.133\ kg/m^2$

$v_b$ is the velocity of the belt = $\pi DN/60 = \pi \times 60 \times 10^{-3} \times 1100/60 = 1.1\pi$

Therefore,

$$T_c = 0.133 \times 1.1\pi^2 = 1.444\ N$$

And

$$T_u = \sigma \times A = 4.0 \times 10^6 \times 9 \times 10^{-5} = 360\ N$$

Thus,

$$T_1 = T_u - T_c = (360 - 1.444)\ N = 358.556\ N$$

Again, we obtain $T_2$ using equation (3.25)

Thus,

$$2.3log\left[\frac{T_1}{T_2}\right] = \mu.\theta cosec\beta$$

Where; $\mu$ the coefficient of friction = 0.3 for rubber-cast iron contact (dry)

$\theta$ the angle of contact at the smaller pulley (in radian $= 2.431\ rad$ )

$\beta$ half the groove angle of the pulley = $(35^o/2)$

Thus,

$$2.3log\left[\frac{358.556}{T_2}\right] = 0.3 \times 2.431cosec(35/2)^{\circ}$$

This gives $T_2 = 31.629\ N$

- The power transmitted by the blower driver belt

This is obtain using equation (3.26). That is,

$$P_b = (T_1 - T_2)v_b$$

By substituting values for the parameters, we have that;

$$P_b = (358.556 - 31.629)1.1\pi = 1129.779\ W = 1.129\ KW$$

### 3.4.7 Design of shafts

Determination of the parameter's values for shaft diameter determination according to the procedures of section 3.4.7 is as shown below

$K_m$ is the combine fatigue and shock factor for bending $= 2$

$K_t$ is the combine fatigue and shock factor for bending $= 1.5$

- Maximum bending moment on the shaft

This is obtained using equation (3.29) and (3.30) that is;

$\sum F_V = 0$

Thus, $R_A + 389.985 + R_B - 382.416 = 0$

$\sum M_{V.A} = 0$

Taking moments about $R_A$, and treating moments tending to cause sagging as positive and those tending to cause hugging as negative gives;

$$4R_B - 382.416(7) + 389.985(11) = 0$$

$$R_B = -403.231$$

Substituting $R_B = -403.231$ into equation (3.39), we get;

$$R_A + 389.985 - 403.231 - 382.416 = 0$$

$$R_A = 395.662\ N$$

Hence, we obtain the maximum bending moment by the sectioning analysis as below;

$$M_{R_A - R_B} \rightarrow 395.662(0.1016) = 40.199\ N.m$$

$$M_{R_B - T_d} \rightarrow 395.662(0.1016 + 0.0762) - 403.231(0.0762) = 39.623\ N.m$$

$$M_{T_d - T_b} \rightarrow 395.662(0.1016 + 0.0762 + 0.1016) - 403.231(0.0762 + 0.1016)$$
$$- 382.416(0.1016) = 0$$

From the above, the maximum bending moment "$M$" induced in the shaft at the section $M_{R_A-R_B}$ is $M = 40.199\ N.m$

- Maximum torsional moment on the shaft

This was obtained using equation (3.31) as shown below;

$$T = (T_1 - T_2)R = (358.884 - 23.532)0.15 = 50.303\ N.m$$

The torsional moment due to the blower belt tension;

$$T = (358.556 - 31.629)0.163 = 53.289\ N.m$$

Therefore, the maximum torsional moment on the shaft $T = 53.289\ N.m$

- The axial load $F_a$

The axial load is same as the weight of disc $W_{disc}$ as calculated earlier.

That is, $F_a = W_{disc} = 12.937\ N$

- The permissible stress in shear and tension

The permissible (allowable) stress in shear of the shaft is obtained as below;

$$\tau_a = \tau_u/f.s = 42\ Mpa/1.5 = 28\ Mpa = 28 \times 10^6\ Nm^{-2}$$

The permissible (allowable) stress in tension of the shaft is;

$$\sigma_a = \sigma_u\ /s.f = 84\ Mpa/1.5 = 56\ Mpa = 56 \times 10^6\ Nm^{-2})$$

Substituting these values hence into equation (3.39) gives

$$\sqrt{(2 \times 40.199 + 1 \times 12.937\, D/8)^2 + (1.5 \times 53.289)^2} = \frac{\pi}{16} \times 28 \times 10^6 D^3$$

This gives $D = 0.027\ m$

Thus, a shaft of $0.030\ m = 30\ mm$ diameter is selected.

Following the same procedures for the blower shaft, similarly, a shaft of diameter $30mm$ was selected

### 3.5.7 design for power requirement of the machine

The total power requirement for running the machine was estimated using the procedures of section 3.5.7 as shown below.

From equation (3.34), we know that that the total power requirement of the machine is given as;

$P_m = P_{d.s} + P_{b.s}$

- Power requirement of the decorticating section ($P_{d.s}$)

The power requirement of the decorticating section $P_{d.s}$ is given by equation (3.35) as;

$P_{d.s} = P_{disc} + P_{shaft} + P_{pulley} + P_{decort}$

- The power required to drive the disc ($P_{disc}$)

By equation 3.37 and 3.39, the power to drive the disc is obtained as follows;

$$W_{disc} = W_{plate} + W_{spikes} + W_{pod} = (\rho v g)_{plate} + n(\rho v g)_{spikes} + W_{pod}$$

$$= (\rho \times \pi r^2 t \times g)_{plate} + n(\rho \times \pi r^2 h \times g)_{spike} + W_{pod}$$

$\rho_{plate}$ the density of the disc material $= 7850\ kgm^{-3}$

$r_{plate}$ the radius of the lower disc $7.620 \times 10^{-2}\ m$

$t_d$ the disc material thickness $= 5mm = 5 \times 10^{-3}\ m$

$n$ the number of spikes on the lower disc$= 16$

$\rho_{spike}$ the density of the spike material$= 7850\ kgm^{-3}$

$r_{spike}$ the radius of the spikes $2.5mm = 2.5 \times 10^{-3}\ m$

$h_{spike}$ the height of the spikes $= 1.5inches = 3.81 \times 10^{-2}\ m$

$v_{disc}$ and $v_{spike}$ the volumetric content of the disc and spike materials respectively.

Thus,

$$W_{disc} = [7850\pi \times (7.62 \times 10^{-2})^2 \times 5 \times 10^{-3} \times 9.8]$$
$$+ 32[7850\pi \times (2.5 \times 10^{-3})^2 \times 3.81 \times 10^{-2} \times 9.8]\ + W_{pod}$$

$$W_{disc} = 9.327N + W_{pod}$$

Now, $W_p$ the weight of equal volume of pod as the capacity of the decorticating chamber given by;

$$\pi r^2 h = \pi \times (7.62 \times 10^{-2})^2 \times 3.81 \times 10^{-2} = 6.95 \times 10^{-4}\ m^3$$

Note that the chambers height is equal as the height of the spikes ($3.81 \times 10^{-2}$).

Weight of $6.95 \times 10^{-4} m^3$ of Bambara nut (by $\rho vg$) gives;

$$W_{pod} = 530 \times 6.95 \times 10^{-4} \times 9.8$$

$$W_{pod} = 3.610\ N$$

Hence

$$W_{disc} = 9.327\ N + W_{pod} = 9.327\ N + 3.610\ N$$

$$W_{disc} = 12.937\ N$$

Therefore, $T_{disc}$ by equation 3.31 is;

$$T_{disc} = (9.327 + 3.610)7.62 \times 10^{-2}$$

$$T_{disc} = 0.986\ Nm$$

Thus, by equation 3.37,

$$P_{disc} = T_{disc}\omega_d = (0.986)\omega_d$$

But,

$$\omega_d = 2\pi N_d/60 = 2\pi \times 200/60 = 20.944\ rads^{-1}$$

Therefore,

$$P_{disc} = (0.986)20.944 = 20.651\ W$$

- Power to drive the shaft $(P_{shaft})$

The power required to drive the shaft is given by equation 3.36, that is;

$$P_{shaft} = T_{shaft} \times \omega_d$$

But,

$$T_{shaft} = W_{shaft} \times r_{shaft} = (\rho \pi r^2 l g)_{shaft} \times r_{shaft}$$

Were,

$T_{shaft}$ is shaft torque;

$W_{shaft}$ is the shaft weight;

$r_{shaft}$ is the radius of the shaft $15mm = 0.015\ m$

$\rho_{shaft}$ is the density of shaft material $= 7850\ kgm^{-3}$

And $l$ is the length of the shaft $= 0.381\ m$

Therefore,

$$T_{shaft} = (7850\pi \times 0.015^2 \times 0.381 \times 9.8) \times 0.015$$

$$T_{shaft} = 0.310\ Nm$$

Thus,

$$P_{shaft} = (0.310)\omega_d = 0.310 \times 20.944$$

$$P_{shaft} = 6.493\ W$$

- Power to drive the pulley$\left(P_{pulleys}\right)$

The power to drive the pulley is calculated in accordance with the procedures as in $P_{shaft}$ above. Thus;

$$P_{pulleys} = (T)_{pulleys} \times \omega_d$$

But,

$$(T)_{pulleys} = (W.r)_{d.pulley} + (W.r)_{b.pulley}$$

Where;

$W_{d.pulley}$ is the weight of the decorticator driven pulley $= 98\ N$

$r_{d.pulley}$ is the radius of the decorticator driven pulley $= 150\ mm = 0.15\ m$

$W_{b.pulley}$ is the weight of the blower driver pulley $= 127.4\ N$

$r_{d.pulley}$ is the radius of the blower driver pulley $= 163\ mm = 0.163\ m$

Thus,

$$T_{pulleys} = 98 \times 0.15 + 127.4 \times 0.163 = 35.466\ Nm$$

Hence;

$$P_{pulleys} = (T_{pulleys})\omega_d = 35.466 \times 20.944$$

$$P_{pulleys} = 742.800\ W$$

Power to decorticate the pod ($P_{pod}$)

The power required for the removal of the kernel by splitting open the pod is a function of the fracture resistance of the pod. To this regard, the force applied by the decorticating member must be set equal to the rupture force of the pod. By the power formula, (equation 3.36) we know that;

$$P_{pod} = T_{pod}\omega_d$$

But;

$$T_{pod} = F_{pod.r}r_{fn}$$

Thus, for $n_{s/f}$ number of spikes per front according to equation 3.41, we have that;

$$T_{pod} = n_{s/f}(F_{pod.r}r_{fn})$$

For the total torque for $n_f$ number of fronts, the torque will be obtained by the sum according to equation (3.52);

$$\sum T_{pod} = \sum_{n=1}^{n=n_f} n_{s/f}\,(F_{pod.r}r_{fn})$$

Therefore, total power requirement for decortication is given by equation (3.53);

$$P_{pod} = \sum T_{pod}\,.\,\omega_d$$

Where;

$P_{pod}$ is the power requirement for pod decortication;

$T_{pod}$ is the torque due to the decorticating force;

$r_{fn}$ is the radius from the axis of rotation of the disc to a front;

Thus, from the present design case the parameters are as follow;

$r_{f1}$ radius to the first front of spike arrays $= 2.5 \times 10^{-2}m$ and $r_{f2}$ the radius to the second front of spikes array $= 6.35 \times 10^{-2}$;

$n_f$ is the number of spikes front or arrays $= 2$

$n_{s/f}$ is the number of spikes per front $= 16$

$F_{pod.r}$ is the rupture force of the pod (Bambara nut); This force is given by Uguru *et al.*, (2021) as force per unit area as $0.4\ N/mm^2$.

From the pressure relation $P = F/A$, we have that, $F = P \times A$

$P$ is the force in unit area $= 0.4\ N/mm^2 = 4 \times 10^5\ N/m^2$

$F = F_{pod.r}$ is the rupture force $(N)$, $A$ is the projected area of the pod = area of the pod contacted during the impact; $A$ is taken as the largest possible area that makes contact with the spike, given as;

$A =$ diameter of the major axis of the pod $(D_m) \times$ diameter of spike.

Average $D_m$ of the variety of peanut used (local 1) was found to be $= 1.206 \times 10^{-2}$ and diameter of spike $= 5\ mm = 5 \times 10^{-3}\ m$

Therefore;

$$A = 1.206 \times 10^{-2} \times 5 \times 10^{-3}\ m = 6.03 \times 10^{-5}\ m$$

Hence;

$$F_{pod.r} = P \times A = 4 \times 10^5 \times 6.03 \times 10^{-5} = 24.12\ N$$

Thus, substituting this value into equation 3.51 to find $T_{pod}$ for the spike front, gives;

Torque for first front array spikes;

$$T_{pod1} = n_{s/f}(F_{pod.r} r_{f1}) = 16 \times 24.12 \times 2.54 \times 10^{-2}$$

$$T_{pod1} = 9.80\ Nm$$

Torque for second front array of spikes

$$T_{pod2} = n_{s/f}(F_{pod.r} r_{f2}) = 16 \times 24.12 \times 6.35 \times 10^{-2}$$

$$T_{pod2} = 24.506\ Nm$$

Hence, total torque according to equation 3.52 is;

$$\sum T_{pod} = (9.802 + 24.506)\ N = 34.308\ Nm$$

Now, total power requirement for decorticating pod by equation 3.53;

$$P_{pod} = \sum T_{pod} \,.\, \omega_d = 24.506 \times 20.944$$

$$P_{pod} = 513.254\ W$$

Therefore, $P_{d.s} = P_{disc} + P_{shaft} + P_{pulley} + P_{pod} = 20.651 + 6.493 + 742.800 + 513.254$

$$P_{d.s} = 1283.198\ W$$

Power to drive the blower $(P_{blower})$

This was computed to be $=$ 84.321 W

Total power required by the machine $(P_m)$ according to equation (3.34) is;

$$P_m = P_{d.s} + P_{b.s} = 1283.198 + 84.321\text{W} = 1367.519\ \text{W}$$

Considering a factor of safety of 1.5, the minimum motor power to drive the machine was computed as $P_m \times f.s = 1367.519 \times 1.5$

Thus, a $2.5HP$ motor is used to run the machine

**Appendix B:** Calculated values of design parameters

| Design parameters | Design values |
|---|---|
| Hopper volume | $V_h = 7.143 \times 10^{-3} m^3$ |
| Delivery channel pipe height | $H_P = 0.1524$ |
| Intra pikes spacing | $2x_f = 2D_{mp} + 3mm$ |
| Intra spike array spacing | $2x_f = 2D_{mp} + 3mm$ |
| Blower air discharge speed | $v_a = 16.122 ms^{-1}$ |
| Blower air discharge rate | $Q = 0.343 m^3 s^{-1}$ |
| Blower shaft speed | $N_f = 1100 rpm$ |
| Diameter of decorticator section driven pulley | $300 mm$ |
| Belt length of decorticating section drive | $L = 1.210 \times 10^3 mm$ |
| Belt angle of wrap on the motor pulley (motor-decorticator drive) | $\alpha = 23.708^{\circ}$ |
| Belt angle of contact on motor pulley (motor-decorticator drive) | $\theta = 2.728 rad$ |
| Tension in the tight side of belt (motor-decorticator drive) | $T_1 = 358.884 N$ |
| Tension in the slack side of belt (motor-decorticator drive) | $T_2 = 23.532 N$ |
| Velocity of belt ($v_b$) (motor-decorticator drive) | $v_b = 3.142 ms^{-1}$ |
| Power transmitted by belt (motor-decorticator drive) | $P_b = 1.054 KW$ |

**Appendix B:** Calculated values of design parameters continue

| Design parameters | Design values |
|---|---|
| Diameter of the blower driven pully | $D_b = 60mm$ |
| Diameter of the blower driver pulley | $D_d = 325mm$ |
| Belt length of blower section drive | $L = 1366.787mm$ |
| Belt angle of wrap on the blower pulley (decorticator-blower drive) | $\alpha = 20.351^{\circ}$ |
| Belt angle of contact on blower pulley (decorticator-blower drive) | $\theta = 2.431rad$ |
| Tension in the tight side of belt (decorticator-blower drive) | $T_1 = 358.556N$ |
| Tension in the slack side of belt (decorticator-blower drive) | $T_2 = 31.629N$ |
| Velocity of belt (decorticator-blower drive) | $v_b = 1.1\pi ms^{-1}$ |
| Power transmitted by belt (decorticator-blower drive) | $P_b = 1.129KW$ |
| Machine power requirement | $P_m = 2.5HP$ |

## Appendix C:

Table 4.1: Results of Effects of Shelling Speed, Plate Clearance, Fan Speed and Feed Rate on the Machine Shelling Efficiency, Cleaning Efficiency, Recovery Efficiency and Percentage Loss

| Std | Run | A:Speed of shelling | B:Plate clearance | C:Speed of Blower | D:Feed Rate | Shelling Efficiency | Recovery Efficiency | Cleaning Efficiency | Percentage Loss |
|---|---|---|---|---|---|---|---|---|---|
| | | rpm | Mm | Rpm | kg/h | % | % | (%) | % |
| 12 | 1 | 300 | 4 | 1200 | 140 | 63.65 | 79.45 | 65.98 | 20.55 |
| 16 | 2 | 300 | 4 | 1400 | 140 | 65.26 | 81.46 | 67.44 | 18.54 |
| 20 | 3 | 250 | 5 | 1300 | 130 | 64.49 | 73.59 | 75.91 | 26.41 |
| 28 | 4 | 250 | 3 | 1300 | 130 | 84.22 | 91.56 | 72.86 | 8.44 |
| 5 | 5 | 200 | 2 | 1400 | 120 | 87.46 | 98.19 | 96.75 | 1.81 |
| 22 | 6 | 250 | 3 | 1500 | 130 | 80.68 | 92.32 | 86.76 | 7.68 |
| 19 | 7 | 250 | 1 | 1300 | 130 | 96.5 | 89.65 | 83.43 | 10.35 |
| 25 | 8 | 250 | 3 | 1300 | 130 | 90.59 | 93.71 | 73.46 | 6.29 |
| 1 | 9 | 200 | 2 | 1200 | 120 | 87.24 | 99.37 | 74.81 | 0.63 |
| 29 | 10 | 250 | 3 | 1300 | 130 | 85.28 | 89.11 | 68.21 | 10.89 |
| 8 | 11 | 300 | 4 | 1400 | 120 | 78.11 | 86.49 | 99.8 | 13.51 |
| 9 | 12 | 200 | 2 | 1200 | 140 | 72.28 | 93.48 | 64.56 | 6.52 |
| 10 | 13 | 300 | 2 | 1200 | 140 | 81.15 | 84.45 | 60.29 | 15.55 |
| 3 | 14 | 200 | 4 | 1200 | 120 | 70.28 | 92.85 | 74.55 | 7.15 |
| 4 | 15 | 300 | 4 | 1200 | 120 | 75.13 | 82.12 | 87.32 | 17.88 |
| 30 | 16 | 250 | 3 | 1300 | 130 | 85.36 | 92.21 | 72.35 | 7.79 |
| 13 | 17 | 200 | 2 | 1400 | 140 | 68.28 | 90.11 | 72.35 | 9.89 |
| 21 | 18 | 250 | 3 | 1100 | 130 | 86.83 | 94.1 | 68.11 | 5.9 |

| Std | Run | A:Speed of shelling | B:Plate clearance | C:Speed of Blower | D:Feed Rate | Shelling Efficiency | Recovery Efficiency | Cleaning Efficiency | Percentage Loss |
|---|---|---|---|---|---|---|---|---|---|
| 24 | 19 | 250 | 3 | 1300 | 150 | 48.39 | 85.83 | 66.76 | 14.17 |
| 6 | 20 | 300 | 2 | 1400 | 120 | 96.28 | 90.29 | 99.12 | 9.71 |
| 14 | 21 | 300 | 2 | 1400 | 140 | 78.27 | 84.68 | 68.72 | 15.32 |
| 27 | 22 | 250 | 3 | 1300 | 130 | 87.42 | 92.62 | 74.67 | 7.38 |
| 17 | 23 | 150 | 3 | 1300 | 130 | 47.2 | 85.82 | 72.52 | 14.18 |
| 2 | 24 | 300 | 2 | 1200 | 120 | 94.63 | 89.54 | 72.65 | 10.46 |
| 26 | 25 | 250 | 3 | 1300 | 130 | 83.76 | 89.18 | 75.11 | 10.82 |
| 15 | 26 | 200 | 4 | 1400 | 140 | 55.65 | 85.43 | 67.11 | 14.57 |
| 7 | 27 | 200 | 4 | 1400 | 120 | 72.49 | 92.28 | 96.22 | 7.72 |
| 23 | 28 | 250 | 3 | 1300 | 110 | 89.32 | 96.16 | 97.22 | 3.84 |
| 18 | 29 | 350 | 3 | 1300 | 130 | 77.88 | 70.85 | 75.65 | 29.15 |
| 11 | 30 | 200 | 4 | 1200 | 140 | 55 | 87.19 | 61.22 | 12.81 |

## Appendix D: Regresional Analysis of Response

Table 4.2: Regresional Analysis of Response of Shelling Efficiency

| Source | Coefficient Estimate | Df | F-value | p-value | |
|---|---|---|---|---|---|
| Model | 86.11 | 1 | 33.44 | < 0.0001 | Significant |
| A-Speed of shelling | 5.21 | 1 | 58.66 | < 0.0001 | |
| B-Plate clearance | -8.09 | 1 | 140.99 | < 0.0001 | |
| C-Speed of Blower | -0.4108 | 1 | 0.364 | 0.5553 | |
| D-Feed Rate | -8.5 | 1 | 155.74 | < 0.0001 | |
| AB | -0.3962 | 1 | 0.2258 | 0.6415 | |
| AC | 0.2675 | 1 | 0.1029 | 0.7528 | |
| AD | 0.6525 | 1 | 0.6122 | 0.4461 | |
| BC | 0.7787 | 1 | 0.872 | 0.3652 | |
| BD | 0.5738 | 1 | 0.4733 | 0.502 | |
| CD | -0.73 | 1 | 0.7662 | 0.3952 | |
| $A^2$ | -5.7 | 1 | 80.02 | < 0.0001 | |
| $B^2$ | -1.21 | 1 | 3.6 | 0.0771 | |
| $C^2$ | -0.394 | 1 | 0.3826 | 0.5455 | |
| $D^2$ | -4.12 | 1 | 41.82 | < 0.0001 | |
| Lack of Fit | 134.78 | 10 | 2.1 | 0.214 | not significant |
| $R^2$ | 0.969 | | | | |
| Adjusted $R^2$ | 0.94 | | | | |
| Predicted $R^2$ | 0.847 | | | | |
| Adeq Precision | 19.0199 | | | | |
| C.V. % | 4.33 | | | | |

Table 4.4: Regresional Analysis of Response of Cleaning Efficiency

| Source | Coefficient Estimate | Df | Mean Square | F-value | p-value | |
|---|---|---|---|---|---|---|
| Model | 72.78 | 1 | 263.25 | 21.68 | < 0.0001 | significant |
| A-Speed of shelling | 0.8338 | 1 | 16.68 | 1.37 | 0.2595 | |
| B-Plate clearance | -0.1938 | 1 | 0.9009 | 0.0742 | 0.7891 | |
| C-Speed of Blower | 5.98 | 1 | 857.17 | 70.58 | < 0.0001 | |
| D-Feed Rate | -9.77 | 1 | 2290.67 | 188.62 | < 0.0001 | |
| AB | 1.82 | 1 | 53.03 | 4.37 | 0.0541 | |
| AC | -0.5281 | 1 | 4.46 | 0.3675 | 0.5535 | |
| AD | -1.21 | 1 | 23.45 | 1.93 | 0.1849 | |
| BC | -1.45 | 1 | 33.44 | 2.75 | 0.1178 | |
| BD | -1.17 | 1 | 21.93 | 1.81 | 0.199 | |
| CD | -3.69 | 1 | 217.49 | 17.91 | 0.0007 | |
| $A^2$ | 0.0789 | 1 | 0.1706 | 0.014 | 0.9072 | |
| $B^2$ | 1.48 | 1 | 59.68 | 4.91 | 0.0425 | |
| $C^2$ | 0.9164 | 1 | 23.03 | 1.9 | 0.1887 | |
| $D^2$ | 2.06 | 1 | 115.84 | 9.54 | 0.0075 | |
| Lack of Fit | 151.63 | 10 | 15.16 | 2.48 | 0.1637 | not significant |
| $R^2$ | 0.9529 | | | | | |
| Adjusted $R^2$ | 0.9089 | | | | | |
| Predicted $R^2$ | 0.7628 | | | | | |
| Adeq Precision | 15.8585 | | | | | |
| C.V. % | 4.56 | | | | | |

Table 4.6: Regresional Analysis of Response of Recovery Efficiency

| Source | Coefficient Estimate | df | F-value | p-value | |
|---|---|---|---|---|---|
| Model | 91.4 | 1 | 19.12 | < 0.0001 | significant |
| A-Speed of shelling | -3.76 | 1 | 78.98 | < 0.0001 | |
| B-Plate clearance | -3.12 | 1 | 54.35 | < 0.0001 | |
| C-Speed of Blower | -0.1283 | 1 | 0.0918 | 0.7661 | |
| D-Feed Rate | -2.73 | 1 | 41.55 | < 0.0001 | |
| AB | 0.2475 | 1 | 0.2275 | 0.6402 | |
| AC | 0.89 | 1 | 2.94 | 0.1069 | |
| AD | 0.505 | 1 | 0.9472 | 0.3459 | |
| BC | 0.4763 | 1 | 0.8425 | 0.3732 | |
| BD | 0.2788 | 1 | 0.2886 | 0.599 | |
| CD | -0.3912 | 1 | 0.5686 | 0.4625 | |
| $A^2$ | -2.84 | 1 | 51.41 | < 0.0001 | |
| $B^2$ | -2.02 | 1 | 25.99 | 0.0001 | |
| $C^2$ | 0.8773 | 1 | 4.9 | 0.0428 | |
| $D^2$ | 0.3235 | 1 | 0.6665 | 0.427 | |
| Lack of Fit | 46.94 | 10 | 1.33 | 0.3975 | not significant |
| $R^2$ | 0.9469 | | | | |
| Adjusted $R^2$ | 0.8974 | | | | |
| Predicted $R^2$ | 0.757 | | | | |
| Adeq Precision | 18.3898 | | | | |
| C.V. % | 2.35 | | | | |

Table 4.8: Regresional Analysis of Response of Percentage Loss

| Source | Coefficient Estimate | Df | F-value | p-value | |
|---|---|---|---|---|---|
| Model | 8.54 | 1 | 74.7 | < 0.0001 | Significant |
| A-Speed of shelling | 3.7 | 1 | 330.04 | < 0.0001 | |
| B-Plate clearance | 2.78 | 1 | 186.46 | < 0.0001 | |
| C-Speed of Blower | -0.06 | 1 | 0.0869 | 0.7722 | |
| D-Feed Rate | 2.65 | 1 | 169 | < 0.0001 | |
| AB | -0.2388 | 1 | 0.9174 | 0.3533 | |
| AC | -0.7625 | 1 | 9.36 | 0.008 | |
| AD | -0.5138 | 1 | 4.25 | 0.0571 | |
| BC | -0.4675 | 1 | 3.52 | 0.0803 | |
| BD | -0.4063 | 1 | 2.66 | 0.124 | |
| CD | 0.3825 | 1 | 2.35 | 0.1457 | |
| $A^2$ | 2.99 | 1 | 246.28 | < 0.0001 | |
| $B^2$ | 1.36 | 1 | 50.86 | < 0.0001 | |
| $C^2$ | -0.9123 | 1 | 22.96 | 0.0002 | |
| $D^2$ | -0.0673 | 1 | 0.1249 | 0.7287 | |
| Lack of Fit | 7.69 | 10 | 0.5324 | 0.8147 | not significant |
| $R^2$ | 0.9859 | | | | |
| Adjusted $R^2$ | 0.9727 | | | | |
| Predicted $R^2$ | 0.9481 | | | | |
| Adeq. Precision | 38.3649 | | | | |
| C.V. % | 8.88 | | | | |

**Appendix E: Results of Simulation**

Table 4.3: Results of Simulation of the Shelling Efficiency

| Run Order | Actual Value | Predicted Value |
|---|---|---|
| 1 | 63.65 | 64.24 |
| 2 | 65.26 | 64.05 |
| 3 | 64.49 | 65.10 |
| 4 | 84.22 | 86.11 |
| 5 | 87.46 | 86.16 |
| 6 | 80.68 | 83.71 |
| 7 | 96.50 | 97.44 |
| 8 | 90.59 | 86.11 |
| 9 | 87.24 | 87.61 |
| 10 | 85.28 | 86.11 |
| 11 | 78.11 | 80.06 |
| 12 | 72.28 | 69.62 |
| 13 | 81.15 | 81.62 |
| 14 | 70.28 | 69.53 |
| 15 | 75.13 | 77.32 |
| 16 | 85.36 | 86.11 |
| 17 | 68.28 | 65.25 |
| 18 | 86.83 | 85.35 |
| 19 | 48.39 | 52.63 |
| 20 | 96.28 | 96.61 |
| 21 | 78.27 | 78.31 |
| 22 | 87.42 | 86.11 |
| 23 | 47.20 | 52.88 |
| 24 | 94.63 | 96.99 |
| 25 | 83.76 | 86.11 |
| 26 | 55.65 | 52.58 |
| 27 | 72.49 | 71.19 |
| 28 | 89.32 | 86.62 |
| 29 | 77.88 | 73.74 |
| 30 | 55.00 | 53.83 |

Table 4.5: Results of Simulation of the Cleaning Efficiency

| Run Order | Actual Value | Predicted Value |
|---|---|---|
| 1 | 65.98 | 67.30 |
| 2 | 67.44 | 67.93 |
| 3 | 75.91 | 78.29 |
| 4 | 72.86 | 72.78 |
| 5 | 96.75 | 97.51 |
| 6 | 86.76 | 88.39 |
| 7 | 83.43 | 79.06 |
| 8 | 73.46 | 72.78 |
| 9 | 74.81 | 74.23 |
| 10 | 68.21 | 72.78 |
| 11 | 99.80 | 99.60 |
| 12 | 64.56 | 66.83 |
| 13 | 60.29 | 63.49 |
| 14 | 74.55 | 75.44 |
| 15 | 87.32 | 84.22 |
| 16 | 72.35 | 72.78 |
| 17 | 72.35 | 75.36 |
| 18 | 68.11 | 64.49 |
| 19 | 66.76 | 61.46 |
| 20 | 99.12 | 96.90 |
| 21 | 68.72 | 69.91 |
| 22 | 74.67 | 72.78 |
| 23 | 72.52 | 71.42 |
| 24 | 72.65 | 75.74 |
| 25 | 75.11 | 72.78 |
| 26 | 67.11 | 66.10 |
| 27 | 96.22 | 92.93 |
| 28 | 97.22 | 100.54 |
| 29 | 75.65 | 74.76 |
| 30 | 61.22 | 63.35 |

Table 4.7: Results of Simulation of the Seed Recovery Efficiency

| Run Order | Actual Value | Predicted Value |
|---|---|---|
| 1 | 79.45 | 78.30 |
| 2 | 81.46 | 80.00 |
| 3 | 73.59 | 77.07 |
| 4 | 91.56 | 91.40 |
| 5 | 98.19 | 97.28 |
| 6 | 92.32 | 94.65 |
| 7 | 89.65 | 89.56 |
| 8 | 93.71 | 91.40 |
| 9 | 99.37 | 99.49 |
| 10 | 89.11 | 91.40 |
| 11 | 86.49 | 84.67 |
| 12 | 93.48 | 93.24 |
| 13 | 84.45 | 84.45 |
| 14 | 92.85 | 91.24 |
| 15 | 82.12 | 81.41 |
| 16 | 92.21 | 91.40 |
| 17 | 90.11 | 89.47 |
| 18 | 94.10 | 95.16 |
| 19 | 85.83 | 87.23 |
| 20 | 90.29 | 90.03 |
| 21 | 84.68 | 84.24 |
| 22 | 92.62 | 91.40 |
| 23 | 85.82 | 87.56 |
| 24 | 89.54 | 88.68 |
| 25 | 89.18 | 91.40 |
| 26 | 85.43 | 84.24 |
| 27 | 92.28 | 90.94 |
| 28 | 96.16 | 98.15 |
| 29 | 70.85 | 72.50 |
| 30 | 87.19 | 86.11 |

Table 4.8: Results of Simulation of the Percentage Loss

| Run Order | Actual Value | Predicted Value |
|---|---|---|
| 1 | 20.55 | 20.78 |
| 2 | 18.54 | 18.96 |
| 3 | 20.16 | 19.53 |
| 4 | 8.44 | 8.54 |
| 5 | 1.81 | 2.41 |
| 6 | 5.35 | 4.77 |
| 7 | 9.25 | 8.41 |
| 8 | 8.22 | 8.54 |
| 9 | 0.63 | 0.84 |
| 10 | 8.60 | 8.54 |
| 11 | 14.60 | 14.75 |
| 12 | 6.52 | 7.21 |
| 13 | 15.55 | 15.58 |
| 14 | 8.10 | 8.62 |
| 15 | 17.88 | 18.09 |
| 16 | 7.79 | 8.54 |
| 17 | 9.89 | 10.31 |
| 18 | 5.90 | 5.01 |
| 19 | 14.17 | 13.56 |
| 20 | 9.71 | 9.79 |
| 21 | 15.32 | 15.63 |
| 22 | 7.38 | 8.54 |
| 23 | 14.18 | 13.10 |
| 24 | 10.46 | 11.26 |
| 25 | 10.82 | 8.54 |
| 26 | 14.57 | 14.60 |
| 27 | 7.72 | 8.33 |
| 28 | 3.84 | 2.98 |
| 29 | 28.27 | 27.89 |
| 30 | 12.81 | 13.36 |

## APPENDIX F: Machine Design of Multi-purpose Decorticator

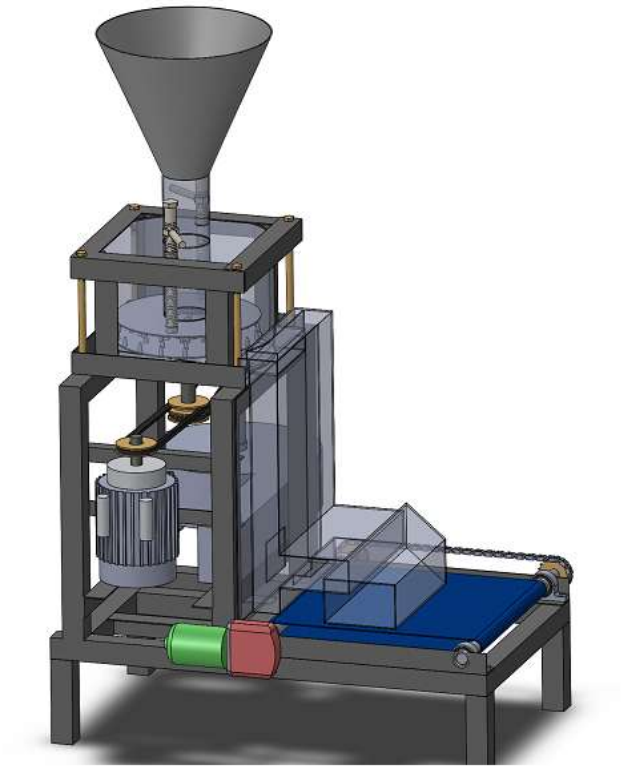

**Figure F1:** Detailed isometric view of Multi-purpose Decorticator

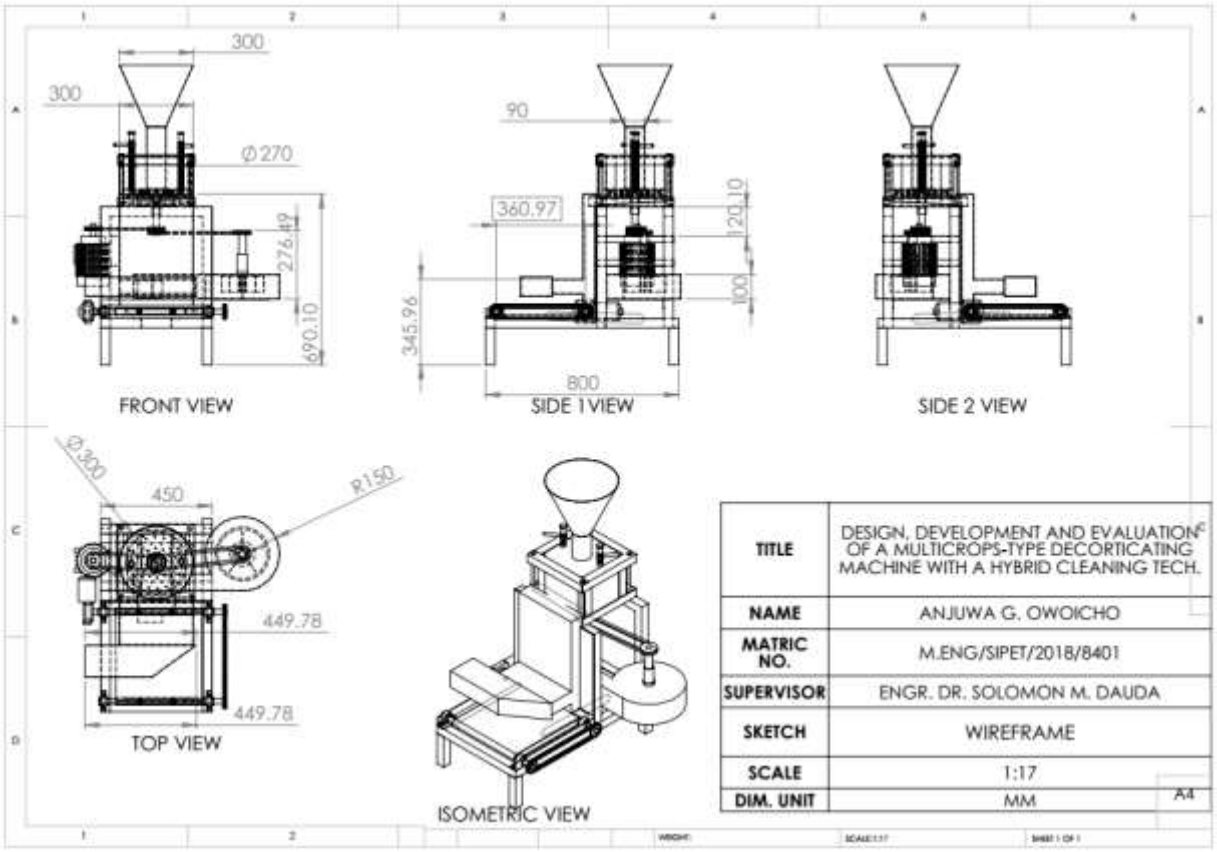


**Figure F2:** Multi-View of Multi-Purpose Decorticator

**Figure F3:** Fabricated View of Multi-Purpose Decorticator